Effiziente Lokalisierung von Nutzern und Geräten in Smarten Umgebungen

Dissertation
zur
Erlangung des akademischen Grades
Doktor-Ingenieur (Dr.-Ing.)
der Fakultät für Informatik und Elektrotechnik
der Universität Rostock

vorgelegt von
Dipl.-Ing. Dominik Lieckfeldt

Rostock, 07. Januar 2010

urn:nbn:de:gbv:28-diss2010-0144-6

Gutachter:
1. Prof. Dr.-Ing. Dirk Timmermann, Institut für Nachrichtentechnik, Universität Rostock, Deutschland
2. Prof. Dr.-Ing. Volker Kühn, Institut für Nachrichtentechnik, Universität Rostock, Deutschland
3. Prof. Dr. Kay Römer, Institut für Technische Informatik, Universität zu Lübeck, Deutschland

Tag der Verteidigung: 12. Juli 2010

Efficient Localization of Users and Devices in Smart Environments

Dissertation in partial fulfillment
of the requirements for the degree of
Doktor-Ingenieur (Dr.-Ing.)
(Electrical Engineering and Computer Science)
in The University of Rostock

submitted by
Dipl.-Ing. Dominik Lieckfeldt

Rostock, 7 January 2010

Doctoral Committee:
1. Prof. Dr.-Ing. Dirk Timmermann, Institute of Applied Microelectronics and Computer Engineering, University of Rostock, Germany
2. Prof. Dr.-Ing. Volker Kühn, Institute of Communications Engineering, University of Rostock, Germany
3. Prof. Dr. Kay Römer, Institute of Computer Engineering, University of Lübeck, Germany

Date of disputation: 12 July 2010

Acknowledgements

This work was partially financed by the German Research Foundation (DFG) within the graduate school Multi modal Smart Appliance ensembles for Mobile Applications (MuSAMA, GRK 1424).

I like to express my sincere gratitude to my supervisor Prof. Dr.-Ing. Dirk Timmermann for providing guidance and encouragement. He made possible writing the thesis by awarding the scholarship within the graduate school and provided the freedom I needed to develop and implement my ideas. I also like to thank Prof. Dr.-Ing. Thomas Kirste and Prof. Dr.-Ing. Volker Kühn for their valuable comments during meetings and my presentations.

Furthermore, I like to thank my colleagues Ralf Behnke, Jiaxi You, Jakob Salzmann and Peter Danielis for the invaluable discussions we had and for supporting me not only during the good times of my thesis. Especially, I like to thank Ralf Behnke and Peter Danielis whose proofreading helped to complete the thesis in time.

I like to thank my family for their constant caring encouragement over the years. I like to express a special thank you to Carolin Greifenberg for her loving support during my work.

Finally, I like to thank the members of the graduate school MuSAMA, especially Christoph Burghardt and Christiane Plociennik, and all staff members at the Institute of Applied Microelectronics and Computer Engineering, University of Rostock as they had a part in the pleasant and prolific working environment.

Contents

LIST OF FIGURES . . . . . **v**

LIST OF TABLES . . . . . **xi**

LIST OF ACRONYMS . . . . . **xii**

1 Introduction **1**
- 1.1 Wireless Sensor Networks 4
- 1.2 Radio Frequency Identification 7
- 1.3 Problem Statement 9
- 1.4 Contribution 11
- 1.5 Notation 12
- 1.6 Outline of Thesis 13

2 Survey of Wireless Localization Techniques **15**
- 2.1 Measurements of RSS 19
- 2.2 Categorization of Algorithms 23
  - 2.2.1 Triangulation 24
  - 2.2.2 Scene Analysis 25
  - 2.2.3 Proximity 26
  - 2.2.4 Evaluation Criteria 27
- 2.3 Selected Estimation Techniques 31
  - 2.3.1 Least Squared Error Method 31
  - 2.3.2 Maximum Likelihood Estimator 33
  - 2.3.3 Multidimensional Scaling 34
  - 2.3.4 Centroid Localization 35
  - 2.3.5 Recursive Bayesian Estimators 36

3 Improving Efficiency and Accuracy of Localization **41**
- 3.1 Model of Energy Consumption 42
- 3.2 Characterization of Energy Efficiency 43

3.2.1 State-of-the-Art . . . 43
3.2.2 Impact of Centralization . . . 44
3.2.3 Approach and Definition of LogarEEL . . . 46
3.2.4 Results and Conclusions . . . 48
3.2.5 Summary . . . 50
3.3 Selection of Efficient Subsets of Sensors . . . 50
3.3.1 Problem Statement . . . 51
3.3.2 Near Optimal Sensor Selection . . . 52
3.3.3 State-of-the-Art . . . 55
3.3.4 New Algorithms for SSP . . . 61
3.3.5 Optimized Scheduling for Distance-based Selection . . . 67
3.3.6 Results and Conclusions . . . 70
3.3.7 Summary . . . 77

4 Device-free Localization using Passive RFID . . . 79
4.1 Survey of Applications of RFID to Smart Environments . . . 83
4.2 Initial Observations Using a Passive RFID-System . . . 92
4.2.1 Set-up and Procedure of Measurements . . . 92
4.2.2 Derivation of Observation Model . . . 94
4.3 Localization Techniques . . . 98
4.3.1 Maximum Likelihood Estimation . . . 99
4.3.2 Centroid of Intersection Points (CIP) . . . 100
4.4 Estimating the Location of Stationary Users . . . 103
4.4.1 Set-up and Procedure of Measurements . . . 103
4.4.2 Characterizing the Impact of Humans on RSS . . . 106
4.4.3 Results and Conclusions . . . 114
4.5 Tracking the Location of Mobile User . . . 118
4.5.1 Set-up of Computer Simulations . . . 118
4.5.2 Results and Conclusions . . . 120
4.6 Summary . . . 121

5 Conclusion and Future Research Directions . . . 123

A Lists . . . 125

B Proofs . . . 127

BIBLIOGRAPHY . . . 151

List of Figures

1.1 Iterative localization helps to localize all location-unaware sensors. (△, ○, ●) denote anchors, blinds and blinds with estimated location, respectively. The shaded area (▒) denotes the region of location-aware sensors. 1.1a - Initial situation. 1.1b - Localization using anchors. 1.1c - First iteration: Anchors and blinds with estimated locations provide location fixes. 6

1.2 Overview on AutoID technologies [27]. 7

1.3 Architecture of bistatic, passive RFID system. Tags are powered and interrogated by the reader over the forward link and respond over the reverse link. Bistatic systems use for either link a separate antenna which mitigates decoupling forward and reverse link signals in the receiver circuits of the reader. 8

2.1 Outline of localization processes. Knowledge about the location of objects is acquired by i) measuring a quantity that depends on location, ii) establishing a model to characterize the dependence iii) feeding model and measured data or derived *Location Related Parameter (LRP)* into an estimator which calculates an estimated location. 16

2.2 Overview on measurement techniques. 16

2.3 *Probability Density Function (PDF)* of estimated distances. Spread of estimates becomes larger the more distant two sensors are. The dotted blue lines and crosses indicate the true distance which deviates from the *Maximum Likelihood Estimator (MLE)* given by the PDFs' peaks. . 24

2.4 Taxonomy of algorithms for localization. 25

2.5 Illustration of bias and variance as evaluation criteria for the accuracy of localization processes. 28

2.6 The *Cramér-Rao-Bound (CRB)* consists of a distance-dependent part and a geometric-dependent part. A favorable geometry is provided by pairs of location-aware sensors whose spatial configuration leads to a large, normalized shaded area of the parallelogram. Those sensor pairs yield a smaller overlapping (green area in (b)) area when estimated distances vary in a particular range. 30
2.7 Overview of localization techniques *Linear Least Squares (LLS)*, MLE and *Multidimensional Scaling (MDS)*. LLS requires more location-aware sensors due to the linearization and works on lines rather than circles (the lower sensor is used for linearization). The MLE searches over the set of possible solutions for the location that maximizes the likelihood. MDS distributes the location-unaware sensors such that the distance constraints are best met in the least squared error sense. . . . 34
2.8 Overview on Extended Kalman Filter procedure. 37
2.9 Overview on Particle Filter procedure. 39

3.1 States of the energy model. 42
3.2 Figure (b) shows the measurement phase: Each node determines distances to adjacent sensors by means of *Received Signal Strength (RSS)* measurements. (c) Aggregation: Distances are transmitted to a central node to be used for localization. (a) Network configuration used for simulations. (△, ○) denote anchors and blinds, respectively. 45
3.3 Average *Logarithmic Energy Efficiency of Localization (LogarEEL)* η of various localization algorithms vs. standard deviation σ of medium-scale fading ($\alpha = 0.5$). 49
3.4 Overview on sensor selection. 52
3.5 Comparison of variance, bias and CRB for (b) circular and (c) linear movement of the mobile anchor under medium-scale fading. Static anchors are at $\alpha = \{0.25, 0.58\}$. Markers (☆, □, ○) denote the curves for variance, CRB and bias, respectively. 53
3.6 Overview on selection procedures showing Zhao's Leadership Passing algorithm. 56
3.7 Flow-chart of algorithms using leadership-passing. The procedure DET_NEXT_LEADER contains the algorithm specific calculation of utility. 57
3.8 Characteristics of wait times $T_{\text{wait},i} = K\left(\frac{\tilde{d}_{j,i}}{r_{\text{tx}}}\right)^{\alpha}$ with parameters K, α. The plot is normalized by K which determines the maximum wait time. Figure (b) shows the flow-chart of algorithm local-dist. 63
3.9 Flow-chart of algorithm local-crb. 64

3.10 Overview on algorithm local-crb. 65
3.11 Figure (a)shows average number of collisions on the MAC layer vs. parameters α and K of wait time. (b) Total simulated energy consumption vs. pairs of K and α as indicated by the blue line in (a). The x-axis depicts the value of K of the parameter set $\{K/T_{\text{mac}}, \alpha\} \in \{\{1.9, 3.28\}, \{2.5, 2.86\}, \{3.0, 2.65\}, \{3.6, 2.53\}, \{4.2, 2.44\}, \{4.8, 2.38\}, \{5.4, 2.34\}, \{6.0, 2.30\}, \{6.6, 2.27\}, \{7.2, 2.25\}, \{9.5, 2.20\}, \{11.9, 2.16\}\}$. 69
3.12 Average ratio of CRB of selected subsets normalized by the optimal CRB as given by algorithm global-crb. 72
3.13 Comparison of algorithms for *Sensor Selection Problem (SSP)*. In this simplified scenario consisting of $N_{\text{A}} = 14$ (▲) uniformly deployed anchors and one location-unaware sensor (●), response order is determined based on the algorithm used and location-aware sensors contribute their measurements without having to compete for wireless channel access. The single location-unaware sensor estimates its location using MLE which uses a *Centroid Localization (CL)* estimate as start point of optimization. 73
3.14 Comparison of algorithms local-crb and local-dist regarding *Mean-Square Error (MSE)* and energy consumption when anchors compete for the shared wireless channel. Results are shown for selection of 4 location-aware sensors and are depicted against pairs of parameters $\{K/T_{\text{mac}}, \alpha\} \in \{\{1.9, 3.28\}, \{2.5, 2.86\}, \{3.0, 2.65\}, \{3.6, 2.53\}, \{4.2, 2.44\}, \{4.8, 2.38\}, \{5.4, 2.34\}, \{6.0, 2.30\}, \{6.6, 2.27\}, \{7.2, 2.25\}, \{9.5, 2.20\}, \{11.9, 2.16\}\}$ whereby only the K/T_{mac} value is given on the axis. 75
3.15 Figure (a) depicts LogarEEL of local-crb and local-dist for subsets of 4 location-aware sensors. (b) Comparison of probability of successful receiving at least n responses vs. packet loss probability using either leadership-passing or scheduling as performed by algorithms local-crb or local-dist. Scheduling of local-crb / local-dist is more robust regarding packet loss and failure of sensors and achieves a higher response arrival rate. 77

4.1 The new approach presented in this chapter tracks back the changes of RSS caused by humans in the vicinity of radio links. The accuracy of the approach depends on the density of radio links: In 4.1b, the user can only be localized to somewhere within the grayed area on the left. In 4.1a, the user can be localized accurately due to its impact on two overlapping radio links. 80
4.2 Passive *Radio Frequency Identification (RFID)* enables inexpensive deployment of a dense field of radio links. (▭ denotes passive RFID tag, ▭▹ denotes a sensor). 81
4.3 Overview on *Device-Free Localization (DFL)* which uses measurements of RSS to obtain an estimate $\tilde{\boldsymbol{\theta}}$ of the user location without requiring the user to carry localization devices. The approach is based on a model relating user location and change of RSS $\Delta\mathbf{s}$. 82
4.4 Referring to radio tomographic imaging, the attenuation on radio links can be modeled as line integrals over a spatial loss field. This model can be used to estimate the user location by detecting occluded radio links. 87
4.5 Set-up of measurements. The test person moves stepwise in the indicated direction while the RFID reader measures the *Received Signal Strength Indicator (RSSI)* of the radio link to the passive tag. 92
4.6 RSSI over time as measured by the deployment of Fig. 4.5. The spikes indicate the times when the test person moved forward. 93
4.7 RSSI versus user location. The shaded area depicts the inner 90% quartile of measurements indicating their spread. (Initial measurements $t < 130\,\mathrm{s}$ and measurements during movements are omitted). 94
4.8 Humans contribute to the fluctuations on the RFID-link and lead to attenuation and amplification according to the phase difference of direct and reflected radio waves at the receiving antenna. 95
4.9 RSSI in dB vs. *Excess Path Length (EPL)* d_{exc}. The blue line denotes the average of measurements and the red line the results provided by fitting the model (4.5). The parameters of the fit are $A = 0.34$, $B = -0.68$, $\lambda = 0.39\,\mathrm{m}$ and $\phi_{\mathrm{refl}} = 2.18$. 97

4.10 Principle of *Centroid of Intersection Points (CIP)* localization. First, insignificant links, i.e. links unaffected by user, are discarded. Second, pairs of forward and reverse links are considered to calculate their *Intersection Point (IP)*. Only pairs of links are considered that do not belong to the same combination of transmitting and receiving antenna and RFID-tag. IPs are weighted using the minimum change of RSSI measured on the corresponding radio links. The estimated user location is the centroid of the weighted IPs. 101
4.11 Measurement set-up of multiple-tag scenario. 104
4.12 Location of tags and test person. Combinations of different subsets $T_i \quad i = 1,\ldots,4$ of tags are used in the evaluation. 104
4.13 Procedure of measurements. Blue triangles and circles denote linear and circular polarized antennas, green rectangles denote passive RFID tags. 105
4.14 Message flow of multi-tag scenario. 106
4.15 Histogram of measured RSS variations on radio links in a bistatic passive RFID system caused by human presence. The EPL d_{exc} is a measure of the distance between test person's location and radio links. 108
4.16 CDF of measured change of RSS. 109
4.17 The figures depict the probability that a significant change of RSS was caused by a user close to the *Line-of-Sight (LOS)* of the affected radio link against the threshold (black curves and right vertical axis). Blue curves corresponding to the left vertical axis depict the mutual information between measurements and EPL. 110
4.18 The figures show the relation and the approximation using (4.15) and (4.16) between EPL d_{exc}, median measurements $\Delta\tilde{s}$ and $\sigma_{\Delta s}$. The results apply for linear polarized antennas and are averaged over all orientations of the user. 112
4.19 Performance of algorithms when using different subsets of tags $(T_1,\ldots,T_4)$ with $|T_1| = 16$, $|T_2 \cup T_1| = 25$, $|T_3 \cup T_2 \cup T_1| = 49$ and $|T_4 \cup T_3 \cup T_2 \cup T_1| = 69$ tags as depicted in Fig. 4.12. MLE yields most accurate location estimates for all sets of tags. 115
4.20 Spatial distribution of MSE for MLE averaged over all orientations (tags in $T_3 \cup T_2 \cup T_1$ used). Each dot represents the true location of the test person. The color of the dots indicate the MSE δ [m^2]: ● ($\delta \leq 0.33$), ● ($0.33 < \delta \leq 0.66$) and ● ($0.66 < \delta \leq 0.96$) 115
4.21 Histogram of errors between measurements and prediction vs. theoretical Gaussian distribution. 117

4.22 Complexity of algorithms in terms of execution time on a Pentium Core 2 Duo CPU@3.3 GHz. 117
4.23 MSE tracking error of a)-c) *Particle Filter (PF)* and d)-f) *Extended Kalman Filter (EKF)*. The four antennas are situated at the corners at (0,0), (0,10), (10,10) and (10,0). Estimated locations are depicted by red crosses, true locations by solid blue dots. 121
4.24 Cumulative histogram of tracking error *Root-Mean-Square Error (RMSE)* $\sqrt{\delta}$ vs. number of tags. Red line with stars denotes PF and blue lines with circles denote EKF. 122

List of Tables

1.1 General mathematical notation. 13

3.1 Simulation parameters. 48
3.2 Overview on related work and comparison with the new approach indicated by a *. 60
3.3 Overview on algorithms. 66
3.4 Parameter values of energy model. Values of energy consumption are based on the work of Polastre et al. in [65] and Shnayder et al. in [75]. 70
3.5 Summary of computer simulation. 71

4.1 Overview of related work. 91
4.2 Calculation of IPs and corresponding weights. 102
4.3 2D-locations (x,y) of antennas used as sender-receiver pairs. 105
4.4 Parameters of fitting the measurements. 113
4.5 Parameters for computer simulations of target tracking. 120

A.1 Algorithms of class local-knowledge in pseudo-code. Code is executed at location-aware sensor s_i. 126

List of Acronyms

AOA Angle-of-Arrival
AutoID Automated IDentification technology
BEB Binary Exponential Backoff
CIP Centroid of Intersection Points
CL Centroid Localization
COTS Commercial Off-The-Shelf
CRB Cramér-Rao-Bound
CSMA/CD Carrier Sense Multiple Access with Collision Detection
DFL Device-Free Localization
EE Energy Efficiency
EKF Extended Kalman Filter
EPL Excess Path Length
GDOP Geometric Dilution of Precision
GPS Global Positioning System
IP Intersection Point
IQR Interquartile Range
IR Infrared Radiation
ISM Industrial, Scientific, and Medical frequency band
LLS Linear Least Squares
LMLE Local Maximum Likelihood Estimator
LPS Local Positioning Systems
LogarEEL Logarithmic Energy Efficiency of Localization
LOS Line-of-Sight
LRP Location Related Parameter
MDS Multidimensional Scaling
MEMS Micro-Electro-Mechanical Systems
MLE Maximum Likelihood Estimator

MSE Mean-Square Error
NLOS Non-Line-of-Sight
PDF Probability Density Function
PF Particle Filter
PLE Path-Loss Exponent
RBE Recursive Bayesian Estimation
ReBEL Recursive Bayesian Estimation Library
RF Radio Frequency
RFID Radio Frequency Identification
RMSE Root-Mean-Square Error
RSS Received Signal Strength
RSSI Received Signal Strength Indicator
SIR Sampling-Importance-Resampling
SSP Sensor Selection Problem
TOA Time-of-Arrival
TDOA Time-Difference-of-Arrival
WSN Wireless Sensor Network

Chapter 1

Introduction

During the past decades, wireless and wired networks have been growing in size and complexity. The global Internet consists of billions of computers, standards for wireless ad-hoc networks have been proposed in order to facilitate large networking of many hundreds or thousands of wireless sensor nodes and the recent development indicates further growth to even larger networks as the devices become smaller and cheaper. This development renders manual configuration and monitoring of such networks very challenging. For example, due to the size of the Internet there exists no single computer which is able to monitor or even configure it as a whole. In addition, application requirements, as in mobile computing applications, demand for ad-hoc networking of devices to provide the user with useful services or to improve, in the case of *Wireless Sensor Networks (WSNs)*, the robustness in harsh environments. Under these circumstances, human administration and configuration of each node is infeasible. Consequently, there exist a high need for automated administration, monitoring and self-configuration in such networks. Smart environments rely on networked communication systems to gather context-information from sensors, make decisions and to eventually assist the user by issuing commands to actuators.

The thesis considers determination of *location* of *sensors* and *users* in *smart environments* as part of this problem. The terms 'sensor', 'location', 'user' and 'smart environment' need to be further explained to understand the wide scope of the problem considered.

First, 'sensor' denotes a device that is capable of communication or of being interrogated by the smart system. Knowledge about a parameter can be obtained by communicating with a sensor. For example, air temperature or quality of radio links can be determined by querying a 'sensor'. As such, 'sensor' is a generic class of objects which includes, among others, wireless sensor motes, laptops and *Radio Frequency Identification (RFID)* transponders. Since the sensing functionality is fundamental to the investigations in the thesis, the word 'sensor' refers to the entire device. A *sensor network* is an arrangement of many sensors that measure any local quantity of interest.

Secondly, 'location' refers to the physical location of a 'sensor' or a 'user', or in other words the space where it is. The 'location' is regarded as pointwise coordinates in the thesis. The thesis focuses on the estimation of the 'location' of users and sensors because of its fundamental importance. In smart environments, knowledge of the distance of users to devices, like a display, is an important context information for the system to support the user. Likewise, the location of mobile devices is interesting to the system as these devices might contribute new ways of support or the user is merely looking for them and needs to be reminded of their 'location'.

Thirdly, the 'user' is a person which the *smart system* provides assistance to. The paradigm of 'ubiquitous computing' describes the depart from the conventional desktop computing and is the guiding theme for smart systems. Rather than using dedicated machines, human-computer interaction in 'smart systems' is said to become transparent to the 'user' since information-processing has been thoroughly integrated into activities and objects of daily living. Due to their numerous potential fields of application, there exist some other terms which refer to the same type of system. Some of the more frequently used terms in this regard are also used in the thesis synonymously, namely smart / intelligent system / environment. Finally, smart environments, which represent the sum of electronic devices and infrastructure they establish and provide, is able to detect 'users' by their interaction with the system and/or by means of sensors.

The location of sensors and users is intuitively important in smart environments. First, measurements of sensors need to be associated with the place where they were measured. For example, the location of a high temperature reading is almost useless without knowing the place of measurement which is needed to infer the location of the

heat source. Furthermore, the user location plays an important role in location-based service provision and whenever the system decides on the most useful reaction to a user interaction. In addition, a reference system of location-aware sensors is needed to be able to determine the relative user location and represent it as coordinates.

To estimate local coordinates of sensors or users, measurements of propagation properties of radio waves between two sensors are used. Among the various types of measurements, like *Time-of-Arrival (TOA)* or *Angle-of-Arrival (AOA)*, the thesis focuses on the *Received Signal Strength (RSS)* of radio communications since it is available on most wireless communications devices with virtually no additional cost. In smart environments, sensors can be battery powered or have a fixed power supply as allowed by the circumstances. Battery-powered sensors have the advantage of being mobile and they require no cabling which is typically an important factor in terms of installation cost. The flexibility of battery powered, mobile sensors allows for ad-hoc extension of the system and for the adaptation of the physical location of sensors to changing application requirements. For example, in case the attendance for a meeting requires movement to a larger room, battery powered sensors can be easily carried to another location with few effort. Another example are networks of sensors monitoring environmental conditions which have to operate in areas where fixed power supplies are not available. However, the downside of battery powered sensors is that every operation has to consider energy preservation in order to prolong the lifetime of sensors.

In light of these considerations, *energy-efficient* operation of sensors is critical to the overall performance of smart systems. The term *efficiency* is used in a wide range of sciences and describes the often encountered tradeoff between the usefulness of an operation and its cost in terms of some relevant quantity. For example, it is known that using multiple RSS measurements instead of only one can increase the accuracy of the estimates. However, retrieval of more measurements consumes more energy while the expected increase of accuracy typically does not scale due to correlations between measurements.

In summary, the thesis considers the problem of estimating the location of users and sensors in terms of energy-efficiency in smart systems. Due to their similarity in this regard, users and sensors are jointly referred to as targets. The process of estimating

the location is denoted as *localization* and regarded as an optimization problem subject to the tradeoff between energy consumption and accuracy of location estimates.

To introduce the particular issues motivating the thesis, in the next sections, WSNs are introduced in Sec. 1.1 and the usefulness of RFID to user localization is outlined in Sec. 1.2. The contributions presented in this thesis are listed in Sec. 1.4, and 1.6 presents the outline and the table of notations used in the thesis.

1.1 Wireless Sensor Networks

The past decade has seen dramatic advances in *Micro-Electro-Mechanical Systems (MEMS)* and *Radio Frequency (RF)* which enabled application of large networks of miniaturized sensors for monitoring and controlling tasks.

For example, the condition of buildings can be monitored by a network of wireless sensors which are embedded in the structure itself [52]. Thereby, reaction to earthquakes and reporting of cracks and structural problems will be possible. The productivity of agriculture can be improved by accurately detecting local nutrition levels and condition of the soil through wireless sensors and directing fertilizer and water in appropriate dosage [1, 44]. Urban-scale sensor networks will enable improved controlling of stoplights and help to avoid jams by proposing alternate routes to motorists and cyclists [21]. Various other applications have seen testbed implementations in the last years [24, 35, 53, 77] which are reviewed, for example, in [5, 9, 11, 70].

Automatic estimation of the local coordinates of sensors is fundamental in these WSNs. For example, the sensors' location is needed by many algorithms like scalable geographic routing and clustering. Even more importantly, measurements of sensors are typically only meaningful if the location of a measurement is known. As these networks require a high degree of self-organization and -configuration, the network has to react locally to the sensed data which is only possible with location-awareness. On the other hand, the need for location-awareness of radio tagged objects, for example assets and equipment in manufacturing logistics or warehousing, can be the driving force for WSNs.

In order to make these applications feasible regarding networks with potentially a large number of nodes, the cost for sensors need to be very low, the lifetime of unattended operations of a sensor will need to be several years or even decades depending on the application and the network must be able to continuously reconfigure itself to adapt to changes. Traditionally, the *Global Positioning System (GPS)* has been used to estimate the location. However, for WSNs, integrating GPS modules on every sensor reduces lifetime and increase device cost. Furthermore, GPS does not work in indoor environments reliably and also trees and buildings can obstruct the *Line-of-Sight (LOS)* to satellites and, thereby, cause reduced accuracy or unavailability of service. Other *Local Positioning Systems (LPS)* rely on base stations with specialized hardware to be deployed in the coverage area. The high cost and often inflexible, stationary deployment of such systems limit their utility for WSNs.

Due to these reasons, the thesis considers WSNs in which a small number of sensors knows their location by means of GPS or by preconfiguration and the majority of sensors is location-unaware and seeks to estimate their locations. Location-aware sensors are called *anchors* since they represent location fixes for other location-unaware sensors which are referred to as *blinds*. The communication range of sensors is limited either due to RF regulations or energy-constraints concerning transmission power, or simply because sophisticated power amplifiers are unavailable in low-cost, low-power hardware. Consequently, it is likely that a number of blinds will not have enough anchors in range to estimate their location. To provide location information also for these sensors, iterative localization methods have been proposed [51]. In iterative localization, the localization procedure is repeated several times whereby in each iteration potentially all sensors with known (anchors) and with estimated locations (former blinds) can be used as location fixes (see Fig. 1.1). Thereby location information spreads throughout the network eventually enabling all blinds to estimate their location.

However, there are two major issues with iterative localization. Firstly, the errors associated with estimated locations propagate since they are used by other blinds as location fixes. Therefore, iterative localization relies on a sophisticated selection mechanism which picks sensors with small location error to limit error propagation. Secondly, querying all sensors with known or estimated locations leads to congestion

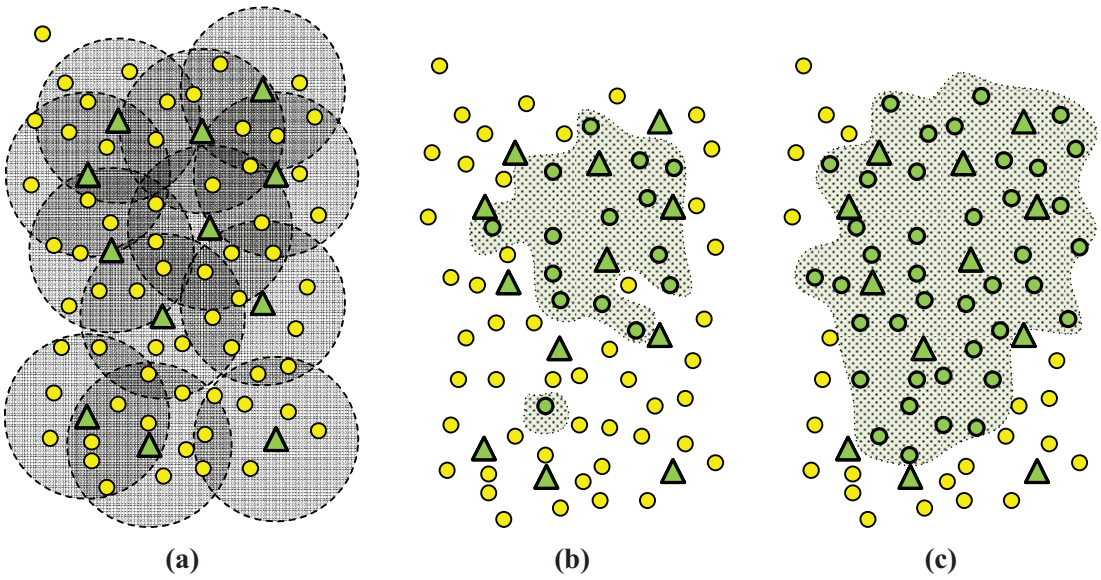

Figure 1.1: Iterative localization helps to localize all location-unaware sensors. (△, ○, ●) denote anchors, blinds and blinds with estimated location, respectively. The shaded area (▒) denotes the region of location-aware sensors. 1.1a - Initial situation. 1.1b - Localization using anchors. 1.1c - First iteration: Anchors and blinds with estimated locations provide location fixes.

and increased energy consumption as a potentially large number of sensors communicates. Consequently, from the perspective of energy-efficiency, it is most important to limit the number of sensors serving as location fixes for location-unaware nodes using a selection method. Recent research considers mobile sensors increasingly frequently [33, 34]. Consequently, the need for such a selection method becomes even more apparent: It is known that indirect methods like odometry or using measurements from accelerometers result in increasingly inaccurate location estimates of mobile targets. Therefore, the mobile sensors in such networks have to track their location as they move using the location fixes of adjacent sensors. In this situation recurring localization is inevitable and, hence, selecting a subset of sensors as location fixes is mandatory.

In summary, the locations of sensors are vital information for the operation of WSNs. Using an initial, small set of location-aware sensors, a selection mechanism to prevent congestion and reduce energy consumption is necessary to provide location

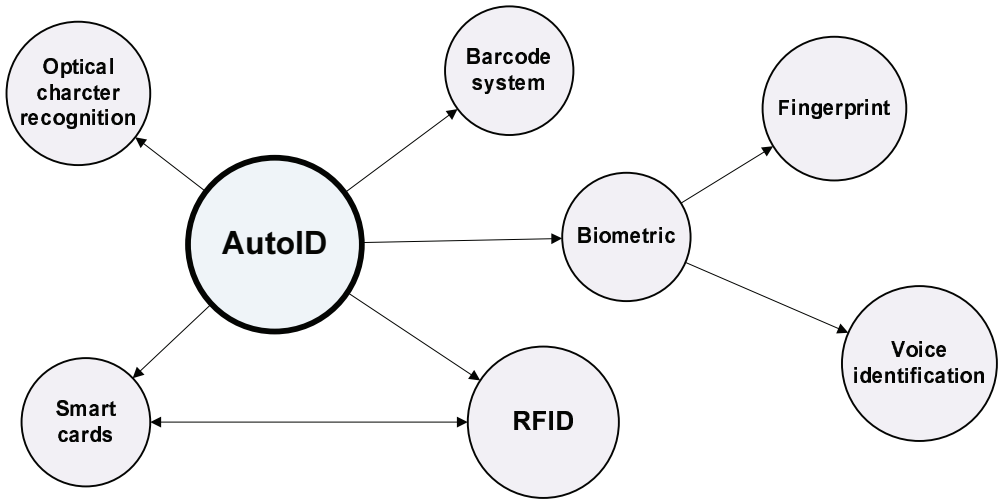

Figure 1.2: Overview on AutoID technologies [27].

information to all sensors. Subsets need to be selected such that their measurements lead to estimated locations with highest accuracy.

1.2 Radio Frequency Identification

Sensors play an important role in manufacturing since they provide fundamental information about the production processes. Controlling and monitoring of conditions of machinery have been carried out using wired communication systems. The potential reduction of installation cost, the widespread application spectrum and the flexibility of low-cost, wireless sensors have been the driving force of the recent boost of automated identification technologies [16, 72]. Figure 1.2 provides an overview about recent approaches. Small, thin-as-paper passive RFID labels, so called *tags*, are discussed in this regard. Passive RFID systems consist of at least one reader device and several passive tags as illustrated in Fig. 1.3. The reader interrogates the tags in range which respond by sending their unique identity number. In contrast to conventional transceiver technology, passive RFID tags are powered by impinging radio energy and do not rely on batteries for their operations. This makes them especially suited for long-term, unattended operations as they incur comparably small installation and maintenance cost.

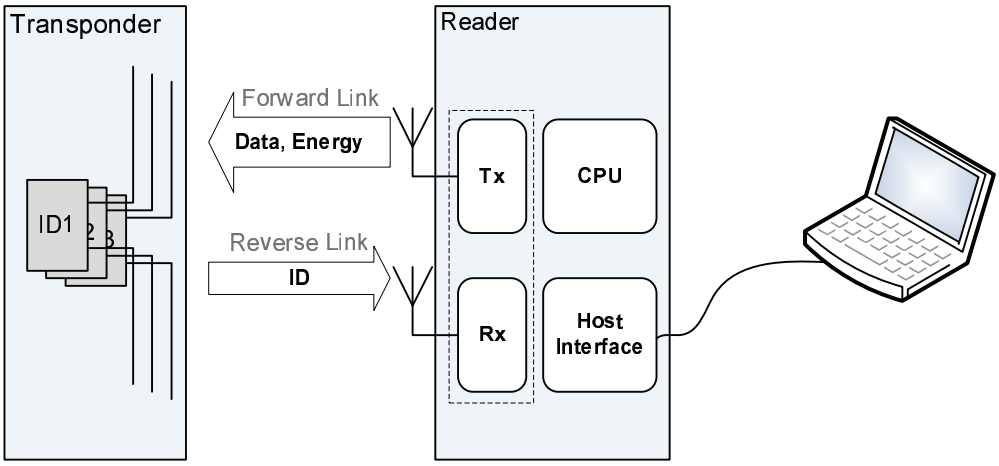

Figure 1.3: Architecture of bistatic, passive RFID system. Tags are powered and interrogated by the reader over the forward link and respond over the reverse link. Bistatic systems use for either link a separate antenna which mitigates decoupling forward and reverse link signals in the receiver circuits of the reader.

RFID is attractive for optimizing product cycles by providing identity and location of goods to the manufacturing management system [78]. Due to their very low cost of several 10s of cent and their small size, they are also very interesting to "bridge the gap" between the physical and virtual world by providing automated identification and, thus, enable many other applications. For example, in assisted living, RFID will help to remind the elderly of the location of their keys or to track their activities in order to detect harmful situations [85]. This application domain will become increasingly important due to the recent demographic development. Therefore, future systems for this kind of applications will need to consider the requirements specific to the care for elderly people [48]. In this regard, the small size and, consequently, the ability to unobtrusively attach passive RFID tags to almost all surfaces and objects in living environments is beneficial compared to conventional LPS which require wearing or attachment of larger battery-powered tags.

In light of these considerations, an LPS which does not require dedicated user cooperation in terms of, wearing tags or cloth with integrated tags, will offer distinguishing advantages over conventional LPS. In particular, applications of *Device-Free Localization (DFL)* to locate victims on disaster sites or to track hostages or snipers in

housings are discussed [84]. Generally, this approach is often referred to as transceiver-free localization or radio tomographic imaging. It exploits the property of humans and mobile objects to attenuate and scatter radio waves. The resultant change of radio propagation properties of a radio link can be measured, analyzed and used to estimate the location of its cause. The number of radio links in the coverage area determines the accuracy of all DFL techniques. Consequently, very low-cost devices are needed to provide a sufficient number of radio links without incuring large additional cost. In this regard, passive RFID will be a valuable alternative to wireless sensor motes due to its small size and very low-cost tags. Furthermore, a detailed yet practical model of how the human body influences radio communications is needed in order to apply DFL to tracking techniques like Kalman or Particle Filters.

In summary, there is need for DFL and tracking as in many situations a cooperation of user to be localized can not be anticipated. Applications like assisted living, localization of victims by first responders and crime reduction can be the driving force to foster such localization techniques. Especially, applications which require high accuracy estimated locations in indoor environments can benefit from passive RFID as a large number of radio links can be realized very cost efficiently without placing to many attention attracting sensors. Accurate DFL and tracking requires a detailed yet practical model of the human impact on radio communications.

1.3 Problem Statement

Before going into the details, it is useful to formally state the considered problem. The thesis considers localization as the process of determining the location of a sensor or a user by means of propagation properties of radio waves. The objective is to calculate an estimate of the location using measurements of RSS which are obtained with sensors. Two types of measurements can be distinguished. First, measurements of RSS which are used to relate two sensors' location are called *direct measurements*. Direct measurements can be used to estimate the location of sensors or users carrying sensors. In contrast, measurements aiming at detecting changes of RSS possibly caused by a user

moving in the vicinity of radio links are referred to as *indirect measurements*. Both, sensor and user location are given in two dimensions (2D). The goal of localization is to find and apply a mapping $\mathcal{L}$ of measurements of RSS $\mathbf{x} \in \mathbb{R}^{N_{\text{meas}}}$ to location $\boldsymbol{\theta} \in \mathbb{R}^2$ for each target.

$$\mathcal{L} : \mathbf{x} \rightarrow \boldsymbol{\theta} \tag{1.1}$$

Different estimators are used for this mapping and reviewed in Chapter 2.

Direct Measurements Localization using direct measurements is a mature field of research and almost all currently available systems utilize direct measurements. New challenges concerning energy-efficiency arise with the continuously growing interest in WSNs and the steadily increasing need for location-based services. The thesis addresses the problem of minimizing the energy consumption during localization of sensors subject to a given minimum accuracy of estimated locations. As will be explained further in the corresponding sections, this problem is related to the *sensor selection problem* (SSP). Since energy-efficiency denotes a specific ratio between the energy spent during localization and its utility to the system, i.e. the accuracy of estimated locations, a measure to numerically characterize this ratio is needed.

Indirect Measurements Device-Free Localization of users exploiting their impact on propagation properties of radio waves currently attracts increasing research interest. Consequently, the challenges are different from those of localization using direct measurements and are more basic. Specifically, many estimators used for localization require analytical observation models of how the user location affects the measurements. Therefore, estimators and especially model-driven recursive Bayesian Filters, like the Kalman or Particle Filters, can benefit from such a model. Furthermore, since accuracy of DFL is expected to increase with the density of radio links, a communication technology is needed which facilitates deployments with dense radio links to improve accuracy while incurring only small cost. The thesis investigates the use of passive RFID and develops and applies the corresponding observation model to DFL.

1.4 Contribution

The work presented in this thesis is based on several publications. In the following we list these publications, group them by subject and indicate the corresponding chapter in the thesis.

Device-free localization with passive RFID Chapter 4 presents a new approach to localization using passive RFID. The new approach distinguishes itself from previous ones as the target does not need to be equipped with a sensor. Detailed theoretical analysis of the impact of humans on passive RFID communications are conducted and the results from real-world measurements are presented.

Lieckfeldt, D.; You, J.; Timmermann, D.: Passive Tracking of Transceiver-Free Users with RFID, International Conference on Intelligent Interactive Assistance and Mobile Multimedia Computing (IMC), 2009

Lieckfeldt, D.; You, J.; Timmermann, D.: Characterizing the Influence of Human Presence on bistatic passive RFID-System, 5th IEEE International Conference on Wireless and Mobile Computing, Networking and Communications (WiMob), Marrakesh, Morocco, 2009.

Lieckfeldt, D.; You, J.; Timmermann, D.: Exploiting RF-Scatter: Human Localization with bistatic passive UHF RFID-Systems, 5th IEEE International Conference on Wireless and Mobile Computing, Networking and Communications (WiMob), Marrakesh, Morocco, 2009.

Sensor selection for energy-efficient localization Section 3.3 considers an algorithm to increase the energy-efficiency of localization in WSN. The idea is to involve only those location-aware sensors in the localization process which lower significantly the uncertainty about the target location. The distinguishing feature of the approach is that the selection is carried out locally without additional communications.

Lieckfeldt, D.; You, J.; Timmermann, D.: Distributed Selection of References for Localization in Wireless Sensor Networks, 5th Workshop on Positioning, Navigation and Communication (WPNC), Leipzig, Germany, 2008.

Lieckfeldt, D.; You, J.; Timmermann, D.: An Algorithm for Distributed Beacon Selection, 4th IEEE International Workshop on Sensor Networks and Systems for Pervasive Computing (PerSeNS), Hong Kong, China, 2008.

Lieckfeldt, D.; Timmermann, D.: Using Cramer-Rao-Lower-Bound to Reduce Complexity of Localization in Wireless Sensor Networks, Baltic Conference Advanced Topics in Telecommunication (BaSoTi), Riga, Latvia, 2007.

Development of a new energy-efficiency measure Section 3.2 presents a generic framework to numerically characterize the energy-efficiency of localization algorithms. The framework which facilitates the identification of the most efficient localization approach is applied to localization in WSN.

Lieckfeldt, D.; You, J.; Behnke, R.; Salzmann, J.; Timmermann, D.: Assessing the Energy Efficiency of Localization, 6th IEEE Wireless Sensor Networks Consumer Communications and Networking Conference (CCNC), Las Vegas, USA, 2009. (Short paper)

Lieckfeldt, D.; You, J.; Salzmann, J.; Behnke, R.; Timmermann, D.: Characterizing the Energy Efficiency of Localization Algorithms in Wireless Sensor Networks, 5th International Wireless Communications and Mobile Computing Conference (IWCMC), Hannover, Germany, 2009.

1.5 Notation

Before going into the details, the general notation when dealing with math is introduced in table 1.1. The thesis considers wireless networks consisting of $N_\mathrm{S} = N_\mathrm{A} + N_\mathrm{B}$ sensors. There are N_A location-aware sensors which are referred to as *anchors* and N_B sensors whose location is unknown which are called *blind*. Furthermore, former blinds can become *reference* if they have been able to determine their location. The following sets of sensors are defined:

$$\mathcal{S} := \{s_1, \ldots, s_{N_\mathrm{S}}\} \quad \text{Set of all sensors} \tag{1.2a}$$

$$\mathcal{B} := \{s_1, \ldots, s_{N_\mathrm{B}}\} \quad \text{Set of blinds } \mathcal{B} \subset \mathcal{S} \tag{1.2b}$$

$$\mathcal{A} := \{s_{N_\mathrm{B}} + 1, \ldots, s_{N_\mathrm{S}}\} \quad \text{Set of anchors } \mathcal{A} \subset \mathcal{S} \tag{1.2c}$$

$$\mathcal{R} := \{s_i : i < N_\mathrm{A}, \boldsymbol{\theta}_i \in \mathbb{R}^2\} \quad \text{Set of references } \mathcal{R} \subseteq \mathcal{B} \tag{1.2d}$$

To facilitate mathematical formulations, the locations $\boldsymbol{\theta}_i = [x, y]^\mathrm{T}$ of sensors are com-

Table 1.1: General mathematical notation.

Notation	Meaning
$\mathbf{a} = [a_1, a_2, \ldots]^{\mathrm{T}}$	Vector
$\mathbf{A}$	Matrix
$\mathcal{S}$	Set
$\|\cdot\|$	2-norm of vector
$[\cdot]^{\mathrm{T}}$	Transpose of matrix/vector
$\|\mathcal{S}\|$	Cardinality of $\mathcal{S}$
$\{\mathbf{A}\}_{i,j}$	Elements i, j of matrix
$E(\mathbf{a}) = [E(a_1), E(a_2), \ldots]^{\mathrm{T}}$	Expected value
$var(\mathbf{a})$	Variance
$\mathcal{S}^{(c)}$	Subset of $setS$ with cardinality c
$\exp\{x\} = e^x$	Exponential function

bined in a matrix.

$$\boldsymbol{\Theta} = [\boldsymbol{\theta}_1, \ldots, \boldsymbol{\theta}_{N_{\mathrm{S}}}]^{\mathrm{T}} \quad \text{Location} \tag{1.3}$$

Where the last N_{A} rows of (1.3) correspond to the location-aware sensors.

The distance $d_{i,j}$ between sensors i at location (x_i, y_i) and j at (x_j, y_j) is given by the Euclidean Distance.

$$d_{i,j} = ||\boldsymbol{\theta}_i - \boldsymbol{\theta}_j|| \quad \text{Distance} \tag{1.4}$$

$$\{\mathbf{D}\}_{i,j} = d_{i,j} \quad \text{Distance-Matrix} \tag{1.5}$$

By convention, $d_{i,j} = 0 \Leftrightarrow i = j$ holds.

1.6 Outline of Thesis

Chapter 2 gives an overview on wireless localization, categorizes different algorithms and reviews estimation techniques which will be used in the thesis.

Chapter 3 considers localization of sensors within WSN and especially focuses on improving the energy efficiency of localization. First, in Sec. 3.2 a measure to numeri-

cally characterize energy efficiency is presented and Sec. 3.3 successfully develops and applies new algorithms for *Sensor Selection Problem (SSP)* in order to improve location error and energy consumption during localization.

Chapter 4 investigates new techniques to backtrack the impact of user on the RSS of radio links. In particular, a bistatic, passive RFID system is used in a real-world testbed in order to validate and evaluate novel models and localization algorithms for DFL.

Finally, chapter 5 concludes and outlines future research directions. As indicated in the thesis, appendices A and B present long lists, definitions and proofs.

Chapter 2

Survey of Wireless Localization Techniques

Before going into the details, this section provides a broad overview about wireless localization using direct measurements. Wireless localization exploits the dependence of propagation properties of radio waves on the relative locations of transmitter and receiver. Typically, *delay*, *phase*, or *signal strength* of the radio waves are measured using one or more antennas. The measurements are then analyzed and often used to estimate LRPs which are distances and angles between sensors. The unavoidable measurement errors propagate to the LRPs and make inferring the location a non-trivial task. To facilitate the review, a deployment of N_A sensors with a-priori known locations $\boldsymbol{\theta}_i$ ($i = 2, \ldots, N_\mathrm{A}+1$) and one location-unaware sensor is considered in the following. The location $\boldsymbol{\theta}_1$ of the location-unaware sensor is to be estimated using measurements of specific RF properties and the index of the single location-unaware sensor is omitted, thus, e.g. $d_{1,i} = d_i$.

Measurements of Delay and Phase Radio waves travel at a finite velocity v. Consequently, given a TOA, i.e. the time it takes a radio wave to travel from transmitter to receiver, the distance separating them can be calculated. In practical systems, the TOA is the time the signal first arrives at the receiver which is the sum of the transmitting time and the propagation delay. At the heart of delay-based localization is the ability

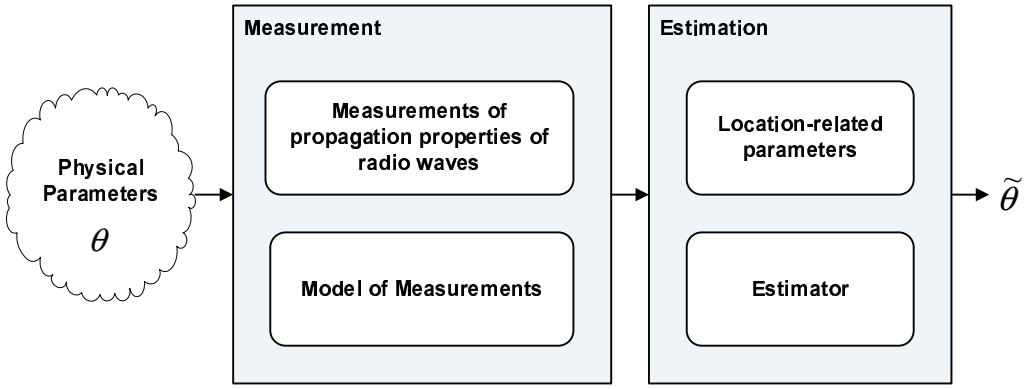

Figure 2.1: Outline of localization processes. Knowledge about the location of objects is acquired by i) measuring a quantity that depends on location, ii) establishing a model to characterize the dependence iii) feeding model and measured data or derived LRP into an estimator which calculates an estimated location.

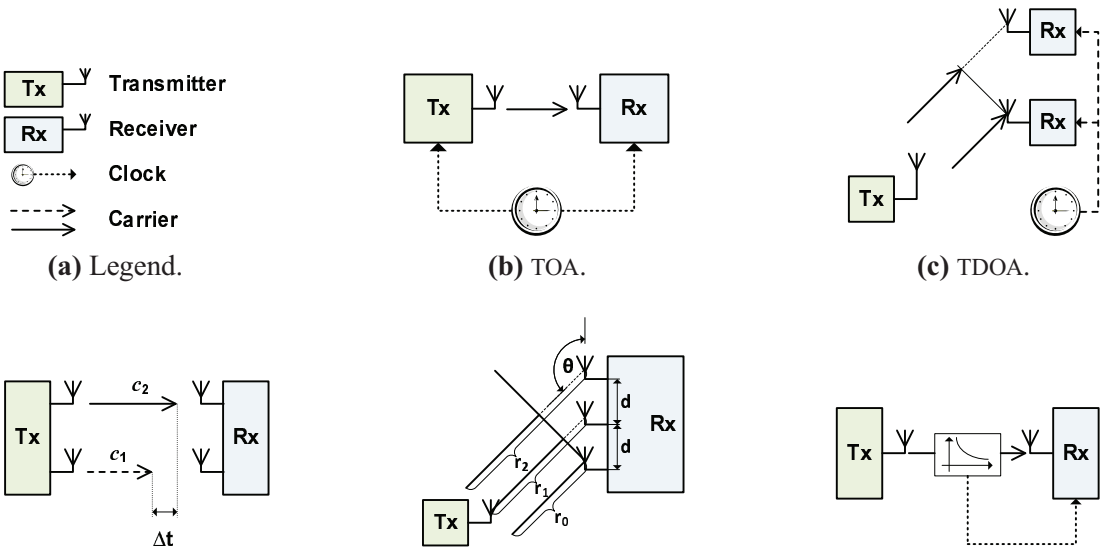

(a) Legend. **(b)** TOA. **(c)** TDOA.

(d) TDOA with different signal types. **(e)** AOA. **(f)** RSS

Figure 2.2: Overview on measurement techniques.

of the receiver to accurately estimate the arrival time of the LOS component of a radio signal. Typically, TOAs are estimated as the delay for which the cross-correlation of the received and the known transmitted signals has a maximum [42]. Consequently, delay-based measurements have two major sources of error. Noise and multipath propagation lead to errors of TOA. Especially in environments with many obstacles, reflections can lead to superposition of multiple time-delayed copies of the transmitted signal at the receiver. Determining the TOA of the LOS component becomes more difficult in such situations.

This approach has often been applied in wireless localization systems and is also part of GPS. Each TOA measurement Δt_i corresponds to a distance and, consequently, defines a circle around the i-th location-aware transmitter on which the receiver resides. The sought location of the receiver can be found by combining multiple TOA measurements and looking for the intersection of the associated circles. Formally stated, the sought location $\boldsymbol{\theta}_1$ is, in the absence of errors, the solution to the following system of equations.

$$v\Delta t_2 = \|\boldsymbol{\theta}_2 - \boldsymbol{\theta}_1\| \tag{2.1a}$$

$$\vdots$$

$$v\Delta t_{N_\mathrm{S}} = \|\boldsymbol{\theta}_{N_\mathrm{S}} - \boldsymbol{\theta}_1\| \tag{2.1b}$$

However, a drawback of this approach is that the time of transmission t_0 needs to be known at the receiver to calculate the TOA. Since this is especially in ad-hoc wireless networks a restricting assumption, alternative approaches have been developed.

In *Time-Difference-of-Arrival (TDOA)*, the difference between multiple TOAs is considered. In this approach, the sensor to be localized would transmit a signal which is received at multiple receiver with common time base. A system of equations similar to that of TOA measurements is obtained by subtracting, e.g. the first equation of (2.1) from all others. Due to this step an additional location-aware sensor is needed in order

to obtain the same number of equations.

$$v(\Delta t_3 - \Delta t_2) = (\|\boldsymbol{\theta}_3 - \boldsymbol{\theta}_1\| - \|\boldsymbol{\theta}_2 - \boldsymbol{\theta}_1\|) \tag{2.2a}$$

$$\vdots$$

$$v(\Delta t_{N_S} - \Delta t_2) = (\|\boldsymbol{\theta}_{N_S} - \boldsymbol{\theta}_1\| - \|\boldsymbol{\theta}_2 - \boldsymbol{\theta}_1\|) \tag{2.2b}$$

In contrast to TOA, each equation of (2.2) presents a range difference and, consequently, the solution space is a hyperbola with focii at the corresponding location-aware sensors. Again, the sought location can be calculated by solving the system of equations. One major advantage of TDOA is that the possibly mobile location-unaware sensor does not need to in sync with the system. Nevertheless, a set of synchronized location-aware sensors is needed which makes this approach attractive for localization systems with fixed installation.

Another approach which neither relies on synchronization nor requires calculation of the difference of TOAs is called the *Cricket location system* and was proposed by Priyantha et al. [66]. The Cricket system uses two signal types, acoustic and RF, which travel at different propagation speeds. The two signals are simultaneously emitted by location-aware sensors. The signals reach the receiver at different times whereby the time between arrivals is proportional to the traveled distance. Assuming that the i-th location-aware sensor transmits two signals with propagation speeds of v_1 and v_2 arriving at $t_i^{'}$ and $t_i^{''}$, a system of equations similar to the TOA case can be formulated.

$$\frac{v_1 v_2}{v_2 - v_1}(t_2^{'} - t_2^{''}) = \|\boldsymbol{\theta}_2 - \boldsymbol{\theta}_1\| \tag{2.3a}$$

$$\vdots$$

$$\frac{v_1 v_2}{v_2 - v_1}(t_{N_S}^{'} - t_{N_S}^{''}) = \|\boldsymbol{\theta}_{N_S} - \boldsymbol{\theta}_1\| \tag{2.3b}$$

Again each equation describes a circle and the solution is the intersection of all circles.

The previously surveyed approaches aimed at inferring the distance between two sensors and combined several of these distances to calculate the location of a location-unaware sensor. Similarly, knowing the directions to several location-aware sensors

can be used for localization. For this purpose, sensors typically use antenna arrays which consist of several closely packed antenna elements ($d \leq \lambda/2$ in figure 2.2e). The received signal at each antenna element has, due to the physical displacement, a slightly different phase which can be used to calculate the AOA α. A system of linear equations can be formulated assuming the receiver's orientation to a global reference system is known.

$$y = k_2 x + b_2 \tag{2.4a}$$

$$\vdots$$

$$y = k_{N_S} x + b_{N_S} \tag{2.4b}$$

Whereby $k_i = \tan\alpha_i$ and $b_i = \frac{y_i}{x_i k_i}$ $i \in \mathcal{A}$.

The RSS is readily available in RF communication systems. Since RSS decreases with the distance between transmitter and receiver, it can be used for localization. Since the thesis focuses on RSS measurements, corresponding models of errors are reviewed in section 2.1.

2.1 Measurements of RSS

Models for RF propagation are key requirements to develop reliable and accurate localization systems. Therefore, associated research fields have attracted significant attention in the community since the beginning of wireless communications. In particular, the objects of the environment present obstructions and reflectors which cause multipath propagation and attenuation of RF signals. The thesis considers estimating distances between sensors from measured RSS as basis for wireless localization.

The RSS of a radio signal denotes its power and is typically measured with virtually no additional cost by the receiver circuit. The *Received Signal Strength Indicator (RSSI)* is an output voltage of the RSSI circuit of a receiver which represents the RSS of the incoming RF signal. Due to its availability with wireless communications and its inexpensiveness, the use of RSSI for localization has attracted considerable research ef-

fort [10, 28, 57, 64, 73]. However, due to the numerous factors that impact RSSI, a feasible model of these errors and their propagation to estimated distances is reviewed in the following.

Measurements of RSS are influenced by numerous factors and are therefore subject to errors which propagate to estimated distances. The errors of estimated distances can be categorized as being either *time-varying* or *static*. Whereas the time-varying errors are caused by noise and interference, static errors are introduced by the environment. For example, objects can obstruct the LOS of a radio link and thereby cause additional attenuation. In literature, these static environment-dependent errors are often modeled as random, mirroring the fact that the environment in which a wireless network operates is unpredictable [60]. In contrast to static errors, time-varying errors can be reduced by performing time-series analysis, e.g. by averaging measurements. For this reason, the thesis focuses on models for static, environment-dependent errors.

Environment-dependent errors comprise the effect of objects in the vicinity of radio links to reflect, attenuate or diffract the signals which leads to multipath propagation and *shadowing* of radio waves. In multipath propagation, multiple delayed and attenuated versions of the transmitted signal reach the receiver over different paths. These signals add constructively or destructively as a function of frequency. Therefore, this type of error source is referred to as *frequency-selective fading* and can be mitigated with spread-spectrum techniques. For example, with direct-sequence spread spectrum techniques the signals are distributed over a large bandwidth so that negative impact of frequency-selective fading is reduced.

Summarizing, the time-varying errors can be dealt with by applying time-series analysis and the environment-dependent frequency-selective fading effects can be reduced by using spread-spectrum techniques. However, shadowing refers to the situation when objects obstruct radio links and, thus, present static errors. Also these objects typically affect not only a narrow frequency band and can not be mitigated by spread-spectrum techniques. Consequently, researchers have investigated this error source which is also referred to as *medium-scale fading*. The computer simulations carried out in the thesis base on medium-scale fading which is typically characterized as lognormal distributed random variable [31]. The details of the model are reviewed in the following.

Modeling Errors of RSS In practical scenarios which comprise obstructions and reflections of radio waves, the RSS is a random variable and specific to each environment. The ensemble mean RSS, which is the average over multiple environments, decays proportional to the distance from the transmitter as $d^{-\varepsilon}$, where ε is the *Path-Loss Exponent (PLE)*. Typically, the ensemble mean RSS $\bar{P}$ is modeled by the *log-distance path loss model* [67].

$$\bar{P}(d) = P_0 - 10\varepsilon \log_{10} \frac{d}{d_0} \tag{2.5}$$

In this model, P_0 denotes an RSS measured in [dBm] at a short reference distance d_0. As stated before, $\bar{P}$ is subject to fluctuations mirroring the random impact of the environment. Since a particular environment can consist of a vast number of objects, the typical first approach for modeling medium-scale fading is to assume an additive white Gaussian noise model.

$$P = \bar{P}(d) + X_\sigma \tag{2.6a}$$

$$X_\sigma \sim N(0, \sigma^2) \tag{2.6b}$$

There exist significant evidence for the validity of this model for many environments ranging from industrial installation to indoor scenarios [31]. Equation (2.6) assumes that measurements of RSS on spatially adjacent radio links are not correlated. However, it is possible that large objects can affect several radio links in a similar manner. There are extensions of (2.6) which address this issue [29, 61]. The correlations are themselves random as they mirror a property of the environment. Therefore, correlations present another simulation parameter and another dimension of parameter space which adds to complexity. Furthermore, real-world measurements are needed that investigate the impact of correlations and the validity of associated computer models for a variety of indoor and outdoor environments. In an effort to use an abstract formulation which facilitates analysis using computer simulations, the thesis considers independent medium-scale fading as expressed by (2.6).

Maximum Likelihood Distance Estimation In order to estimate the distance between the location-unaware and the i-th location-aware sensor using a measurement of RSS P_i $(i \in \mathcal{A})$, the *Probability Density Function (PDF)* $f(P_i|\boldsymbol{\theta}_1;\boldsymbol{\theta}_i)$ is considered. This function presents for a given configuration of sensor locations the probability of measuring P_i between the location-unaware and the i-th location-aware sensor. Using (2.6), $f(P_i|\boldsymbol{\theta}_1;\boldsymbol{\theta}_i)$ becomes

$$f_{P|\boldsymbol{\theta}}(P_i|\boldsymbol{\theta}_1;\boldsymbol{\theta}_i) = \frac{1}{\sqrt{2\pi}\sigma} \exp\left\{ -\frac{(P_i - \bar{P}(\|\boldsymbol{\theta}_1 - \boldsymbol{\theta}_i\|))^2}{2\sigma^2} \right\} \tag{2.7}$$

However, since the task is to obtain an estimate of $d_i = \|\boldsymbol{\theta}_1 - \boldsymbol{\theta}_i\|$ from noisy measurements, the loglikelihood function $L(d_i|P_i) = \log f(P_i|\boldsymbol{\theta}_1;\boldsymbol{\theta}_i)$ of the observations is considered.

$$L(d_i|P_i) = \log \frac{1}{\sqrt{2\pi}\sigma} - \frac{(P_i - \bar{P}(d_i))^2}{2\sigma^2} \tag{2.8}$$

Only the second term needs to be further considered, since the first term does not depend on locations. The value d_i which maximizes (2.8) is regarded as the *Maximum Likelihood Estimator (MLE)* of distance. Usually, searching for extrema requires calculating the first derivative. However, since (2.7) is Gaussian, the maximum can simply be found by setting the second summand of (2.8) to zero and solving for d_i using (2.5). Consequently, a best estimate $\tilde{d}_i$ of the distance given a measurement P_i in the maximum-likelihood sense can be obtained.

$$\begin{aligned} 0 &= P_i - \bar{P}(\tilde{d}_i) \\ &= P_i - P_0 + 10\varepsilon \log_{10} \frac{\tilde{d}_i}{d_0} \\ &\vdots \\ \tilde{d}_i &= d_0 10^{\frac{P_0 - P_i}{10\varepsilon}} \end{aligned} \tag{2.9}$$

Finally, it is noted that the estimated distances of (2.9) are lognormal distributed as derived in appendix B.2.

$$f(\tilde{d}_i|d_i) = \frac{K\log_{10}e}{\sqrt{2\pi}\sigma\tilde{d}_i}\exp\left\{-K^2\frac{\left(\log_{10}\tilde{d}_i-\log_{10}d_i\right)^2}{2\sigma^2}\right\} \tag{2.10}$$

The constant factor is $K = 10\varepsilon$. Figure 2.3 shows PDFs for several values of the true distances. The MLE of distances is the maximum of each PDF. It is shown that the spread of estimates increases with the true distance. Intuitively, one would assume that the longer a radio link the stronger the impact of the environment on the measurements is. Consequently, the potentially larger number of obstacles on longer links is mirrored by the increasing spread. It is pointed out that the model (2.6) assumes constant variance of the RSS in [dBm]. The increasing spread of estimates is the result of the transformation of a Gaussian distributed parameter (P_1 [dBm]) to a lognormal distributed (distance) one. Furthermore, it is noted that the estimated distances $\tilde{d}$ are biased, meaning that they do not approach the true distance when increasing the number of measurements [1].

Summarizing, distances can be estimated from RSS measurements but the associated measurement errors affect the estimates. Section 2.2 reviews algorithms used in the thesis which calculate an estimate of the location given measurements of RSS. These algorithms are typically designed such that propagation of measurement errors is reduced.

2.2 Categorization of Algorithms

Sophisticated algorithms are used to reduce the effect of measurement errors and to achieve highest accuracy. Typically, at the heart of a localization algorithm is an estimator which combines the measurements to reduce the effect of errors. Algorithms can be distinguished by the way the measurements are used to estimate locations. This motivates the following categorization.

[1] The term bias is further explained in section 2.2.4

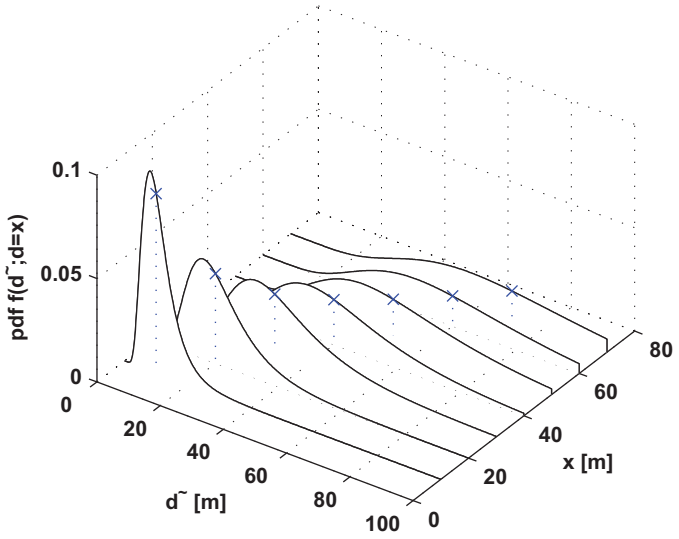

Figure 2.3: PDF of estimated distances. Spread of estimates becomes larger the more distant two sensors are. The dotted blue lines and crosses indicate the true distance which deviates from the MLE given by the PDFs' peaks.

As explained in the beginning of this section, measurements can be used to determine distances and angles between sensors. Knowledge of these parameters gives rise to applying the well known relations between edges and vertices of a triangle to estimate the location. Besides this *triangulation*, *pattern*-based approaches aim at learning a direct mapping of specific combinations of measurement values to location. In contrast, *proximity*-based approaches utilize constraints on angles and distances instead of pointwise values [49, 54]. Each of the aforementioned approaches is surveyed in the following.

2.2.1 Triangulation

Triangulation refers to the utilization of relations between edges and vertices in a triangle to determine, e.g. the third vertex given the first two and all edges. In literature, such approaches are often referred to as *range-based* and *fine-grained*, since corresponding algorithms are most often based on distances to location-aware sensors and are able to determine the true target location in the absence of measurement errors. Typically, as described in the beginning of this section, associated algorithms establish a system of

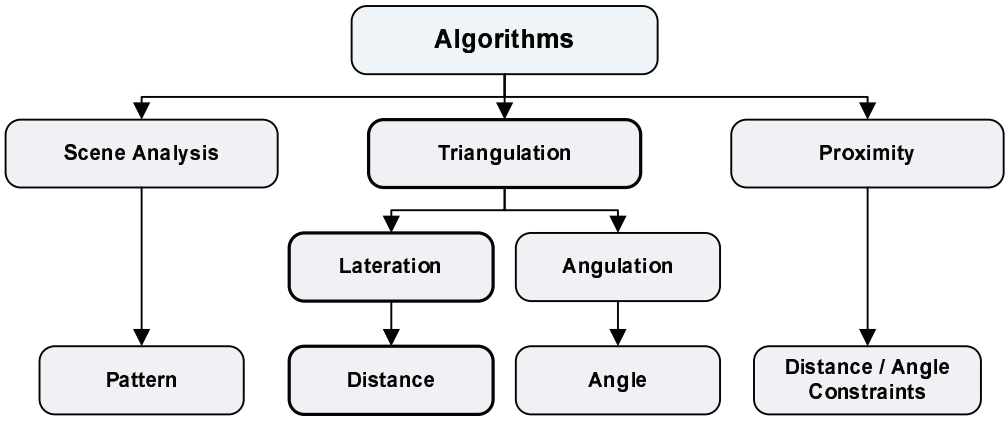

Figure 2.4: Taxonomy of algorithms for localization.

equations relating estimated distances or angles to a-priori known locations of specific sensors. Whereas there exist a single solution in the error-free case, there is probably no such point in case of perturbed measurements. In this situation, the point can be considered a feasible solution which represents the least difference to the measurements, i.e. which has the smallest residual, in a least-squares or maximum-likelihood sense.

As triangulation-based methods require solving a system of typically non-linear equations (2.1)–(2.3), the implementation of corresponding methods involve either a linearization of the problem or a search over the set of feasible locations. Despite the reduction in complexity, a linearization can cause a degradation of accuracy of estimated locations. On the other hand, search-based approaches incur relatively high computational effort and might lead to local instead of the sought global optimum in case an appropriate starting point for the search is not provided.

2.2.2 Scene Analysis

The presence of objects, walls and humans affects radio communications and such situations are encountered especially in indoor environments and cause multipath and attenuation of radio waves. One way to mitigate the impact of these effects on localization is to conduct a-priori measurements for each possible target location and store the results. Later, the location of a specific online measurement is associated with the best

matching a-priori measurement. Consequently, the measurements are directly mapped to an estimated location.

In practice, conducting a-priori measurements for every possible target location is infeasible due to the tremendous time effort. Therefore, only a subset of candidate locations is considered such that measurements at other possible target locations can be interpolated. In addition, corresponding approaches need to consider and be able to cope with changes of the environment during online measurements. Specifically, the movement of humans and also opening doors can lead to different characteristics of radio propagation which are not included in a-priori measurements and thus reduce accuracy of estimated locations. Consequently, the main challenges of this approach are 1) Adopting to changes of the environment during online measurements, 2) Interpolating measurements for non-measured target locations and finding feasible mappings of measurements to target locations.

2.2.3 Proximity

Proximity-based localization typically utilizes constraints on angles and/or distances relative to location-aware sensors to restrict the *area* of candidate locations. The most basic constraint is connectivity information which constrains the receiver to be within communication range of the transmitter. The area can be further narrowed by intersecting multiple of such constraints. The radiation pattern of antennas and the use of antenna arrays and beamforming techniques enable constraining the location of a sensor to reside within a sector.

Typically, the mass center of the constraint area, often simply referred to as centroid, is regarded as an estimate of location [17]. Basically, connectivity can be regarded as binary quantized RSS measurement since the RSS of a transmission must exceed a threshold at the receiver to be correctly demodulated. Consequently, proximity-based localization has to cope with the same propagation effects as the other methods. Furthermore, the estimated locations are generally biased and yield even in the absence of measurement errors inaccurate locations. However, combinations of proximity- and triangulation-based algorithms can yield improved performance. On the one hand, determining a narrow area of candidate locations as a starting point for triangulation-

based localization can improve success rate of finding the global optimum and increase speed of convergence. For this purpose, the estimated locations of proximity-based algorithms, which tend to be computationally less complex, present a good choice. On the other hand, incorporating RSS measurements to refine proximity-based localization has been reported to improve accuracy of estimated locations [12].

The previous categorization of algorithms illustrated that different approaches are possible in order to achieve highly accurate estimated locations. Since a comparison of localization algorithms can only base on reasonable performance metrics, section 2.2.4 covers corresponding evaluation criteria and elaborates on the optimal performance of localization algorithms.

2.2.4 Evaluation Criteria

The most sophisticated estimator is not able to fully recover the true location from perturbed measurements. The major performance metric of an estimator is its ability to reliably achieve estimates with small error, i.e. small deviation from the true location. However, the estimates are themselves random since they are derived from measurements subject to random errors. Consequently, the error of estimates is random and needs to be characterized accordingly. A common approach is to use the *bias* and *variance* of locations. The bias denotes the average deviation of the estimates from the true location whereas the variance indicates their spread around the average. The *Mean-Square Error (MSE)* δ is the sum of the two components, squared bias and variance, and is applied in diverse scientific disciplines to assess the performance of estimators.

$$\delta = E\left(\left\|\boldsymbol{\theta} - \tilde{\boldsymbol{\theta}}\right\|^2\right) \tag{2.11a}$$

$$= var(\tilde{\boldsymbol{\theta}}) + bias(\tilde{\boldsymbol{\theta}})^2 \tag{2.11b}$$

Figure 2.5 illustrates bias and variance. To evaluate the MSE, the expected value can be approximated by the average over N realization of the estimation.

$$\delta = \lim_{N\to\infty} \frac{1}{N} \sum_{j=1}^{N} \left\|\boldsymbol{\theta} - \tilde{\boldsymbol{\theta}}_j\right\|^2 \tag{2.12}$$

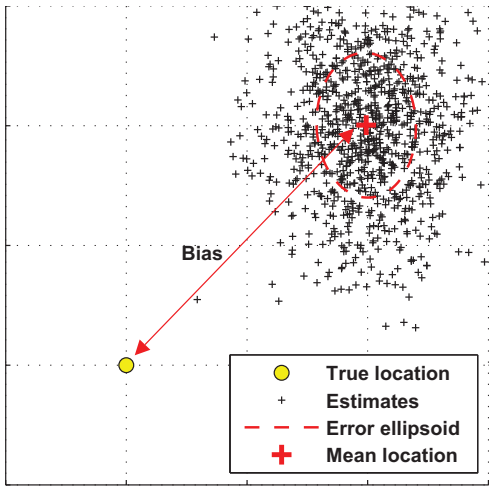

Figure 2.5: Illustration of bias and variance as evaluation criteria for the accuracy of localization processes.

For practical investigations, the value for N is a tradeoff between a high value ensuring a reliable approximation of the MSE and a low value to keep the run time of computer simulations low.

Cramer-Ráo-Bound on Localization Error

Intuitively, it is clear that one can learn less about the true parameter value from a measurement the stronger the noise power is. The *Cramér-Rao-Bound (CRB)* provides a means to numerically characterize the limits of estimators and provides an instrument to determine how well the best estimator can perform under the specified conditions. Specifically, the CRB provides a lower bound on the variance of unbiased ($bias = 0$) estimators [39]. The CRB does not rely on any specific estimator and solely bases on the uncertainty of measurements X and how they add when multiple measurements are combined. To illustrate the concept, the 1-dimensional case is considered where the locations of sensors consist of a single parameter, i.e. $\theta = z$. Any unbiased estimator $\tilde{z}$ must satisfy

$$var(\tilde{z}) \geq \frac{1}{-E\left(\frac{\partial^2 \log f(X;z)}{\partial z^2}\right)} \tag{2.13}$$

The concept of CRB states that the larger the curvature $-E\left(\frac{\partial^2 \log f(X;z)}{\partial z^2}\right)$ of a PDF the more information a measurement contains about its parameters. For example, a high curvature is tantamount to a PDF which is very focused whereas a small curvature indicates that the PDF takes on significant values for a wider range of parameter values.

The thesis considers localization in two dimensions whereby the RSS of communications between a location-unaware sensor at $\boldsymbol{\theta}_1$ and several location-aware sensors at $\boldsymbol{\Theta} = [\boldsymbol{\theta}_2, \ldots, \boldsymbol{\theta}_{N_\mathrm{S}}]^\mathrm{T}$ are measured. The joint conditional PDF of the observed RSS $\mathbf{P} = [P_2, \ldots, P_{N_\mathrm{S}}]^\mathrm{T}$ is the summation over the loglikelihoods of all RSS measurements whose PDFs are given in (2.7).

$$l(\mathbf{P}|\boldsymbol{\theta}_1;\boldsymbol{\Theta}) = \sum_{i=2}^{N_\mathrm{S}} l_i, \quad \text{where} \quad l_i = \log f_{P|\boldsymbol{\theta}}(P_i|\boldsymbol{\theta}_1;\boldsymbol{\theta}_i) \tag{2.14}$$

Consequently, (2.13) has to be extended to be applicable for parameter vectors. The CRB for parameter vectors is given by the following equation.

$$cov(\tilde{\boldsymbol{\theta}}) \geq \mathbf{F}_{\boldsymbol{\theta}}^{-1} \tag{2.15}$$

$$\mathbf{F}_{\boldsymbol{\theta}} = \begin{bmatrix} \sum_{i=1}^{N_\mathrm{A}} -E\left(\frac{\partial^2 l_i}{\partial x^2}\right) & \sum_{i=1}^{N_\mathrm{A}} -E\left(\frac{\partial^2 l_i}{\partial x \partial y}\right) \\ \sum_{i=1}^{N_\mathrm{A}} -E\left(\frac{\partial^2 l_i}{\partial y \partial x}\right) & \sum_{i=1}^{N_\mathrm{A}} -E\left(\frac{\partial^2 l_i}{\partial y^2}\right) \end{bmatrix} \tag{2.16}$$

Whereby $\mathbf{F}_{\boldsymbol{\theta}}$ denotes the *Fisher-Information matrix* [39]. The CRB $\sigma^2_{\min}$ has been applied to the sensor localization problem by Patwari et al. and is reviewed in the following [63].

$$var\left(\tilde{\boldsymbol{\theta}}_1\right) \geq \sigma^2_{\min} = \frac{1}{a} \frac{\sum_{i=2}^{N_\mathrm{S}} d_i^{-2}}{\sum_{i=2}^{N_\mathrm{S}-1} \sum_{j=i+1}^{N_\mathrm{S}} \left(\frac{d_{1\perp i,j} d_{i,j}}{d_i^2 d_j^2}\right)^2} \tag{2.17a}$$

$$a = \left(\frac{10\varepsilon}{\sigma \ln 10}\right)^2 \tag{2.17b}$$

Where the distance $d_{1\perp i,j}$ denotes the shortest distance from location-unaware sensor to the line segment connecting sensors i and j.

Basically, a low value of (2.17) indicates a, on average, highly accurate location

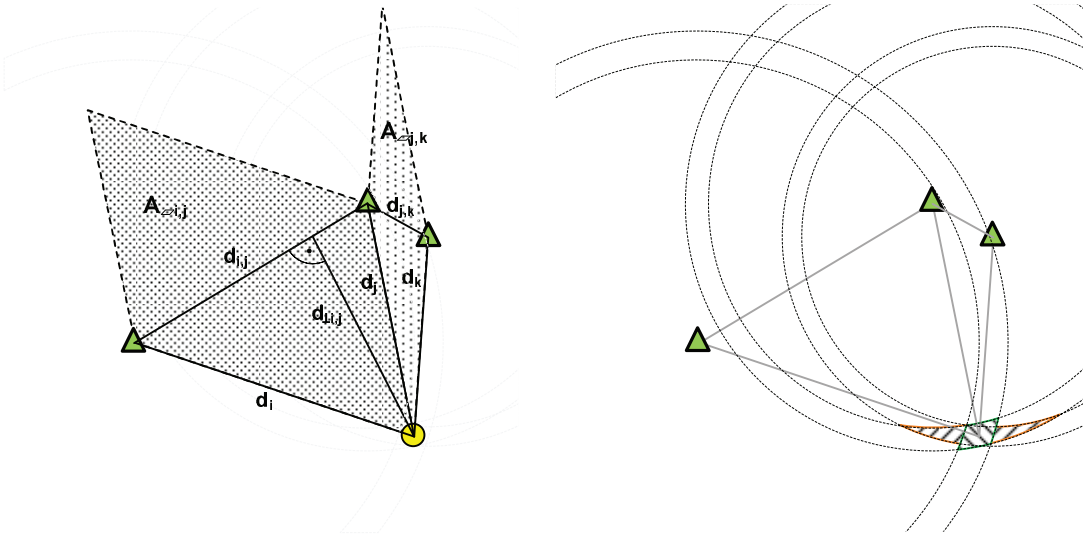

Figure 2.6: The CRB consists of a distance-dependent part and a geometric-dependent part. A favorable geometry is provided by pairs of location-aware sensors whose spatial configuration leads to a large, normalized shaded area of the parallelogram. Those sensor pairs yield a smaller overlapping (green area in (b)) area when estimated distances vary in a particular range.

estimate whereas a high CRB mirrors a configuration of sensor locations and measurement uncertainty that would yield inaccurate location estimates with high probability. The CRB consists of a distance-dependent term in the enumerator and a geometry-dependent one in the denominator. The uncertainty about the measurements is represented by the first factor $\frac{1}{a}$ which includes both the PLE and the variance of medium-scale fading. Figure 2.6 illustrates the components of the CRB. First, the larger the distances between location-aware and location-unaware sensors the larger the CRB as indicated by the enumerator of (2.17). In addition, the geometric configuration of each pair of location-aware sensors affects the denominator. Specifically, the CRB is impacted by the *Geometric Dilution of Precision (GDOP)* as explained in the following. Considering the triangle given by two location-aware sensors and the location-unaware sensor, a parallelogram can be constructed as indicated in figure 2.6a. $A_{i,j}$ denotes the area of parallelogram given by the vectors from the location-unaware sensor to sensors i and j normalized by the length of vectors, i.e. distances d_i and d_j.

Figure 2.6b shows, in a simplified manner, how errors of distances propagate to the uncertainty of estimated locations. The shaded areas denote the regions where the location-unaware sensor resides with high probability if the measurements of the two leftmost or the two rightmost location-aware sensors are combined. It is shown that the area for the two rightmost sensors (orange) is larger than that of the two leftmost sensors (green). This results in a higher uncertainty of the estimated location as indicated by corresponding values of A^{-1}.

Summarizing, the range of localization algorithms can be divided into triangulation, scene-analysis and proximity, each of which exploits the dependence of radio propagation properties between location-aware and location-unaware sensors in a different way. The MSE is used to compare the various localization algorithm against each other regarding bias and variance of estimated locations. The CRB can be used to assess the best performance of unbiased estimators and, hence, provides a means to characterize the best possible performance regarding the spatial configuration of sensors. At the beginning of the section, it was mentioned that each algorithm contains an estimator which maps the measurements or parameters, like distances or angles derived from measurements, to estimated locations. Section 2.3 reviews the estimators used in the thesis.

2.3 Selected Estimation Techniques

Another determining characteristic of wireless localization techniques is the way the sought location is calculated from perturbed measurements and derived geometrical quantities. Especially in complex indoor environments, the errors associated with measurements demand for sophisticated estimators to mitigate the impact on location estimates. Consequently, the choice of the estimator is another distinctive feature of wireless localization techniques.

2.3.1 Least Squared Error Method

For decentralized *Linear Least Squares (LLS)* localization which belongs to the class of triangulation, RSSI is used to estimate the distance between communicating sensors.

Based on the erroneous distances $\tilde{d}_i$ ($i = 2, \ldots, N_S$) to several location-aware sensors, a location-unaware sensor at $\boldsymbol{\theta}_1$ can estimate its location by solving the following system of equations:

$$(x_1 - x_i)^2 + (y_1 - y_i)^2 = \tilde{d}_i^2 \tag{2.18a}$$

The system of equations typically does not have a unique solution, due to measurement errors. However, a solution minimizing the sum of the squared error of each equation can be found by solving (2.19).

$$\tilde{\boldsymbol{\theta}}_1 = \arg\min_{\boldsymbol{\theta}_1 \in \mathbb{R}} \sum_{i=2}^{N_S} \left(\|\boldsymbol{\theta}_1 - \boldsymbol{\theta}_i\| - \tilde{d}_i \right)^2 \tag{2.19}$$

Since this operation typically requires a search over the solution space, a less complex approach is to linearize (2.18) and utilize an LLS estimator. Equations (2.18) can be linearized by subtracting the location of the i-th location-aware sensor from all other equations ($i = 1, \ldots, j-1, j+1, \ldots, N_A$) [56].

$$\left(x_1 - x_j + x_j - x_i\right)^2 + \left(y_1 - y_j + y_j - y_i\right)^2 = \tilde{d}_i^2 \tag{2.20}$$

Expanding and regrouping the terms leads to

$$(x_1 - x_j)(x_i - x_j) + (y_1 - y_j)(y_i - y_j) = \frac{1}{2}(\tilde{d}_j^2 - \tilde{d}_i^2 + d_{i,j}^2) \tag{2.21}$$

In matrix-vector notation, this system of equations has the form $\mathbf{Ax} = \mathbf{b}$ which can be solved by LLS [45]. Without loss of generality, $j = 2$ is assumed.

$$\tilde{\boldsymbol{\theta}}_{\text{lls}} = \frac{1}{2} (\mathbf{A}^T \mathbf{A})^{(-1)} \mathbf{A}^T (\tilde{d}_2^2 \mathbf{1} - \tilde{\mathbf{d}} + \mathbf{d}) + \boldsymbol{\theta}_2 \tag{2.22}$$

$$\mathbf{A} = \begin{bmatrix} x_3 - x_2 & y_3 - y_2 \\ \vdots & \vdots \\ x_{N_S} - x_2 & y_{N_S} - y_2 \end{bmatrix} \tag{2.23}$$

Here, $\tilde{\mathbf{d}} = [\tilde{d}_3^2, ..., \tilde{d}_{N_S}^2]^T$ and $\mathbf{d} = [d_{2,3}^2, ..., d_{2,N_S}^2]^T$ denote the estimated distances and the known distances between location-aware sensors. $\mathbf{1}$ denotes a column vector of size $N_S - 2$ containing only ones to facilitate the addition.

The major advantage of LLS is its small computational complexity and the ability to distribute the operations over many sensors. Consequently, the estimator has been applied to the localization task in resource-constraint WSN [69]. However, the linearization makes this method susceptible to errors especially if the sensor used as reference in (2.20) is far away from the location-unaware sensor.

2.3.2 Maximum Likelihood Estimator

The MLE, which belongs to triangulation-based approaches, jointly estimates the unknown locations of N_B sensors given all measurements to N_A location-aware sensors [63]. Each sensor is indexed and the first $i = 1, 2, \ldots, N_B$ sensors have unknown locations whereas sensors $i = N_B + 1, N_B + 2, \ldots, N_S$ are location-aware. Given the estimated distances $\tilde{d}_{i,j}$ and equation (2.10), the negative loglikelihood of the location-unaware sensors' location can be formulated as

$$L = -\sum_{i=1}^{N_S} \sum_{j=i+1}^{N_S-1} \log\left(\frac{K \log_{10} e}{\sqrt{2\pi}\sigma \tilde{d}_{i,j}}\right) - K^2 \frac{\left(\log_{10} \tilde{d}_{i,j} - \log_{10} \left\|\boldsymbol{\theta}_i - \boldsymbol{\theta}_j\right\|\right)^2}{2\sigma^2} \tag{2.24}$$

It is assumed that the pairwise measurements of RSS are symmetric, i.e. the following holds for the estimated distances $\tilde{d}_{i,j} = \tilde{d}_{j,i}$. The location which minimizes (2.24) is the MLE $\tilde{\boldsymbol{\theta}}_i$ of the location of the i-th location-unaware sensor.

The first summand does not depend on $\boldsymbol{\theta}$ and can be discarded in the following. The sum over the terms in brackets of the second summand depend on $\boldsymbol{\theta}$ and should be minimized in order to obtain the MLE (2.25).

$$\tilde{\boldsymbol{\theta}}_{\text{mle},i} = \arg \min_{\{\boldsymbol{\theta}_i \in \mathbb{R}\}} \sum_{i=1}^{N_S} \sum_{j=i+1}^{N_S-1} \left(\log_{10} \frac{\tilde{d}_{i,j}}{||\boldsymbol{\theta}_i - \boldsymbol{\theta}_j||}\right)^2 \tag{2.25}$$

It is noted that the MLE is obtained by minimizing the negative loglikelihood which is tantamount to maximizing the positive likelihood function. The MLE of estimated

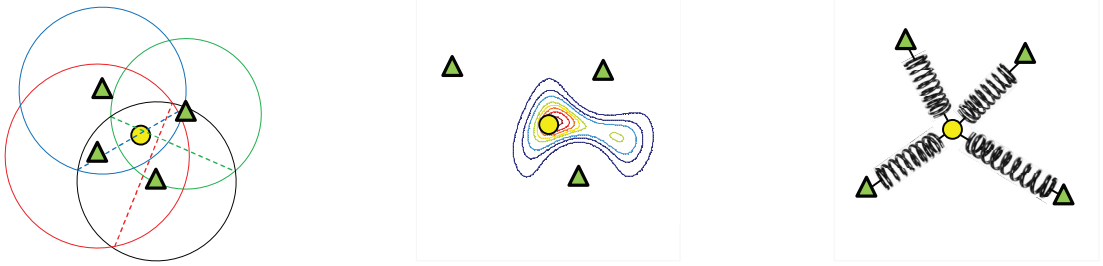

(a) LLS. **(b)** MLE. **(c)** MDS.

Figure 2.7: Overview of localization techniques LLS, MLE and MDS. LLS requires more location-aware sensors due to the linearization and works on lines rather than circles (the lower sensor is used for linearization). The MLE searches over the set of possible solutions for the location that maximizes the likelihood. MDS distributes the location-unaware sensors such that the distance constraints are best met in the least squared error sense.

distances is denoted by $\tilde{d}_{i,j}$ and given in (2.9). This algorithm is centralized since (2.25) has to be calculated at one sensor knowing all required distances and locations.

To reduce the complexity and to enable decentralized calculation of the MLE, only the local likelihood is considered, meaning that (2.25) is calculated on each location-unaware sensor with the locally available estimated distances to adjacent location-aware senors. This leads to a slightly different form of (2.25) which is referred to as *Local Maximum Likelihood Estimator (LMLE)*:

$$\tilde{\boldsymbol{\theta}}_{\mathrm{lmle},i} = \arg \min_{\{\boldsymbol{\theta}_i \in \mathbb{R}\}} \sum_{j=N_\mathrm{B}+1}^{N_\mathrm{S}} \left(\log_{10} \frac{\tilde{d}_{i,j}}{||\boldsymbol{\theta}_i - \boldsymbol{\theta}_j||} \right)^2 \tag{2.26}$$

Since this estimator utilizes fewer information than the MLE, it is expected that accuracy of estimates will tend to be lower.

Both variants require a search over the solution space to find the optimal solution which is implemented as a conjugate gradient decent optimization.

2.3.3 Multidimensional Scaling

Multidimensional Scaling (MDS), which belongs to class triangulation, is a set of statistical techniques originally developed to display the structure of distance-like data as

a geometrical picture. Since MDS works on distance information between objects its applicability for localization of wireless devices has been discussed in [74]. It is noted that MDS belongs to the class of centralized localization algorithms.

Starting with a square matrix $\mathbf{D}$ of pairwise distances between sensor nodes, MDS tries to find the relative arrangement of sensor locations that best fits $\mathbf{D}$ ($\{\mathbf{D}\}_{i,j} = \tilde{d}_{i,j}$). Often the MSE between the measured and the resultant distances is used to define the goodness of a fit. Estimates of location following the MSE objective can be obtained in the following way where $\mathbf{I}$ is the identity matrix:

1. Double center $\mathbf{D}$: $\mathbf{D}_{\mathrm{c}}$.
2. Compute Eigenvalues and -vectors: $\mathbf{D}_{\mathrm{c}} = \mathbf{U}\mathbf{V}\mathbf{U}^{\mathrm{T}}$.
3. Obtain intermediate coordinates $\check{\boldsymbol{\theta}}$ using the two[2] largest Eigenvalues v_1, v_2 and the corresponding Eigenvectors $\mathbf{u}_1, \mathbf{u}_2$: $\check{\boldsymbol{\theta}} = [\mathbf{u}_1, \mathbf{u}_2]\,\mathbf{I}\,[\sqrt{v_1}, \sqrt{v_2}]^{\mathrm{T}}$.
4. Determine the similarity transform $\mathbf{T}$ that transforms the estimated locations of anchors to their true locations and perform the same transformation on all intermediate coordinates.

$$\tilde{\boldsymbol{\theta}}_{\mathrm{mds}} = \mathbf{T}\check{\boldsymbol{\theta}}^{\mathrm{T}} \tag{2.27}$$

The estimator is implemented using the MatLab-functions `cmdscale.m` and `procrustes.m` to obtain $\check{\boldsymbol{\theta}}$ and $\mathbf{T}$, respectively.

2.3.4 Centroid Localization

Centroid Localization (CL), which belongs to proximity-based approaches, is a technique which utilizes the concept of neighborhood to estimate locations [17]. The idea of CL is to regard sensors that are within communication range as being geographically close to each other. Consequently, using connectivity information to location-aware sensors, a location-unaware sensor can calculate its location as the centroid of their

[2]For 2D (3D) coordinates the two (three) largest Eigenvalues should be used.

locations.

$$\tilde{\boldsymbol{\theta}}_{\mathrm{cl}} = \frac{1}{N_{\mathrm{A}}} \sum_{i=2}^{N_{\mathrm{S}}} \boldsymbol{\theta}_i \tag{2.28}$$

While this approach has its advantages, namely to be very simple in terms of computations, its accuracy strongly depends on the communication range of sensors and generally provides only coarse location information compared with the other algorithms discussed so far. However, its simplicity makes it especially suited to provide a start point for search-based algorithms like MLE.

2.3.5 Recursive Bayesian Estimators

Recursive Bayesian Estimation (RBE) is a mathematical framework for estimating an unknown PDF recursively over time using mathematical models of measurements and the process. Regarding the topic of the thesis, RBE considers the evolution of the time-variant state, e.g. $\boldsymbol{\theta} = [x,y]^{\mathrm{T}}$, of a target and its continuous estimation using perturbed measurements of RSS[3]. Specifically, let $\boldsymbol{\theta}^{(t)}$ and $\mathbf{x}^{(t)}$ denote the state and measurements at time t. Given the models

$$\boldsymbol{\theta}^{(t)} = f(\boldsymbol{\theta}^{(t-1)}) + \mathbf{w}^{(t-1)} \quad \text{process model} \tag{2.29a}$$

$$\mathbf{x}^{(t)} = h(\boldsymbol{\theta}^{(t)}) + \mathbf{v}^{(t)} \quad \text{measurement model} \tag{2.29b}$$

with the corresponding covariance matrices of the zero-mean, multivariate Gaussian noises

$$\mathbf{Q}^{(t)} = E\left(\mathbf{w}^{(t)}\mathbf{w}^{(t)^{\mathrm{T}}}\right) \quad \text{process noise covariance} \tag{2.30a}$$

$$\mathbf{R}^{(t)} = E\left(\mathbf{v}^{(t)}\mathbf{v}^{(t)^{\mathrm{T}}}\right) \quad \text{measurement noise covariance} \tag{2.30b}$$

RBEs estimate the state $\tilde{\boldsymbol{\theta}}^{(t)}$ at time t using only the knowledge of the previous state estimate and the current measurements. As they do not require storage of all previous

[3]Typically, the state includes other parameters like velocity or acceleration of target.

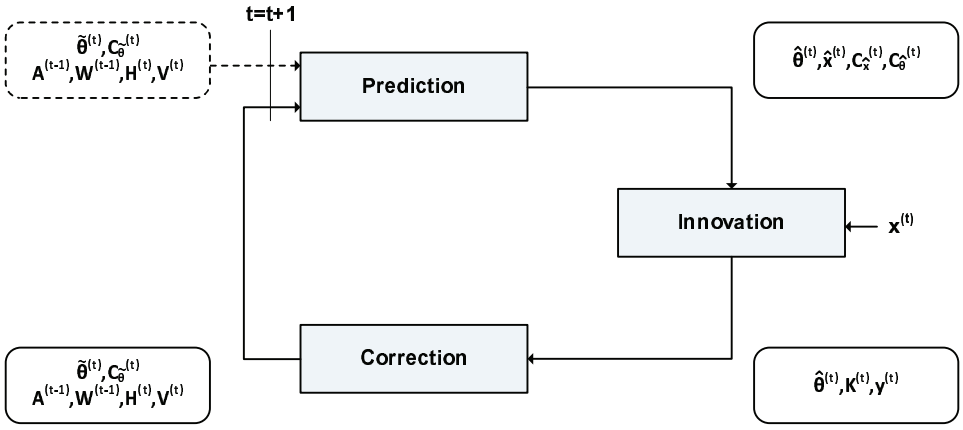

Figure 2.8: Overview on Extended Kalman Filter procedure.

estimates and measurements and work recursively, they are especially suited to online localization algorithms. In the following, two RBEs are reviewed in more detail since they are used in section 4.5. A description which is slightly different from the commonly known ones is presented to emphasize the similarities between both estimators.

Extended Kalman Filter

In RBE, the *Extended Kalman Filter (EKF)* is a non-linear variant of the Kalman filter which linearizes about the current mean and covariance of state and measurements [82]. Its procedure can be divided in a *prediction*, *innovation* and *correction* step as illustrated in figure 2.8.

In the prediction step, the current state and measurements are predicted using the corresponding models.

$$\hat{\boldsymbol{\theta}}^{(t)} = f\left(\tilde{\boldsymbol{\theta}}^{(t-1)}\right) \qquad \text{pred. state} \tag{2.31a}$$

$$\mathbf{C}_{\hat{\theta}}^{(t)} = \mathbf{A}^{(t-1)}\mathbf{C}_{\tilde{\theta}}^{(t-1)}\mathbf{A}^{(t-1)^{\mathrm{T}}} + \mathbf{W}^{(t-1)}\mathbf{Q}^{(t-1)}\mathbf{W}^{(t-1)^{\mathrm{T}}} \qquad \text{pred. state covariance} \tag{2.31b}$$

$$\hat{\mathbf{x}}^{(t)} = h\left(\hat{\boldsymbol{\theta}}^{(t)}\right) \qquad \text{pred. measurements} \tag{2.31c}$$

$$\mathbf{C}_{\hat{\mathbf{x}}}^{(t)} = \mathbf{H}^{(t)}\mathbf{C}_{\tilde{\theta}}^{(t-1)}\mathbf{H}^{(t)^{\mathrm{T}}} + \mathbf{V}^{(t)}\mathbf{R}^{(t)}\mathbf{V}^{(t)^{\mathrm{T}}} \qquad \text{pred. meas. covariance} \tag{2.31d}$$

Basically, the EKF extends the original Kalman filter by including first order approximations of the possibly non-linear state and measurements model in the estimation process.

$$\mathbf{A}^{(t-1)} = \left.\frac{\partial f}{\partial \boldsymbol{\theta}}\right|_{\tilde{\boldsymbol{\theta}}^{(t-1)}} \qquad \mathbf{W}^{(t-1)} = \left.\frac{\partial f}{\partial \mathbf{w}}\right|_{\tilde{\boldsymbol{\theta}}^{(t-1)}} \tag{2.32a}$$

$$\mathbf{H}^{(t)} = \left.\frac{\partial h}{\partial \boldsymbol{\theta}}\right|_{\hat{\boldsymbol{\theta}}^{(t)}} \qquad \mathbf{V}^{(t)} = \left.\frac{\partial h}{\partial \mathbf{v}}\right|_{\hat{\boldsymbol{\theta}}^{(t)}} \tag{2.32b}$$

The predictions present the state under the assumption the process model was not subject to errors. However, the movement patterns of users are typically too complex to be modeled accurately causing the predictions to deviate from the true state. The deviation can be characterized by the difference between the predicted and the actual measurements in the innovation step.

$$\mathbf{y}^{(t)} = \mathbf{x} - \hat{\mathbf{x}}^{(\mathbf{t})} \qquad \text{innovation} \tag{2.33a}$$

$$\mathbf{K}^{(t)} = \mathbf{C}_{\hat{\theta}}^{(t)} \mathbf{H}^{(t)^{\mathrm{T}}} \mathbf{C}_{\hat{\mathbf{x}}}^{(t)^{-1}} \qquad \text{Kalman gain} \tag{2.33b}$$

In the correction step, the information about how well the predictions explain the measurements are incorporated in the final state estimate.

$$\tilde{\boldsymbol{\theta}}_{\mathrm{ekf}}^{(t)} = \hat{\boldsymbol{\theta}}^{(t)} + \mathbf{K}^{(t)} \mathbf{y}^{(t)} \qquad \text{state estimate} \tag{2.34a}$$

$$\mathbf{C}_{\tilde{\theta}}^{(t)} = (\mathbf{I} - \mathbf{K}^{(t)} \mathbf{H}^{(t)}) \mathbf{C}_{\hat{\theta}}^{(t)} \qquad \text{state covariance} \tag{2.34b}$$

As the EKF is based on a linearization of the non-linear process and measurement models, it can loose track in case the current state estimate is too different from the true state. Furthermore, it requires the models to be continuously differentiable.

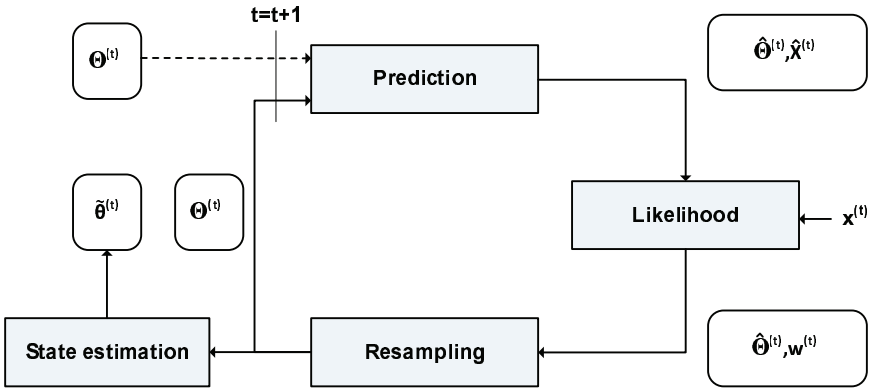

Figure 2.9: Overview on Particle Filter procedure.

Particle Filter

The basic principle of the *Particle Filter (PF)* is to model the PDF over the state space by n_p discrete particles (2.35).

$$\{\boldsymbol{\Theta}\}_{:,i} = \hat{\boldsymbol{\theta}}_i \; (i = 1, \ldots, n_\mathrm{p}) \tag{2.35}$$

Each particle represents an individual hypotheses about the target state which evolves by recursively applying the process model to it and evaluating its likelihood regarding measurements. The distinctive features of PFs are that they approach the optimal performance of Bayesian estimators when increasing the number of particles. Furthermore, they are able to track arbitrary, possibly multi-modal probability densities.

The general principal of a PF is illustrated in figure 2.9. Given an initial vector of particles $\{\boldsymbol{\Theta}^{(t-1)}\}_{:,i} = \hat{\boldsymbol{\theta}}_i^{(t-1)}$ at time t, the process model (2.29a) is applied to each particle and a prediction of the measurements $\hat{\mathbf{x}}^{(t)}$ is calculated using (2.29b). The deviation between predicted and actual measurements $\mathbf{x}^{(t)}$ is evaluated using the likelihood function $l(\boldsymbol{\Theta}^{(t)}{}_{:,i}|\mathbf{x}^{(t)})$ and used to apply weights w_i to each particle i.

$$w_i^{(t)} = l(\boldsymbol{\Theta}^{(t)}{}_{:,i}|\mathbf{x}^{(t)}) \tag{2.36}$$

In particular, particles representing a target state which is not well explained by the current measurements are assigned a small weight and vice versa. The form of the like-

lihood function depends on the observation model and is further explained in Chap. 4. In the resampling step, the effective particle set size is calculated.

$$n_{\mathrm{p,eff}} = \frac{1}{\sum_{i=1}^{n_\mathrm{p}} {w_i^{(t)}}^2} \tag{2.37}$$

If $n_{\mathrm{p,eff}}$ is smaller than a threshold, then *Sampling-Importance-Resampling (SIR)* is applied. SIR denotes a mechanism to delete particles with small weight and spawn new ones at particle locations in state-space with large weight. Thus, it is ensured that the majority of particles resides in the region of state-space with high likelihood.

The actual state estimate is calculated as the mean of the state values given by all particles and is input to the next estimation cycle.

$$\tilde{\boldsymbol{\theta}}_{\mathrm{pf}}^{(t)} = \frac{1}{n_\mathrm{p}} \sum_{i=1}^{n_\mathrm{p}} \hat{\boldsymbol{\theta}}_i \tag{2.38}$$

Chapter 3

Improving Efficiency and Accuracy of Localization

Experimental deployments of WSNs in the past years have shown that sensor networks can be used in a vast number of applications and proved valuable for smart environments [22, 32]. As illustrated in the previous sections, location of sensors and users are important in the growing field of intelligent environments. Typically, battery-powered sensors participate in the localization process either because these sensors require location-awareness for their operations or because they are attached to an object or person to be localized. Energy-efficient operation is in any case mandatory to prolong the sensors' life time.

This chapter considers the tradeoff between energy consumption and accuracy of location estimates which is summarized by the term *Energy Efficiency (EE)*. Since EE is an abstract term, section 3.2 proposes, *Logarithmic Energy Efficiency of Localization (LogarEEL)*, a measure to quantify numerically the EE of localization algorithms. LogarEEL is used to compare the EE of several well-known centralized and decentralized localization algorithms. Section 3.3 investigates new distributed algorithms for the SSP. In particular, the localization procedure is regarded as a selection problem where the task is to pick the subset of location-aware sensors that yields the smallest MSE of location estimates among all subsets of the same size and, thus, can be considered as the most energy-efficient subset for this task.

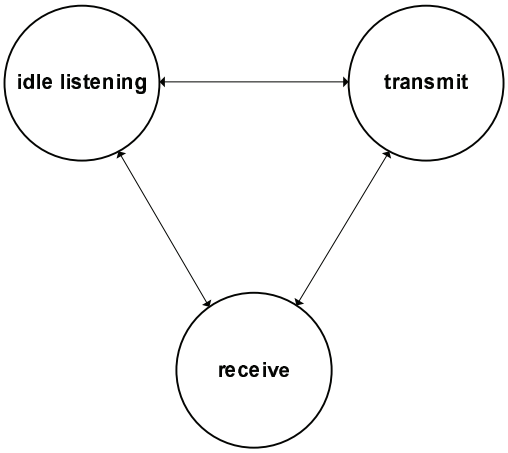

Figure 3.1: States of the energy model.

3.1 Model of Energy Consumption

Since this section focuses on improving the EE of localization, it is necessary to state the model of energy consumption which will be used in the computer simulations. The model should be simple enough to facilitate implementation and it should consider the major sources of energy consumption in sufficient detail to include major aspects. The major sources of energy consumption of wireless sensors are communication and idle energy consumption [86]. Since transmitting a single bit over the wireless channel dissipates $O(10^{-6})$ J whereas execution of a single instruction requires $O(10^{-9})$ J, thus, three orders of magnitude less energy than communications, calculations are discarded in the energy model [79]. Clearly, sensors participating in the localization process will remain active until their task is completed. Hence, it is reasonable to assume the following model of energy consumption:

$$e_i(t) = e_{\text{tx},i}(t) + e_{\text{rx},i}(t) + e_{\text{idle},i}(t) \tag{3.1}$$

$$E(t) = \sum_i e_i(t) \tag{3.2}$$

The basic idea of the energy model is to consider the major sources of energy consumption which are *transmitting* $e_{\text{tx},i}$ and *receiving* $e_{\text{rx},i}$ and *idle listening* $e_{\text{idle},i}$ energy consumption of the i-th sensor. The model assumes a three state sensor model with

idle listening, transmitting and receiving states as illustrated in figure 3.1. In each state, sensors dissipate a specific amount of energy over time.

The specifics of centralized and decentralized localization algorithms which generate different communication overhead are considered in section 3.2.2. Regarding computer simulations, the relation between congestions on the MAC layer and energy consumption is important. Therefore, section 3.3.6 elaborates on this issue.

3.2 Characterization of Energy Efficiency

Although the term energy efficiency is often used in the context of WSN, it is rarely defined clearly and many works considering EE of WSNs by comparing the total energy consumption in the investigated scenarios rather than the ratio of utility of operations and resources spent. This section focuses on a new definition of EE, called *Logarithmic Energy Efficiency of Localization (LogarEEL)*, with the goal to facilitate the comparison of localization algorithms using computer simulations. Before elaborating on the details of LogarEEL, the requirements a feasible measure of EE should meet are motivated.

A measure to quantify the EE of localization algorithms is an important tool as it enables tradeoffs between accuracy and energy consumption in the design phase as well as during runtime of the WSN. In the design phase, engineers can choose between different localization algorithms to meet the requirements of the application concerning accuracy while minimizing the energy consumption. To do so, the performance concerning MSE and complexity of algorithms is typically compared. To facilitate selection of the most energy-efficient algorithm, a bounded measure of EE is needed which summarizes both MSE and energy consumption. The boundedness property can be achieved by a suitable normalization. Furthermore, the usability of a measure of EE can benefit if it is intuitively usable. In particular, a high EE should be mirrored by a large value of the measure and vice versa.

3.2.1 State-of-the-Art

This section reviews several approaches to characterize the EE of localization in WSNs.

Feng et al. investigate localization based on lateration using RSS measurements [26]. The authors consider the *utility* defined as the ratio of energy consumption and decrease of the CRB on localization error to characterize the impact of a specific node on the overall EE of localization. Specifically, a location-aware sensor is more energy efficient the smaller its utility is. Although utility is lower bounded and based on the CRB it lacks objectivity since the energy consumption is not normalized and has unit W/m^2. In addition, the proportionality criteria is not met since low utility denotes high efficiency.

Reichenbach et al. compare several localization algorithms regarding the *Power-Error-Product* (PEP) [68]. The PEP is the product of location error and energy spent for localization. Therefore, a small PEP denotes high EE. Although, PEP is an interesting approach which motivated LogarEEL, it lacks a feasible normalization and its usability is reduced since it is inversely-proportional to the general understanding of efficiency.

In many other works, efficiency is only used as a term and not defined explicitly. This section's contribution is the definition of LogarEEL as a measure to characterize the EE of localization. The distinctive features of LogarEEL are: It is normalized since it is based on the best achievable accuracy of an unbiased location estimator and the energy needed to (asymptotically) achieve this accuracy. Hence, it is bounded and corresponds to the general understanding that a high value denotes high efficiency.

3.2.2 Impact of Centralization

In wireless localization, algorithms can be classified either *centralized* or *decentralized*. Despite their comparably large communication overhead, centralized algorithms typically incorporate more measurements and, thus, information in the localization process and consequently yield estimated locations with potentially higher accuracy than decentralized ones. In addition, centralized algorithms, like MDS and MLE reviewed in Sec. 2.3, typically jointly estimate the location of several location-unaware sensors at once.

In contrast thereof, decentralized algorithms utilize the locally available information only rather than querying distant sensors for their measurements. Therefore, they are preferable in energy-limited wireless networks. The algorithms, which have been

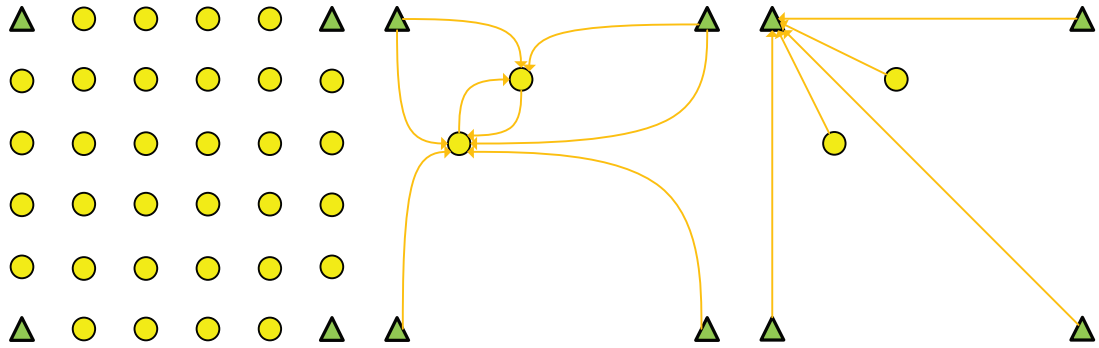

(a) Sample network. **(b)** Measurement phase. **(c)** Distribution phase.

Figure 3.2: Figure (b) shows the measurement phase: Each node determines distances to adjacent sensors by means of RSS measurements. (c) Aggregation: Distances are transmitted to a central node to be used for localization. (a) Network configuration used for simulations. (▲, ●) denote anchors and blinds, respectively.

explained in Sec. 2.3, can be classified either centralized or decentralized regarding whether or not global information is required at one specific sensor. Since the centralized algorithms inherently estimate the locations of all involved location-unaware sensors, a fair comparison with decentralized approaches should consider two different situations: 1) *Individual localization* of a single location-unaware sensor and 2) Joint localization of all blinds which is referred to as *total localization*. It is noted that while being penalized in terms of cost in the first situation, centralized approaches are expected to achieve improved efficiency with total localization.

Since knowledge about all distances is required for centralized localization, the localization process can be divided into a measurement phase, where sensors determine their distance to all neighbors, and an aggregation phase, where this information is transmitted to a central node (see figures 3.2b and 3.2c). Specifically, in the measurement phase each node would broadcast a message to its neighbors. Having received such a broadcast, sensors would use the RSS of the transmission to infer the distance to the sender. Consequently, in a sample network, N_S transmissions and $N_S(N_S-1)$ receptions are required to determine all distances[1]. In addition, communicating the distance

[1]In case links are symmetric, i.e. $d_{i,j} = d_{j,i}$, $\binom{N_S}{2}$ receptions and $N_S - 1$ transmissions are required.

information to a central station requires at least $N_S - 1$ transmissions and receptions. Hence, using (3.1) the cost of individual, centralized localization becomes

$$C_{\text{ind,cent}} = (2N_S - 1)E_{\text{tx}} + (N_S^2 - 1)E_{\text{rx}} \tag{3.3}$$

Whereby the idle energy consumption is discarded as it is constant for all algorithms. It is noted that for total, centralized localization all N_B location-unaware sensors are localized with the same cost. Therefore, the per sensor cost equals the average over all blinds.

$$C_{\text{tot,cent}} = \frac{1}{N_B} C_{\text{ind,cent}} \tag{3.4}$$

In contrast, the decentralized approaches considered in this work rely solely on the distances to location-aware sensors and, therefore, only require a total of N_A transmissions and, at each location-unaware sensor, N_A receptions. Thus the cost of individual and total localization for the decentralized algorithms becomes

$$C_{\text{ind,decent}} = N_A E_{\text{tx}} + N_A E_{\text{rx}} \tag{3.5}$$

$$C_{\text{tot,decent}} = \frac{1}{N_B}(N_A E_{\text{tx}} + N_A N_B E_{\text{rx}}) \tag{3.6}$$

3.2.3 Approach and Definition of LogarEEL

In general, efficiency is the ratio between *gain* (G) and *cost* (C). Regarding localization, high efficiency denotes highly accurate location estimates for which to obtain only few resources had to be spent. In order to quantify this formulation more mathematically, the relation between the MSE of location and the energy E_i attributed to localize sensor i are considered and the EE $\breve{\eta}_i$ of a localization algorithm is defined as:

$$\breve{\eta}_i = \frac{1/\delta_i^2}{E_i} = \frac{G_i}{C_i} \tag{3.7}$$

Here, E_i denotes the energy consumption due to the localization of sensor i. However, this expression does not allow for statements like "the best" efficiency, since (3.7) has

no upper bound. A reasonable way to improve the expressiveness of (3.7) is to normalize both gain and cost.

Concerning the error of localization, the CRB provides a means to assess the best possible performance of unbiased estimation and can be calculated in closed-form 2.2.4. Hence, the CRB is used to normalize the MSE and, therefore, limits the range of the normalized gain $\tilde{G}$ to $0 \leq \tilde{G} \leq 1$:

$$\tilde{G}_i = \frac{1}{\delta_i^2 / \delta_{\text{crb},i}^2} \tag{3.8}$$

Next, the energy consumption of localization is considered, as the cost. In order to maintain the boundedness property, the cost have to be normalized. The fundamental information of the considered localization process are distances estimated using measurements of RSS. Consequently, the energy consumption for retrieving / estimating these distances is regarded as normalizing factor. Consequently, the normalized cost $\tilde{C}_i$ for sensor i can be formulated.

$$\tilde{C}_i = \frac{C_i}{N_{\text{A}}(E_{\text{rx}} + E_{\text{tx}})} \tag{3.9}$$

Due to the possible range and the fact that most feasible estimators do not approach the CRB and have strongly varying accuracy, the log scale is used on the original definition of the EE (3.7). Furthermore, since accuracy and energy consumption might have different importance to the overall system performance, a weighting factor α is introduced to account for this. Thus, LogarEEL is defined as

$$\eta_i = 10 \log_{10} \left(\frac{\tilde{G}_i^{\alpha}}{\tilde{C}_i^{1-\alpha}} \right) \tag{3.10}$$

$$= 10\alpha \log_{10}(\tilde{G}_i) - 10(1-\alpha) \log_{10}(\tilde{C}_i) \tag{3.11}$$

α has range $[0,1]$ and can be used to either emphasize gain or cost of localization. LogarEEL's upper bound is connected to the best possible accuracy given by the CRB and the least energy consumption needed to infer the required distance estimates. An increase of η by 1.5 dB constitutes doubling the EE $\tilde{G}/\tilde{C}$ (assuming $\alpha = 0.5$).

Table 3.1: Simulation parameters.

Parameter	Variable	Value
Deployment area	-	$1\,\mathrm{m} \times 1\,\mathrm{m}$
# location-unaware sensors	N_B	21
# location-aware sensors	N_A	4
Path loss exponent	ε	2
Tx,Rx energy	$E_\mathrm{tx}, E_\mathrm{rx}$	1 a.e.u.
Gain-cost weighting	α	0.5
Number of trials	-	5000

3.2.4 Results and Conclusions

For the simulations, a fully connected regular network of 25 sensors is considered where the $N_\mathrm{A} = 4$ location-aware sensors reside at the corners (see Fig.3.2a). During simulations the MSE of localization as given in Sec. 2.2.4 is calculated approximately on the basis of $N = 5000$ independent trials. Each trial consists of estimation of distances based on perturbed RSS measurements, whereby the measurement model of (2.6a) is assumed. Based on MSE, the normalized gain and cost are averaged over all location-unaware sensors and used to calculate LogarEEL using (3.11). Regarding cost, individual and total localization are considered independently whose specifics have been analyzed in section 3.2.2. Table 3.1 provides an overview of the simulation parameters.

Fig. 3.3b plots LogarEEL of MLE (2.25), LMLE (2.26), LLS (2.22) and MDS (2.27) vs. standard deviation σ of RSS measurements within the sample network. In general, the centralized approaches are advantageous for total localization since they inherently estimate all location-unaware sensor locations. Confidence intervals are omitted, as they are typically much smaller than 1 dB. In addition, results of LMLE and LLS are omitted for individual localization since the graphs are just $5\log_{10}\frac{C_{tot,decent}}{C_{ind,decent}} \approx -1.4\,\mathrm{dB}$ below those of total localization in the considered scenario.

For localization of a single sensor (individual node localization) it is shown that with equally weighted gain and cost (i.e. $\alpha = 0.5$), LMLE achieves the highest EE. This result emphasizes the point that the increase in accuracy of centralized MLE does

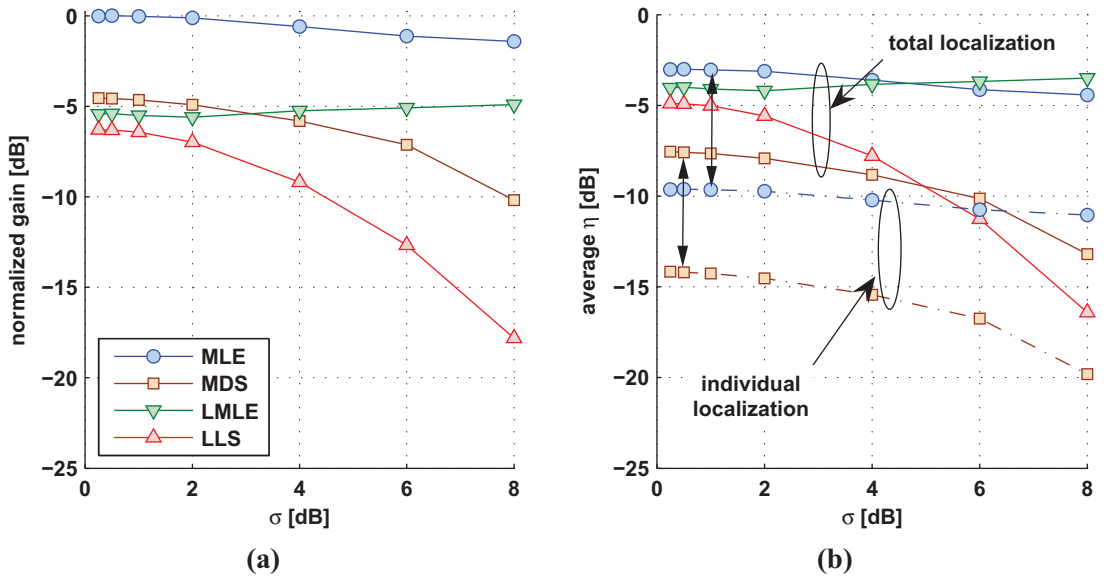

Figure 3.3: Average LogarEEL η of various localization algorithms vs. standard deviation σ of medium-scale fading ($\alpha = 0.5$).

not outweigh the additional cost for measuring and distributing the estimated distances compared to decentralized LMLE. For small values of σ, LLS shows relatively high EE with regards to LMLE. However, LLS exhibits the highest degradation for growing σ. This behavior is caused by the strong susceptibility of linear least squares based optimization to large errors which is also observed for MDS, however, slightly less pronounced.

Concerning total localization, the centralized approaches show increased values of LogarEEL since their cost is independent of the actual number of sensors to be localized and, therefore, the average cost per sensor strongly decreases compared with individual localization. The decentralized approaches also have slightly increased efficiency, due to decreased cost, but the improvement is smaller compared with that of the decentralized methods.

In general, LogarEEL of both MLE and LMLE are relatively insusceptible to changes of σ which indicates that their performance is strongly connected to the CRB. Figure 3.3a shows that the normalized gain of MLE is approximately zero for small σ which is tantamount to nearly equal values of MSE and CRB in this range. This em-

phasizes the objectiveness of LogarEEL since the performance of MLE, which is able to approach the best possible accuracy as given by the CRB, is relatively unaffected by changes of parameters of the wireless channel.

3.2.5 Summary

LogarEEL has been introduced as a measure to characterize the EE of localization algorithms in WSN. Since LogarEEL is upper bounded and normalized to the best achievable accuracy, it constitutes an improvement over existing measures of EE of localization which are either unbounded or dependent on nuisance parameters. Furthermore, a weighting factor is introduced which can be used to emphasize the impact of either accuracy of location estimates or the associated energy consumption.

As an example, the EE of some well-known localization algorithms were investigated, namely MLE, LLS and MDS. The intention of the investigations were to show that LogarEEL produces expected results for known localization algorithms and, therefore, to support its utility to evaluating EE. The results support the general understanding that centralized approaches have difficulties to cope with decentralized approaches in terms of EE when a single sensor need to be located. Furthermore, the susceptibility of MSE-based localization methods, namely LLS and MDS, to large errors is mirrored by their decreasing EE. In contrast, MLE-based approaches show little sensitivity. Summarizing, the decentralized LMLE which optimizes only the local likelihood yields the highest EE for single-node localization whereas the Multidimensional Scaling approach achieved the smallest.

3.3 Selection of Efficient Subsets of Sensors

Typically, due to coverage or robustness-reasons WSN are deployed redundantly, meaning that several sensors are eligible for any specific task [5]. While such approach provides increased resilience to errors it also makes necessary, from the perspective of resource management, a selection mechanism that selects subsets of all eligible sensors and, thereby, reduces the network's resource consumption. Of course, a smart selection

mechanism would chose subsets such that a given quality criteria is maximized for the task.

In the following, it is assumed that the parameters PLE and standard deviation of medium-scale fading are known or have been determined with sufficient accuracy a-priori.

3.3.1 Problem Statement

In the SSP the task is as follows: Given a set $\mathcal{S}$ of sensors, find the subset $\mathcal{H}^{(c)}$ of c sensors that achieves the required accuracy of information while meeting the energy constraints of the sensors [71].

In the context of localization, estimates of location with smallest error are sought while requiring the sensor network only to consume little energy. Since energy is consumed for activation, communications, sensing and, therefore, depends on the number of sensors involved, SSP becomes the task of choosing the subset of references that achieves smallest localization error among all subsets of the same size.

The SSP can be formalized as follows:

$$\begin{aligned} \text{Minimize} \quad & E\left(||\boldsymbol{\theta} - \tilde{\boldsymbol{\theta}}||^2\right) && (3.12)\\ \text{Subject to} \quad & \mathcal{H}^{(c)} \subseteq \mathcal{R} && (3.13)\\ & \tilde{\boldsymbol{\theta}} = f(\mathcal{H}^{(c)}) && (3.14)\\ & |\mathcal{H}^{(c)}| = c \end{aligned}$$

In literature, this optimization task is often described as finding the optimal trade-off between *utility* and cost, where utility denotes some measure of the desired property, i.e. accuracy of location estimates. Typically, SSP is regarded as the problem of sorting subsets of sensors in descending order of their utility and to retrieve information from the first subset in the list which meets a given accuracy-cost-ratio. The process of sensor selection for localization can be divided into three steps which are depicted in Fig. 3.4. In the first step, the sensors are sorted according to their utility. Then sensors need to be informed or be given means to determine themselves when to contribute their measurements which constitutes sensor scheduling based on utility. Finally, sensors

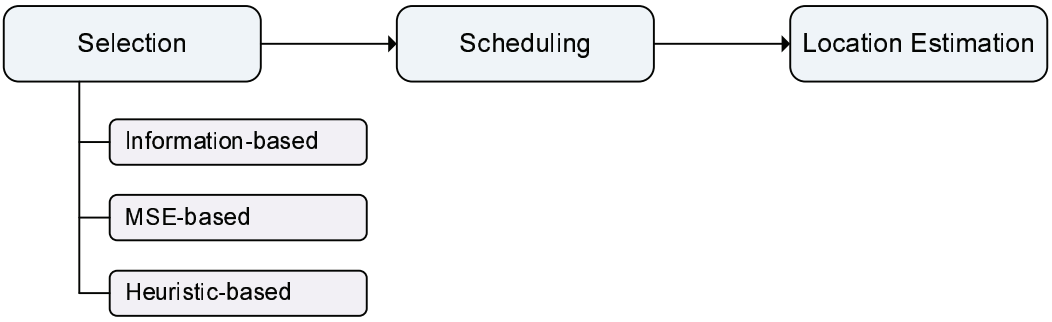

Figure 3.4: Overview on sensor selection.

respond as scheduled and the location-unaware sensor calculates its location using the responses.

The main challenge of SSP is twofold: 1) Find a utility-function that is able to sort sensors correctly despite measurement errors and 2) Reduce the additional resource consumption introduced by the sensor selection process. This section first investigates how subsets can be selected in a near optimal way in terms of MSE. Then Sec. 3.3.3 reviews the state-of-the-art and Sec. 3.3.4 introduces new algorithms to solve SSP. In Sec. 3.3.5, the issue of MAC collisions is dealt with and an improved scheduling is proposed. Finally, the new algorithms are evaluated in terms of CRB, MSE and regarding their sensitivity to MAC collisions in Sec. 3.3.6.

3.3.2 Near Optimal Sensor Selection

In general, a subset of location-aware sensors should be selected such that the average MSE of location estimates is minimized over all possible subsets of the same cardinality. Consequently, utility in this regard is inversely proportional to MSE. Let $\mathcal{H}^{(c)}$ be the set of all subsets with cardinality c $\mathcal{H}^{(c)} := \{\mathcal{H} \mid \mathcal{H} \subseteq \mathcal{R};\ |\mathcal{H}| = c\}$ and determine the subset $\tilde{\mathcal{H}}_{\text{opt}}^{(c)}$ that minimizes the average MSE:

$$\tilde{\mathcal{H}}_{\text{opt}}^{(c)} = \arg \min_{\{\mathcal{H} \in \mathcal{R}, |\mathcal{H}| = c\}} E\left(\delta(\mathcal{H})\right) \tag{3.15}$$

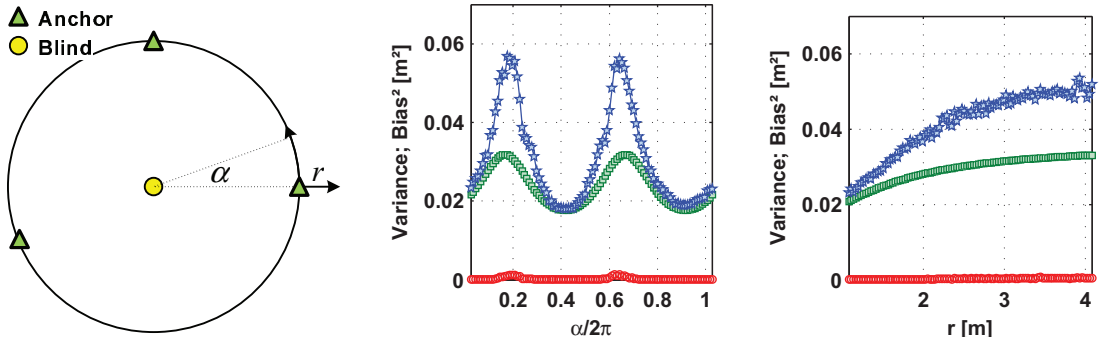

(a) Scenario. **(b)** $r = 1\,\mathrm{m}$ **(c)** $\alpha = 0°$

Figure 3.5: Comparison of variance, bias and CRB for (b) circular and (c) linear movement of the mobile anchor under medium-scale fading. Static anchors are at $\alpha = \{0.25, 0.58\}$. Markers (☆, □, ○) denote the curves for variance, CRB and bias, respectively.

This function basically returns the subset $\tilde{\mathcal{H}}_{\mathrm{opt}}^{(c)}$, which minimizes the average MSE. Thereby, it is assured, that the references in $\mathcal{H}_{\mathrm{opt}}^{(c)}$ contribute on average most to accurate localization.

Impact of Geometry on Mean Square Error

The MSE of localization is related to variance and bias of location estimates. Therefore, the two are investigate in the following in more detail. Specifically, the dependence of MSE on geometric properties of location-aware and location-unaware sensors' locations are considered as a basis for SSP. Recognizing that the error of localization stems from defective estimated distances, it is natural to consider the corresponding error propagation from distances to location estimates. To facilitate explanations, a simple scenario is considered and the CRB, variance and bias of location estimates are investigated using computer simulations.

In particular, a scenario of three anchors and one blind is considered. Two anchors are situated on the circle with center at the blind's location as depicted in Figure 3.5a. The location of the third anchor is varied as indicated by the arrows. Figure 3.5 (b)–(c) show variance, squared bias and CRB vs. different movement patterns of the third

anchor. Localization is performed using MLE while distances are i.i.d. lognormal distributed.

The figures indicate that both variance and bias, and consequently also the MSE, depend on the relative locations of anchors and blind. It is shown that the variance is dominating the MSE and extrema of variance, squared bias and CRB approximately coincide. In order to reduce average MSE, the subsets are selected such that variance is reduced. Since the CRB provides a lower bound on the variance of any unbiased estimator, it is regarded as a means to characterize the utility of any subset of anchors. From these considerations, it is concluded that the CRB σ^2_{min} is a feasible selection criteria. Under this assumptions, (3.15) can be reformulated.

$$\begin{aligned} \mathcal{H}_{\text{opt}}^{(c)} &= \arg \min_{\{\mathcal{H}\in\mathcal{R},|\mathcal{H}|=c\}} \sigma^2_{\text{min}}(\mathcal{H}) \\ \tilde{\mathcal{H}}_{\text{opt}}^{(c)} &\approx \mathcal{H}_{\text{opt}}^{(c)} \end{aligned} \tag{3.16}$$

The subsets $\mathcal{H}_{\text{opt}}^{(c)}$ yield on average the smallest variance of location estimates among all subsets of cardinality c.

This optimization requires complete knowledge of σ^2_{min} of each subset. This information can be obtained by letting the anchors communicate their estimated distances to every other anchor in range. In practice, several issues arise due to this requirement. First, the goal of sensor selection is to limit resource consumption while maintaining a specific level of accuracy. However, gathering complete data as required by (3.16) typically means spending more resources for communication than necessary. Second, it is likely that the data needed by a blind for localization, i.e. distances to adjacent anchors calculated using RSSI, have been obtained during gathering of complete data. Consequently, subsequent sensor selection is rendered unnecessary. As a result, the selection process needs to be fully distributed in order to maintain the benefits of sensor selection, namely, resource preservation while assuring that most important anchors communicate first with the blind.

It is noted that extrema of MSE of other estimators, like LLS, might not coincide with those of the CRB. For these estimators an alternative formulation of the error covariance of location estimates can be found as shown in [30, 39].

3.3.3 State-of-the-Art

In the following, the state-of-the-art of SSP is reviewed and summarized in Table 3.2. The distinguishing characteristic is the way each algorithm calculates the utility of sensors. Therefore, it is used as main classification criteria. In the context of localization and target tracking, SSP has long been spotted as an interesting field of research. A survey of the recent advances is provided by Rowaihy et al. [71]. The literature on SSP can be divided into 1) works that consider the problem from an information-theoretic point of view. Such works aim at decreasing the uncertainty about the target location. 2) Works that utilize a formulation of the MSE of target location for SSP. These works work on error covariance matrices of measurement or target location which are readily available in the context of probabilistic filters and tracking applications like EKF, for example. 3) Algorithms that do not fall in any aforementioned class typically use heuristics to characterize the utility of sensors.

Further categorization regarding centralization, complexity and accuracy will be given in the text and are summarized at the end of Sec. 3.3.3.

Reviewing Sensor Selection Criteria

Information-based Approaches In [91], Zhao et al. investigate a sensor selection scheme which is referred to as *leadership-passing*. In this scheme, the leadership token is passed from sensor to sensor such that each sensor's measurement about the target location optimizes a specific information-measure, like the *entropy* or *mutual information*. Specifically, the current leader uses measurements of previous leaders and its own measurement to determine, using the knowledge about the location of adjacent location-aware sensors, which of them is the best next leader.

Zhao et al. start off with regarding the tracking problem as the task of minimizing the uncertainty about the target location. They utilize a grid-based description of the posterior distribution p of target location. Following the idea of sequential Monte-Carlo sampling, each anchor's observation $\mathbf{x}$ is incorporated into the posterior one after another. The utility of a sensor is given by the effect of its measurements to decrease the uncertainty of the posterior distribution. Thereby, "best" sensor in terms of tracking and localization is one whose current measurement would result in the posterior distribution

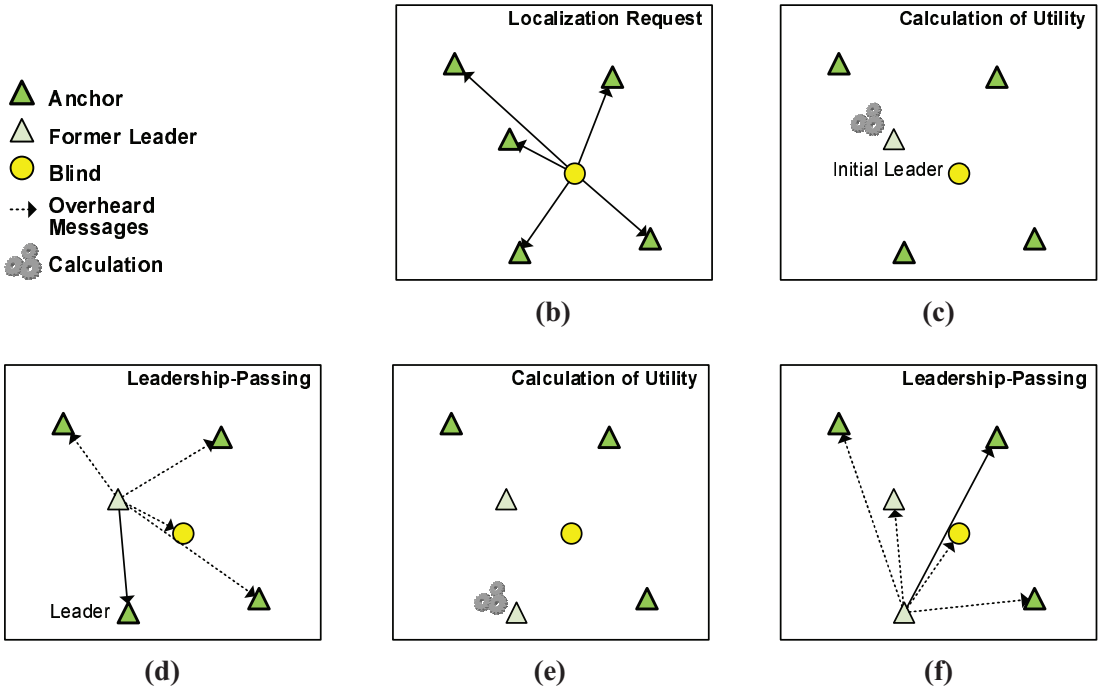

Figure 3.6: Overview on selection procedures showing Zhao's Leadership Passing algorithm.

with smallest entropy among the measurements of all other sensors. Assuming 1D locations $\theta = x$, the entropy H_p of the discrete posterior can be calculated using (3.17).

$$H_p = -\sum_x p(x) \log p(x) \tag{3.17}$$

They recognize that calculation of H_p requires as input the target distribution which, in turn, assumes knowledge of *all* measurements prior to selection. However, avoiding the aggregation of unimportant measurements is key to the EE of SSP and, consequently, H_p can not be used. Several information measures are discussed which are two entropy-based measures and one that uses Mahalanobis distance of target distributions. The investigations are extended in a co-work of Zhao where a comparison of sensor selection using an extended set of selection criteria is presented [20].

Although entropy-based measures provide an accurate way to characterize the utility of a sensor for tracking and localization, they incur a high computational burden.

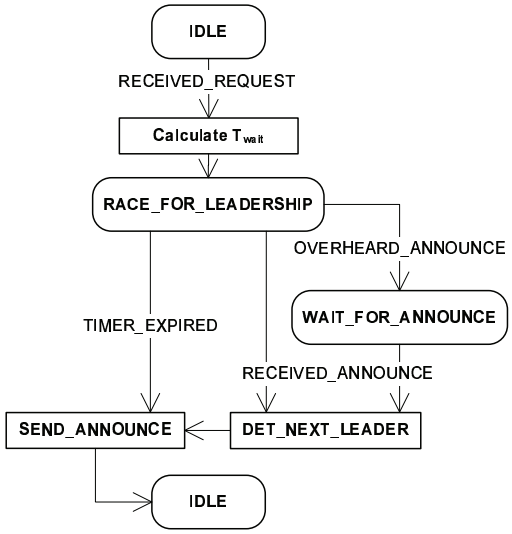

Figure 3.7: Flow-chart of algorithms using leadership-passing. The procedure DET_NEXT_LEADER contains the algorithm specific calculation of utility.

In addition, the accuracy of selection depends strongly on the choice of the first leader. Moreover, leaders represent a single-point-of-failure since loss of any response would abort the selection process.

Liu et al. consider target tracking using WSNs [50]. In particular, they focus on applications where distance and bearing information can be obtained from acoustic sensors. The utility of sensors is evaluated on the basis of mutual information about the future target state and the current sensor measurement. In this context, the sensor with the largest measurement value is initialized as leader and subsequent leaders are selected based on mutual information.

The method of Liu et al. constitutes an approach which utilizes all locally available information to solve the SSP. However, calculation of mutual information is complex and is not applicable in situations where sensors do not have sufficient computing power or for application that require low-latency location estimates.

Several extensions to the work of Zhao et al. have been proposed, e.g. in [25, 81]. In [81], Wang et al. propose to use the reduction in entropy of the target posterior distribution as an indicator of the utility of a sensor (see Figure 3.7 and 3.6). Specifically, they project the posterior onto the sensing view of a sensor to reduce complexity and

calculate the difference between the entropy of the projected posterior with and without the sensor's measurement. This approach is more energy efficient and provides a good approximation of the optimal response order. Although, computational complexity is reduced, calculation of the posterior is necessary and thus complexity is comparable to Zhao's approach using Mahalanobis Distance.

In [92], Zou et al. propose a sensor selection algorithm for target localization which is based on sensors' distances to the maximum of a grid-based representation of target location distribution. Specifically, the selection process starts with a sensor detecting a target and notifying the cluster-head. Given the sensor's location and the detection event, the cluster-head calculates the probability distribution of target location p on predefined grid-points. The cluster-head subsequently queries the sensor that has minimal distance to the maximum of p and updates p. The process continuous until a specific number of sensors has been queried.

Grid-based approaches are able to model a wide range of probability distributions. Hence the work is applicable to many scenarios of target localization. However, centralized calculation of utility means that failures at a single node, the cluster-head, can abort the selection process. Furthermore, explicitly querying sensors means additional communication compared to Zhao's leadership passing while accuracy remains below that of [25, 50, 81, 91].

MSE-based Approaches MSE-based approaches to SSP aim at optimizing the MSE of location estimates. Kaplan et al. propose in [37] and [38] two related selection algorithms that are based on target tracking using an Extended Kalman Filter (EKF) and measurements of target bearings. Compared with the information-driven approaches, these algorithms work on the covariance matrix of location estimates instead of considering the entropy or mutual information.

The authors propose a *global node selection* (GNS) and an *autonomous node selection*(ANS) scheme. Both schemes regard the tracking process as a series of snapshots. Each snapshot starts with searching the best initial tuple of anchors from an initial sensor set which can be inherited from the previous snapshot or be a predefined one. The search step has complexity $O(N^2)$ for an initial set of cardinality N since all combinations of two sensors are considered. After that, additional sensors are added one after

another while ensuring that each sensor decreases the expected MSE using either a local utility measure in ANS or global knowledge in GNS.

The approaches have in common a high computational burden due to the initial search for the best tupel. In addition, even though the ANS uses a utility measure which can be calculated with local knowledge, a high message overhead is introduced as the local utility needs to be compared with a threshold value and the threshold needs to be communicated to candidate sensors beforehand.

Feng et al. pursue a different approach and investigate optimal placement of anchors and clusters in a WSN [26]. They utilize the CRB to determine optimal transmission ranges and anchor placement and present a protocol which selects anchors. The basic idea is to activate only as many anchors as needed to ensure that every point in the deployment area is covered by three anchors to enable localization. The anchors are selected such that the average CRB in that area is minimized. The main difference compared with the scenario considered in the thesis, is that a sink node is assumed which performs centralized calculations and that the focus is rather on increasing the coverage of localization as to increase its accuracy given an upper limit on the number of location-aware sensors to be used.

Heuristic-based Approaches In [14, 23, 51], range measurements are weighted according to their variance and distance or location-aware sensors are selected based on the difference between distances and estimated locations [6]. Others apply tests to detect outliers in order to exclude them from calculations or just choose the nearest location-aware sensors for estimation of location [58, 66]. For coarse-grained localization, it has been reported in [19] that choosing the nearest three location-aware sensors increases localization accuracy when estimating distances with the DV-Hop method.

Furthermore, in [18], localization errors are simulated to decide where additional location-aware sensors have to be placed to decrease errors effectively. However, this leads to large computational overhead on references.

In [76], geometry of the situation is considered. Here, the set of all anchors is divided into groups of three. The sensors of one group form a triangle whose angles must meet a certain requirement for this group to be selected for localization. Drawbacks of

Table 3.2: Overview on related work and comparison with the new approach indicated by a *.

	Distributed	Robust	Complexity	Message overhead	Acc.
Information-Driven					
Chu, Zhao et al. [20, 91]	yes	no	average	low	average
Liu et al. [50]	yes	no	high	low	high
Wang et al. [81]	yes	no	average	low	average
MSE-Driven					
Kaplan et al. [37]	no	yes	average	high	high
Kaplan et al. [38]	yes	yes	average	high	average
Lieckfeldt et al. [47]*	yes	yes	low	low	average
Others					
Zou et al. [92]	no	no	average	average	low

this approach are high computational complexity as all possible groups of sensors are considered and the need for global knowledge to be available.

In [13], Bian et al. consider the problem of sensor selection and argue that "sensor selection should be based upon a trade-off between application-perceived benefit and energy consumption of the selected sensor set". Specifically, they concentrate on the following architecture of sensor networks: The application layer can select different sets of sensors for a task, for example by interrogating the set of sensors with highest utility to measure the temperature. Bian et al. consider three different classes of utility functions for this purpose, namely, submodular and supermodular function and a class to characterize geometric covering objectives. Submodularity denotes utility functions with diminishing return when increasing the size of the sensor set. That means, that when adding additional sensors to a set the increase of its utility becomes smaller and smaller. For this class of utility functions it is shown that a solution in polynomial time can be found.

Bian et al. consider a scenario for which it is most important to prevent unimportant sensors to be activated and to perform measurements, and in which centralized calculation of utility is feasible. However, in the scenario considered in this work, the focus is to evaluate utility in a distributed manner and to limit communications to the minimum whereas measurements of RSS are readily available without extra cost.

Summary

Existing approaches either do not avoid that insignificant location-aware sensors communicate during localization process or they require global knowledge which also assumes additional communication. Furthermore, while the impact of geometry has often been stated in literature, the author is not aware of any work that uses a simple utility function which considers both geometry and distance information for the selection process and is fully distributed. Another distinction is that in previous works responses are typically scheduled by the leadership passing technique. However, this technique is susceptible to failures of sensors and, hence, can be regarded as less robust to this kind of errors as will be illustrated in Sec. 3.3.6.

3.3.4 New Algorithms for SSP

This section presents two algorithms for distributed sensor selection which require minimal communications and use simple math for calculating utility. The first algorithm uses distance information for evaluating the utility of a location-aware sensor. A more general formulation of distance-based selection is contributed to the state-of-the-art which enables optimized scheduling of responses as will be explained in Sec. 3.3.5. The second algorithm uses the CRB as utility measure [47]. The CRB has the desirable property to summarize GDOP and distance-related accuracy degeneration while requiring less complex calculations for important channel models. After providing a general description of the selection process the details of each algorithm are explained.

The following terms are introduced to facilitate the investigations:

- The selection process is initiated by a localization *request* which is broadcasted by the *requester*.
- All location-aware sensors which have received the request are summarized by the set $\mathcal{H}$.
- *Responders* are those location-aware sensors which have already contributed their measurements by sending a *response* to the originator of the request.

- All location-aware sensors keep track of the current state of the selection process by storing related responses. The set of all responses received by sensor $s_i \in \mathcal{H}$ is denoted by $\mathcal{S}_{\text{resp},i}$.

Selection Procedure

Starting with the initial request for localization, all location-aware sensors in transmission range of the requester estimate their distance to the requesting blind. Each is assigned a wait time $T_{\text{wait},i}$ $(s_i \in \mathcal{R})$ which delays its response and is key to avoid additional communication. Wait times are based on distance and/or CRB with the aim to ensure that sensors will respond in approximately the same order as optimal (see (3.16)). Naturally, such approach has to deal with measurement errors and collisions on the MAC layer while minimizing the total wait time to preserve energy as will be explained later in this section.

Sensors obtain local information from the blind's initial localization request and subsequently by overhearing the responses of other sensors. It is emphasized that local information is not explicitly exchanged but will be made available to other sensors during the process without additional communication.

Distance-based Selection

In algorithm *local-dist*, each reference uses the ratio of transmission range r_{tx} of the blind's request and the estimated distance to calculate the delay of its response. In contrast to [46], a more general formulation of the wait time is used which enables finding a tradeoff between total wait time and collision probability as investigated in Sec. 3.3.5. The following family of functions with parameters K and α are considered to calculate the wait time.

$$T_{\text{wait},i} = K\left(\frac{\tilde{d}_{1,i}}{r_{\text{tx}}}\right)^{\alpha} \qquad s_1 \in \mathcal{B}, \quad s_i \in \mathcal{R} \tag{3.18}$$

$$T_{\text{wait}} = \sum_i T_{\text{wait},i} \qquad \text{Total wait time} \tag{3.19}$$

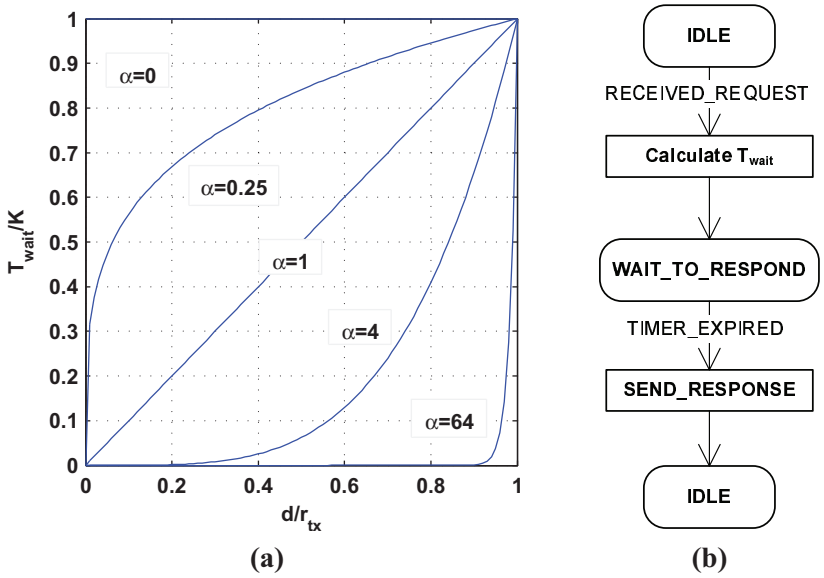

Figure 3.8: Characteristics of wait times $T_{\text{wait},i} = K\left(\frac{\tilde{d}_{j,i}}{r_{\text{tx}}}\right)^{\alpha}$ with parameters K, α. The plot is normalized by K which determines the maximum wait time. Figure (b) shows the flow-chart of algorithm local-dist.

Consequently, the range of the wait time is $T_{\text{wait},i} \in [0, K]$ whereas the upper bound may be violated due to defective distance estimation. Figure 3.8 depicts the characteristics of $T_{\text{wait},i}$ for different parameter choices. Parameters K and α can be used to change the total wait time T_{wait} and the collision probability.

CRB-based Selection

In the following, a new approach to sensor selection is investigated which aims at minimizing both variance and bias of location estimates while requiring no additional communication and only simple calculations. The new approach bases on the use of the CRB which has been demonstrated to reflect the characteristics of MSE in Sec. 3.3.2. In algorithm *local-crb*, the CRB is calculated using estimated distances between location-aware sensors and blind. Responses are broadcast and include the originator's address and location and its estimate of the distance to the requester. After the first reference has answered, subsequent references can use the additional information provided by

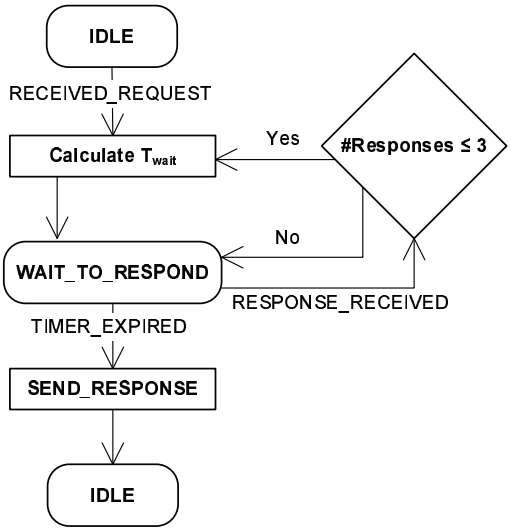

Figure 3.9: Flow-chart of algorithm local-crb.

the former responses, namely distance estimates of other sensors. Without loss of generality, the requester is referred to as s_1 and the location-aware sensors involved in the selection process denoted by $s_i,\ i > 1$.

Starting with the localization request of the blind, any location-aware sensor receiving that request performs distance-based selection using (3.18) until at least one responder's message has been overheard (Fig. 3.10). Each sensor stores responses and associated information. Using the information of the first response, each reference evaluates the CRB and determines whether its measurement would lead to a CRB larger than the transmission radius of the localization request. This situation can occur if a sensor is collinear or nearly collinear with the previous responder and the blind. In order to prevent collinearity, such sensors further delay their response.

Eventually, another location-aware sensor responds and, again, each of the remaining sensors s_i evaluates their utility using CRB. This time, they can calculate the current CRB $\sigma^2_{\min}(\mathcal{S}_{\text{resp},i})$ using the information of the first two responders and compare it with the new CRB $\sigma^2_{\min}(\mathcal{S}_{\text{resp},i} \cup s_i)$ assuming they would respond next. The final wait time

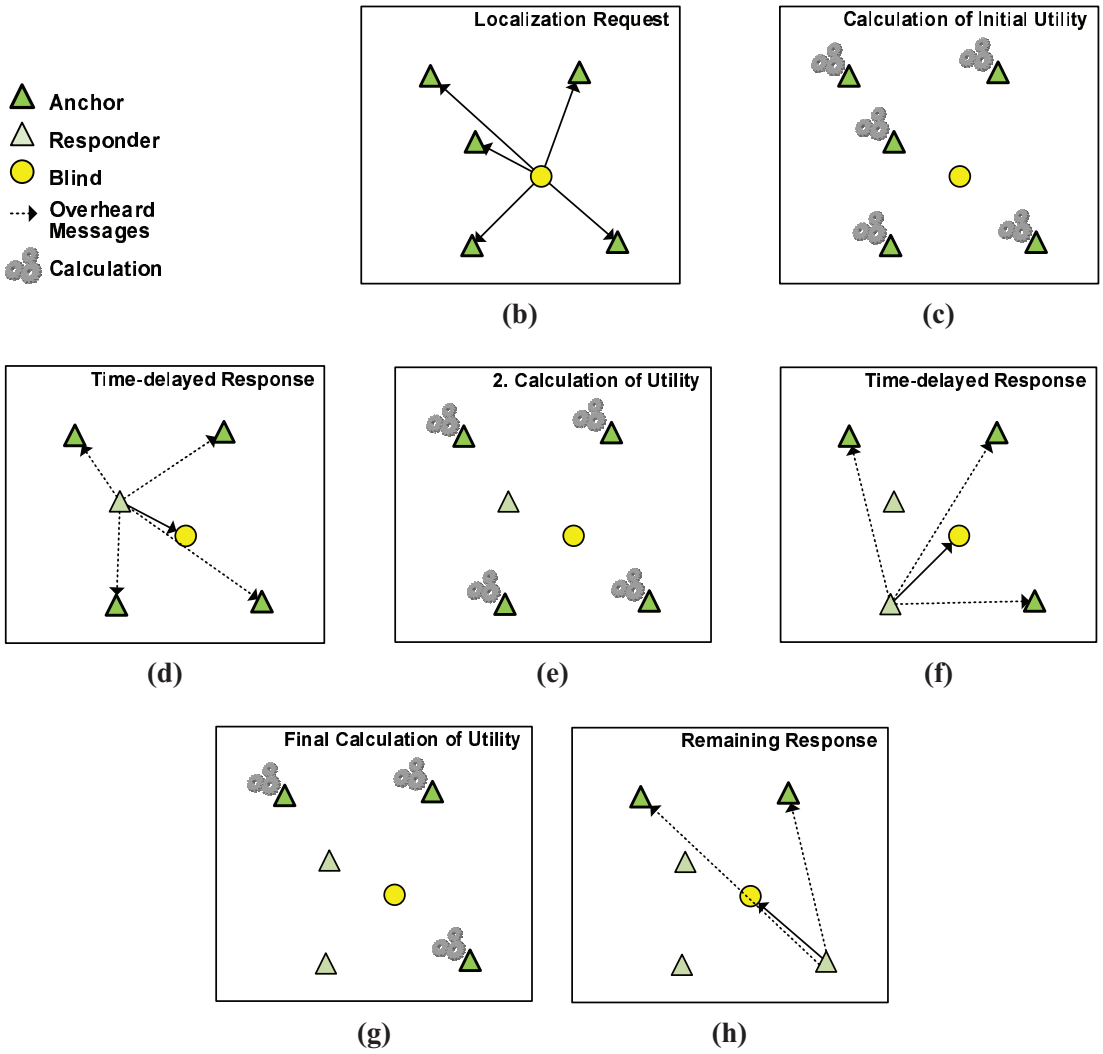

Figure 3.10: Overview on algorithm local-crb.

for subsequent responses is calculated based on the decrease of CRB $\Delta\sigma^2_{\min}$.

$$T_{\text{wait},i} = \begin{cases} \tilde{K} \cdot \Delta\sigma_{\min}^{\tilde{\alpha}} & \left|\mathcal{S}_{\text{resp},i}\right| \geq 2 \\ K \cdot \left(\frac{\tilde{d}_{1,i}}{r_{\text{tx}}}\right)^{\alpha} & \left|\mathcal{S}_{\text{resp},i}\right| < 2 \end{cases} \tag{3.20}$$

$$\Delta\sigma_{\min} = \frac{\sigma^2_{\min}(\mathcal{H}_i \cup s_i)}{\sigma^2_{\min}(\mathcal{H}_i)} \tag{3.21}$$

Table 3.3: Overview on algorithms.

algorithm	Knowledge	Metric used
global-crb	global	CRB
local-dist	local	Distances
local-crb	local	Distances, CRB
local-mDist	local	Mahalanobis distance
local-mInfo	local	Mutal information
local-heuristic	local	Approximation of mutual information

Since the characteristics of $\Delta\sigma^2_{\min}$ are different compared with $\frac{\tilde{d}_{1,i}}{r_{\text{tx}}}$, the algorithm needs to use different values $\tilde{K}$ and $\tilde{\alpha}$ for each phase. The process continuous either until a predefined number of references has responded, the selection process is aborted by the blind or any other suitable trigger.

In practice the CRB is calculated using defective distances and, consequently, errors need to be considered explicitly. One way of doing this is to incorporate a model for the errors as is part of the information-driven approaches in Sec. 3.3.3. However, these approaches have high computational complexity which motivate investigating alternatives which require only simple computations yet consider the impact of geometry on localization error.

In particular, the denominator of CRB in equation (2.17) becomes a complex number if the distance $d_{2,3}$ between any two pairs of location-aware sensors and their distance estimates $d_{1,2}, d_{1,3}$ to the blind do not satisfy $d_{1,2} + d_{1,3} >= d_{2,3}$. The author found empirically that using the absolute value represents a reasonable tradeoff between utility of CRB to SSP and low computational complexity.

Table A.1 gives an outline of the algorithms local-dist and local-crb in pseudo code. The code is executed by location-aware sensor s_i.

Issues of Distributed Selection Methods

Two major issues of local-crb and local-dist are the *hidden terminal problem* and that the order of responses determined by an algorithm is subject to *collisions* of responses on the MAC layer. For the investigations, it is assumed that blinds reduce transmission

power to half the maximal transmission range while location-aware sensors respond with maximum transmission range. This effectively mitigates the hidden terminal issue. Furthermore, it is assumed that each responder is aware of the location of all other adjacent location-aware sensors. This assumption holds since this information can be easily obtained by sensors by overhearing transmissions of their neighbors.

Collisions on the MAC layer occur whenever the wait times of two sensors differ only by a small value and the radio transmission of the two interferes with each other. Generally, the problem of distributed access to a shared communication medium is well investigated. Typically, MAC schemes can be divided into two different approaches. First, collisions are avoided by multiplexing the communications in the frequency, time or space domain. Second, concurrent medium access is allowed and collisions are detected and resolved as they occur. A simple concurrent MAC scheme is *Carrier Sense Multiple Access with Collision Detection (CSMA/CD)* with *Binary Exponential Backoff (BEB)*. Only the latter approach is considered in this work, due to its simplicity and since it does not require control packets to be send. While effectively improving packet delivery rate, CSMA/CD with BEB can perturb the response order of sensors in situation where many collisions have to be resolved. Consequently, collisions have to be avoided in order to maintain the response order as determined by the algorithms. One way of doing this in a fully distributed way without excess communications is to adapt the parameters of wait times which is investigated in Sec. 3.3.5.

3.3.5 Optimized Scheduling for Distance-based Selection

Sec. 3.3.4 outlined some issues when using distances to schedule responses. One important issue is that the anticipated response order can be perturbed by collisions on the MAC layer. Before elaborating on the issue, the details of the considered multiple access scheme need to be stated. The computer simulations discussed in the following sections assume CSMA/CD with BEB. Each sensor can sense whether the channel is idle. A collision occurs whenever a sensor tries to respond during the response of another sensor. The situation becomes more difficult in case the responses of multiple sensors were delayed and their responses need to be rescheduled such that the original response order is preserved. However, this is difficult to achieve without requiring addi-

tional communications. Consequently, collisions not only disturb the correct response order but also add significantly to energy consumption since recurring carrier sensing and retransmissions are required.

This section considers adapting parameters α and K to minimize the collision probability. As a prerequisite, the parameters' impact on collision probability and the total wait time is investigated. A parameter set $(\alpha_{\text{opt}}, K_{\text{opt}})$ is sought using numerical analysis which presents an optimum concerning the total energy consumption of the localization procedure.

It is assumed in the following that sensors are uniformly deployed and are aware of their true distances to adjacent sensors. Furthermore, it is assumed that radio propagation delays are small compared to MAC packet length in seconds and, thus, can be disregarded. This assumption readily holds for common sensor platforms like the cc1010 and for the ZigBee standard. In both cases, radio waves travel several kilometers during one bit duration which renders propagation delay for the current investigations negligible.

Collisions occur whenever two sensors schedule their responses such that the time between the start of the first response and the start of the second response is smaller than the packet transmit time T_p.

$$\text{“Collision”} \Leftrightarrow \left| T_{\text{wait},i} - T_{\text{wait},j} \right| \leq T_{\text{p}} \tag{3.22}$$

Using eq. (3.18) and given the location of one sensor s_i and its distance $\tilde{d}_{1,i}$, one obtains the following disc-shaped interval which represents the area around the requester in which no other sensor but s_i should be situated to avoid collisions

$$\text{“Collision”} \Leftrightarrow b_{\text{low}}(\tilde{d}_{1,i}) \leq \tilde{d}_{1,j} \leq b_{\text{up}}(\tilde{d}_{1,i}) \qquad j \neq i, s_i, s_j \in \mathcal{H} \tag{3.23a}$$

$$b_{\text{low}}(d) = \begin{cases} \sqrt[\alpha]{d^\alpha - \frac{T_{\text{p}} r_{\text{tx}}^\alpha}{K}} & d^\alpha \geq \frac{T_{\text{p}} r_{\text{tx}}^\alpha}{K} \\ 0 & \text{else} \end{cases} \tag{3.23b}$$

$$b_{\text{up}}(d) = \min\left(r_{\text{tx}}, \sqrt[\alpha]{d^\alpha + \frac{T_{\text{p}} r_{\text{tx}}^\alpha}{K}} \right) \tag{3.23c}$$

Since sensors are independently deployed, one can calculate the average number of

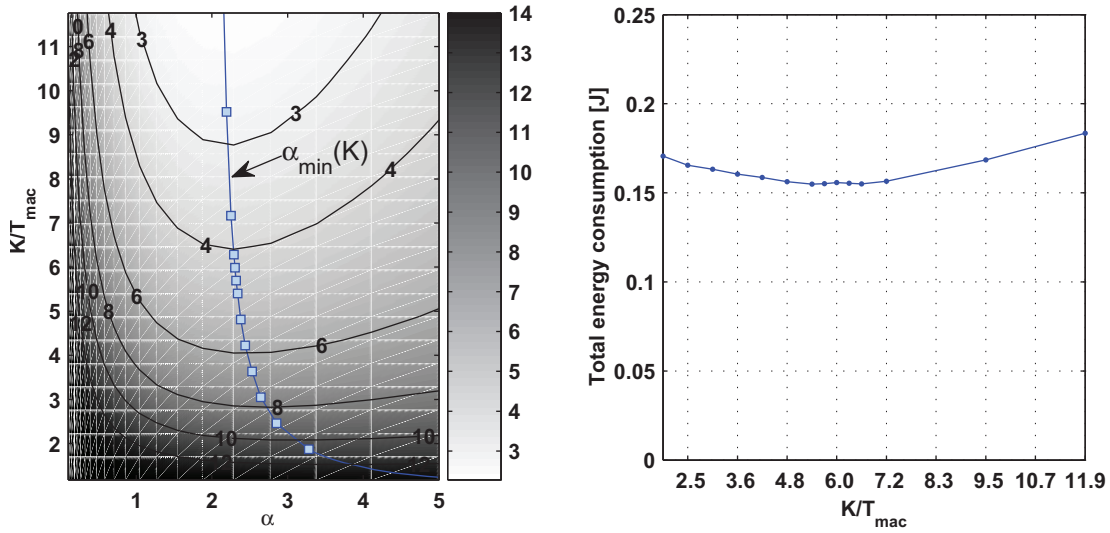

(a) $\bar{N}_{\text{coll}}$ vs. K, α **(b)** Energy consumption vs. K, α

Figure 3.11: Figure (a)shows average number of collisions on the MAC layer vs. parameters α and K of wait time. (b) Total simulated energy consumption vs. pairs of K and α as indicated by the blue line in (a). The x-axis depicts the value of K of the parameter set $\{K/T_{\text{mac}}, \alpha\} \in \{\{1.9,3.28\},\ \{2.5,2.86\},\ \{3.0,2.65\},\ \{3.6,2.53\},\ \{4.2,2.44\},\ \{4.8,2.38\},\ \{5.4,2.34\},\ \{6.0,2.30\},\ \{6.6,2.27\},\ \{7.2,2.25\},\ \{9.5,2.20\},\ \{11.9,2.16\}\}$.

collisions N_{coll} as a function of d using the node density ρ which has unit $[1\,\text{m}^{-2}]$.

$$N_{\text{coll}}(d) = \rho \cdot \int_{b_{\text{low}}(d)}^{b_{\text{up}}(d)} 2\pi x \, dx \tag{3.24}$$

Using eq. (3.24), one can calculate the average number of collisions for a selection process by multiplying each N_{coll} with its probability $P(N_{\text{coll}})$ and integrating the product of N_{coll} and its probability over all possible values of d.

$$\begin{aligned} \bar{N}_{\text{coll}} &= \int_0^{r_{\text{tx}}} N_{\text{coll}}(x) \cdot P\left(N_{\text{coll}}(x)\right)\, dN_{\text{coll}}(x) \\ &= 2\frac{\rho}{r_{\text{tx}}^2} \int_0^{r_{\text{tx}}} \vartheta \cdot \int_{b_{\text{low}}(\vartheta)}^{b_{\text{up}}(\vartheta)} 2\pi\varsigma \, d\varsigma \, d\vartheta \end{aligned} \tag{3.25}$$

Since the integration limits of the inner integral depend on the outer integral, an ana-

Table 3.4: Parameter values of energy model. Values of energy consumption are based on the work of Polastre et al. in [65] and Shnayder et al. in [75].

	Transmit	Receive	Idle listening	Carrier Sense
Energy [Joule/bit]	$3.12 \cdot 10^{-6}$	$2.34 \cdot 10^{-6}$	$1.59 \cdot 10^{-6}$	$2.5 \cdot 10^{-6}$

lytical solution to eq. (3.25) is difficult to obtain. However, one can utilize numerical integration to evaluate and investigate $\bar{N}_{\text{coll}}$.

Fig. 3.11a depicts $\bar{N}_{\text{coll}}$ for various values of α and K. Dark areas indicate parameter sets which yield many collisions. A solid blue line shows the parameter combination which lead to the least collisions for a specific K. It is shown that $\alpha \approx 2.2$ yields good results for a large range of K values. For small K the optimal α shifts to larger values. For a practical parameter choice, not only the collision probability has to be considered but also the total energy consumption which is depends on the total wait time and therefore also on K.

The total energy consumption of SSP is investigated using computer simulations. Idle listening, transmitting and receiving messages contribute to the total energy dissipated by all sensors. Table 3.4 presents the energy consumption attributed to transmitting or receiving one bit and for idle listening which base on typical values for sensor motes[2].

Figure 3.11b shows that $K/T_{\text{mac}} = 5.4$ $\alpha = 2.34$ yield minimum energy consumption and represent the best tradeoff between Mac collision probability and total wait time. In particular, energy consumption is approximately 10 % larger at $\{K/T_{\text{mac}}, \alpha\} = \{1.9, 3.28\}$ compared with the minimum. Section 3.3.6 completes the analysis of optimized scheduling by analysing the dependence of MSE on $\{K, \alpha\}$.

3.3.6 Results and Conclusions

The algorithms of Sec. 3.3.4 are analyzed in the following using computer simulations. Four different investigations focus on analyzing the CRB, the MSE without and with considering MAC contention. Finally, the impact of packet loss on the success rate of

[2]The values base on the CC1010 transceiver module distributed by Texas Instruments.

Table 3.5: Summary of computer simulation.

	Simulation			
Parameter	Analysis of CRB	Analysis of MSE	MSE vs. MAC contention	Impact of Packet Loss
Radio channel	$\varepsilon = 2.3$ $\sigma = 3.92\,\mathrm{dB}$	$\varepsilon = 2$ $\sigma = 2\,\mathrm{dB}$	$\varepsilon = 2$ $\sigma = 2\,\mathrm{dB}$	n/a
Error model	ideal	Eq. (2.6a)	Contention, Eq. (2.6a)	Packet Loss
Figure of merit	CRB	MSE	MSE, Energy	Success Rate
Estimator	n/a	Eq. (2.26)	Eq. (2.26)	n/a
Request [bit]	n/a	n/a	61	n/a
Response [bit]	n/a	n/a	85	n/a
#Trials	n/a	2000	1000	n/a
#Deployments	10000	80	80	n/a

algorithms is investigated. The simulations assume a fully connected uniform deployment of anchors in a circular area of radius $r_{\mathrm{tx}} = 100\,\mathrm{m}$ with one blind at its center. The algorithms perform sensor selection as described in Sec. 3.3.4 and utilize true distances or RSSI with log-normal errors to estimate distances as indicated in the text. Each deployment consists of several trials during which selection is carried out repeatedly while using different realizations (trials) of estimated distances. The parameters of the simulations and the investigated values are summarized in Tab. 3.5

Reference Algorithms

Selection based on *global knowledge* requires additional communication among anchors, for example, to exchange and compare estimates $\tilde{d}_{i,j}$ of the distance to the blind. Naturally, the algorithms of class global knowledge are expected to perform better than those of class local knowledge because more information of the network topology is available.

To provide a reference for the evaluation, the *global-crb* algorithm is used which regards the true CRBs of each anchor as its utility. This algorithm selects near optimal

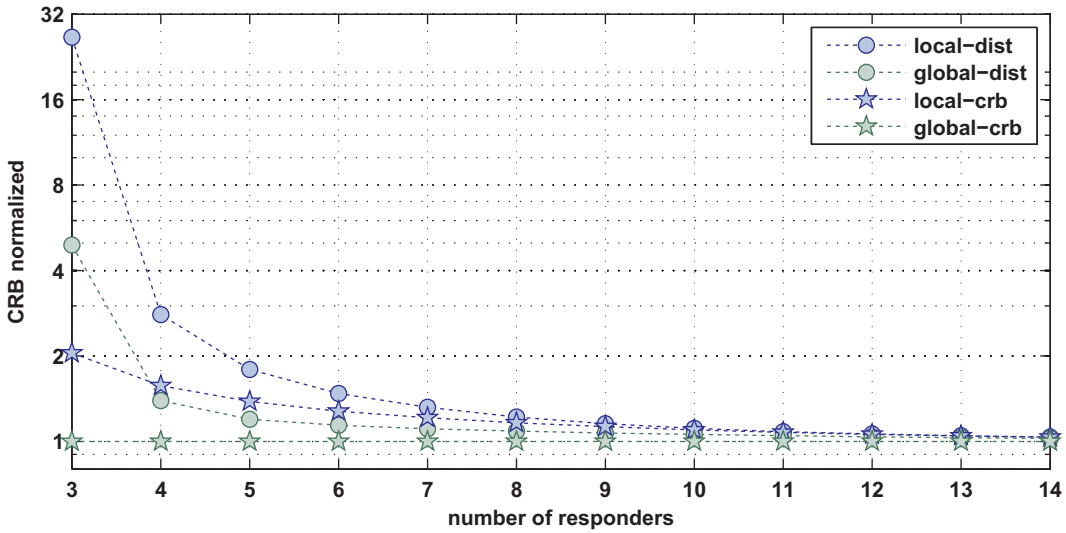

Figure 3.12: Average ratio of CRB of selected subsets normalized by the optimal CRB as given by algorithm global-crb.

subsets in terms of (3.15). The subsets are given in (3.26).

$$\hat{\mathcal{H}}_{\text{opt}}^{(c)} = \arg \min_{\{\mathcal{H}\in\mathcal{A},|\mathcal{H}|=c\}} \sigma_{\min}^2(\mathcal{H}) \tag{3.26}$$

Results

Analysis of CRB First, the CRB of the subsets selected by algorithms local-dist and local-crb is investigated and compared with their counterparts that use global knowledge. In [47], a scenario was investigated which is different from the currently introduced one: A time division multiple access (TDMA) communication protocol was considered. However, responses were scheduled using probabilities calculated in a very similar way to eqs. (3.18) and (3.20).

Figure 3.12 depicts on the y-axis the average CRBs normalized by the CRB of algorithm global-crb versus the number of anchors in the selected subset. The figure shows the average increase of CRB of each algorithm compared with that of global-crb. Specifically, for subsets of size 3, algorithm local-dist selects subsets that yield on average a 32-times worse CRB compared with global-crb. It is shown that the algorithms of class global knowledge have a better overall performance despite for $c = 3$. Here,

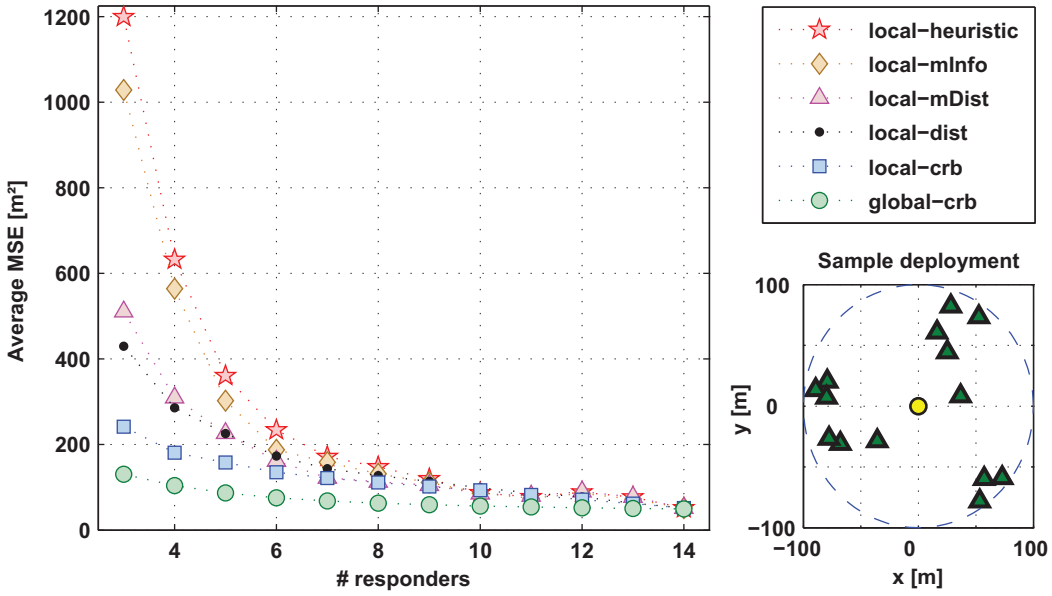

Figure 3.13: Comparison of algorithms for SSP. In this simplified scenario consisting of $N_A = 14$ (▲) uniformly deployed anchors and one location-unaware sensor (●), response order is determined based on the algorithm used and location-aware sensors contribute their measurements without having to compete for wireless channel access. The single location-unaware sensor estimates its location using MLE which uses a CL estimate as start point of optimization.

local-crb performs better as it prevents unfavorable sensors from responding which would lead, otherwise, to a CRB larger than the transmission range (see line 27 in table A.1). Furthermore, local-crb achieves a significantly lower CRB than local-dist.

The investigations show that sensor selection based on the CRB improves the lower bound on MSE compared with distance-based selection. The next investigations relax the requirement of synchronization associated with TDMA communications and evaluates the newly proposed algorithms in terms of MSE.

Analysis of MSE In this paragraph, the set of algorithms is extended and the MSE of localization is evaluated. The MLE is utilized to determine locations from perturbed distances and apply scheduling of responses as described in Sec. 3.3.4. Centroid Localization is used to provide a starting point for the optimization procedure of MLE. Additionally, the algorithms reviewed in Sec. 3.3.3 of Liu et al. (local-mInfo) [50], of

Zhao et al. (local-mDist) [91] and of Wang et al. (local-heuristic) [81] are considered in the comparison. The algorithms that utilize a grid-based representation of location distribution assume initially a uniform distribution over the deployment area. The resolution of the grid is 50×50 points which constitutes a resolution of 2 m. The computer simulation consists of 80 different random deployments. For each deployment, SSP is conducted in 2000 trials whereby in each trial the measurements of RSS are i.i.d. log-normal distributed, as described in Sec. 2.1. The figure of merit is the average MSE over all deployments.

Fig. 3.13 depicts the average MSE of location estimates against the size of the selected subset. The figure shows that global-crb yields the subsets which achieve smallest MSE of all selection algorithms, however, using global knowledge and true distances. The algorithms local-mInfo and local-heuristic achieve largest location error while local-mDist and local-dist show average accuracy of location estimates using estimated distances.

The large MSE of local-mInfo and local-heuristic has the following major reason. Both algorithms strongly rely on the selection of the first two responders. If these show an unfavorable spatial configuration, the subsequent selection is very likely negatively affected due to leadership-passing. In particular, the spatial configuration of sensors can be such that selecting a third location-aware sensor causes the CL start point for MLE to be far away from the true location of the requester. In such situations, MLE might only find a local optimum which leads to large location error. In contrast, local-crb and local-mDist favor subsets of location-aware sensors with favorable geometrical configuration which means that subsets are more likely to be evenly distributed around the location-unaware sensor. Therefore, these algorithms effectively lead to more accurate CL estimates and, therefore, a better total localization accuracy.

The impact of resolution of the posterior representation on algorithms local-mInfo, local-mDist and local-heuristic is minor since all algorithms use the same resolution but show different location errors.

The algorithm local-mDist, which uses the Mahabanolis distance of location distribution and basically considers solely the impact of geometry on MSE, achieves average MSE. Since distance-based selection, represented by algorithm local-dist, achieves slightly smaller MSE compared with local-mDist, it is concluded that the impact of

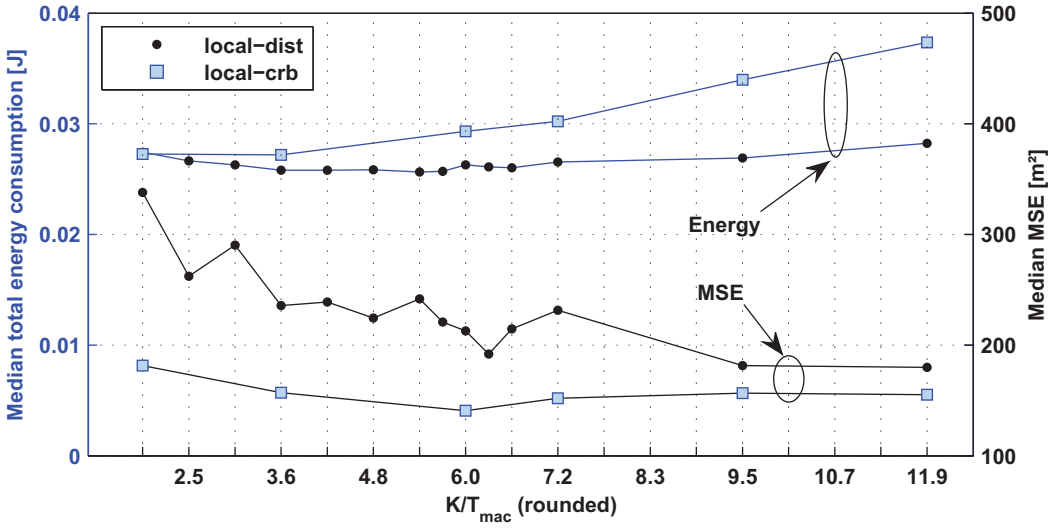

Figure 3.14: Comparison of algorithms local-crb and local-dist regarding MSE and energy consumption when anchors compete for the shared wireless channel. Results are shown for selection of 4 location-aware sensors and are depicted against pairs of parameters $\{K/T_{\text{mac}}, \alpha\} \in \{\{1.9, 3.28\}, \{2.5, 2.86\}, \{3.0, 2.65\}, \{3.6, 2.53\}, \{4.2, 2.44\}, \{4.8, 2.38\}, \{5.4, 2.34\}, \{6.0, 2.30\}, \{6.6, 2.27\}, \{7.2, 2.25\}, \{9.5, 2.20\}, \{11.9, 2.16\}\}$ whereby only the K/T_{mac} value is given on the axis.

geometry influences the MSE less strongly than the distance to the location-unaware sensor. However, considering both the impact of geometry and distance on MSE, as is done by algorithm local-crb, achieves smallest MSE among all algorithms with local knowledge. Especially for small subsets of three anchors, selection using local-crb yields at least 50% smaller location error than any other algorithm. This advantage withers, however, for subsets with more than ten anchors, where all algorithms show comparable performance.

Analysis of MSE regarding MAC collisions This paragraph focuses on algorithms local-dist and local-crb, investigates the impact of collisions on MSE using computer simulations. The simulations are identical to those of the previous paragraph with the exception that responders have to compete to access the wireless channel. Due to complexity of simulations, the 80 deployments were analyzed in only 1000 trials. Access to

the shared communication medium is performed using CSMA/CD which utilizes BEB to reduce packet loss in the presence of MAC collisions.

The parameters of wait time, K and α, are varied from values yielding high collision probability (3.25) to values yielding low collision probability but increased total energy consumption. The simulations show that the median MSE of local-dist decreases with increasing K which is tantamount to decreasing collision probability (Fig. 3.14). As expected, collisions perturb the calculated response order and, therefore, lead to larger localization errors. In this regard, algorithm local-crb shows a slightly different behavior since its MSE is less affected and has a minimum at $K/T_{\text{mac}} = 6$, $\alpha = 2.30$. This result emphasize that the optimized scheduling developed for local-dist does not apply for local-crb.

For small subsets of 4 location-aware sensors, local-crb achieves 46% to 14% smaller localization error compared with local-dist while requiring 0% to 32% more energy. Furthermore, local-crb achieves a better EE compared with local-dist in terms of LogarEEL (Fig. 3.15a). In particular, local-crb is 42% more energy efficient than local-dist for parameters $\{K/T_{\text{mac}} = 7.2, \alpha = 2.25\}$.

Impact of packet loss The considered algorithms utilize two different approaches to schedule the responses. While the proposed local-crb and local-dist algorithms perform distributed scheduling and delay responses based on deterministically calculated wait times, algorithms local-mDist, local-mInfo and local-heuristic apply the leadership-passing approach which elects a leader to contribute its measurement to the localization process. The next leader is determined based on previously contributed measurements. The latter approach can be regarded as quasi-centralized since each selection decision is made by a single sensor. Consequently, leadership-passing is sensitive to packet loss and failure of leader nodes which can lead to abort of the selection process. Fig. 3.15 depicts the probability of receiving at least n responses using either leadership-passing or local-crb / local-dist for different packet loss rates. The figure shows that local-dist and local-crb are more resilient to packet loss compared with leadership-passing and deliver 85% of responses with a probability of 0.97 for a packet loss rate of 0.05 while leadership passing's success probability is only 0.54.

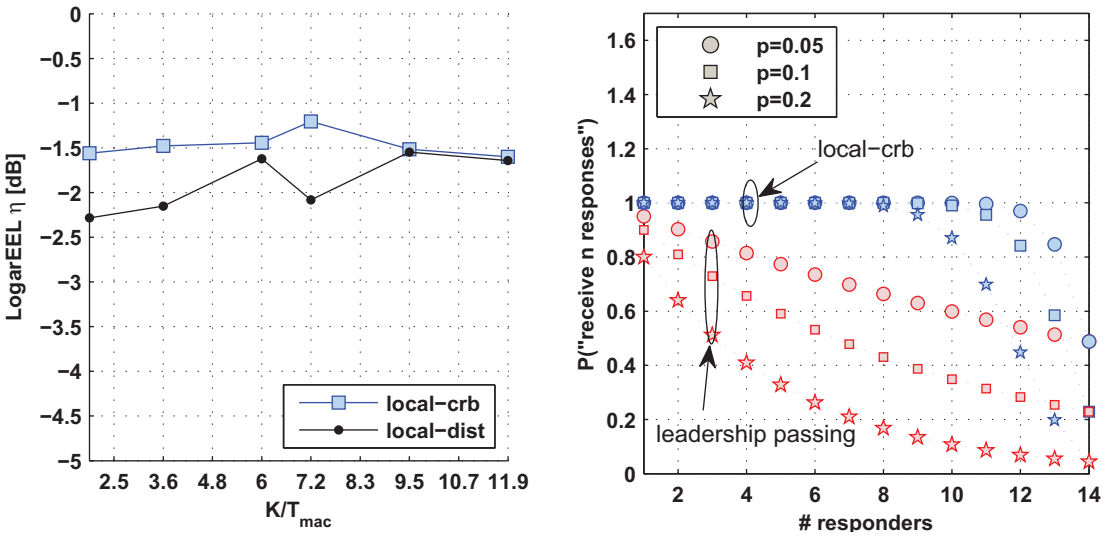

(a) Energy efficiency.

(b) Impact of packet loss.

Figure 3.15: Figure (a) depicts LogarEEL of local-crb and local-dist for subsets of 4 location-aware sensors. (b) Comparison of probability of successful receiving at least n responses vs. packet loss probability using either leadership-passing or scheduling as performed by algorithms local-crb or local-dist. Scheduling of local-crb / local-dist is more robust regarding packet loss and failure of sensors and achieves a higher response arrival rate.

3.3.7 Summary

A new algorithm to select efficient subsets for localization, referred to as local-crb, has been developed and analyzed using computer simulations (Sec. 3.3.4). The new algorithm utilizes the CRB, a lower bound on the variance of unbiased estimation, to characterize the utility of anchors to localization. The available anchors are scheduled in descending order of their utility by delaying their responses. The main advantages of the proposed algorithm are its low computational complexity, the fully distributed calculation of CRB which saves resources by avoiding additional communications and its comparatively high accuracy of location estimates.

Furthermore, an extension and reformulation of existing distance-based sensor selection has been investigated in Sec.3.3.4. The corresponding algorithm, referred to as local-dist, determines the utility of anchors using the distance to the location-unaware sensor whereby utility is smaller the more distant an anchors is. Anchors respond in

descending order of utility similarly to local-crb with the difference that the mathematical formulation of delays allows for optimizing the tradeoff between MAC collisions and total time of the selection process for randomly deployed networks. This way the energy consumption associated with the selection process have been minimized. The major advantage of this approach is that computations are even more simple than that of local-crb. However, location estimates using small subsets yield larger location errors. Although optimization of local-dist's scheduling achieved 10% savings of energy, the applicability of the result depends on whether the sensors are actually uniformly deployed.

In comparison with the reference algorithms, the presented approaches yield subsets which achieve average localization accuracy while being significantly less complex. Especially algorithms local-mInfo, which utilize grid-based representation of the location posterior, requires significant computation capabilities at the sensors leading to long delays during the selection process. However, performance of local-mInfo and local-heuristic strongly depend on a good selection of the first three location-aware sensors. Simulations have shown that these algorithms yield highest location error among the investigated algorithms. The major reason for this is that the start point for MLE is calculated using CL. Regarding local-mInfo and local-heuristic, this leads to start points far away from the true location and, therefore, to poor location estimates (Sec. 3.3.6).

Another disadvantage of leadership passing is that it calculates utility in a quasi-centralized way because typically only a single sensor decides on the next location-aware sensor to contribute its measurements. Consequently, corresponding algorithms are vulnerable to packet loss and might abort unintentionally whenever a message is lost, e.g. because of transmission errors or failure of sensors. In comparison, algorithms local-crb and local-dist can improve the success rate of responses significantly (Fig. 3.15b).

Chapter 4

Device-free Localization using Passive RFID

Although the Global Positioning System (GPS) has been accepted as a localization system for outdoor environments, its capabilities are very limited indoors since the satellite signals are typically strongly attenuated by walls and ceilings and, consequently, reception is limited inside buildings. However, especially localization of objects and persons plays an important role in intelligent environments. As illustrated in Sec. 1, location of users and devices are fundamental for these systems to provide assistance. Caring for the elderly constitutes another important potential application of intelligent environment which raises different requirements. Typically, intelligent systems, which are to provide assistance to elderly people, have to take explicitly into account that users might not "cooperate" with the system in the sense that they can forget to equip themselves with required devices or sensors. Consequently, a localization system is anticipated which does not or only weakly rely on user carried devices or sensors, which can provide sufficiently accurate estimates of the user's locations and which has very small installation and maintenance cost.

The main challenge for wireless localization systems is to provide accurate locations despite disturbances on the radio channel. Since the methods typically rely on measuring properties of radio propagation, the presence of obstacles in the vicinity of a radio link is known to influence the RSS on that link. Typically, these changes are re-

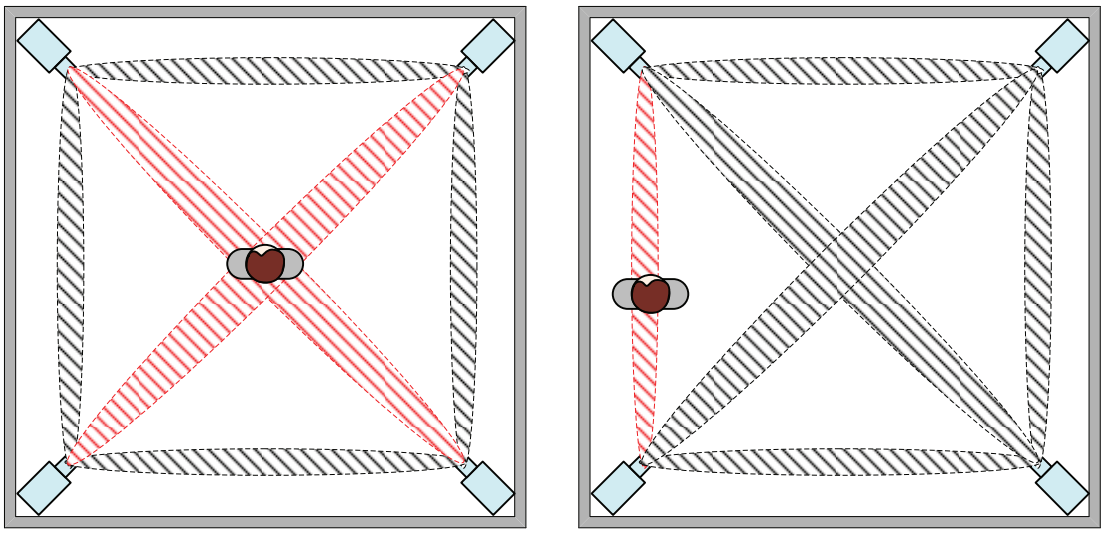

(a) **(b)**

Figure 4.1: The new approach presented in this chapter tracks back the changes of RSS caused by humans in the vicinity of radio links. The accuracy of the approach depends on the density of radio links: In 4.1b, the user can only be localized to somewhere within the grayed area on the left. In 4.1a, the user can be localized accurately due to its impact on two overlapping radio links.

garded as non-deterministic impact factor. The reason for this is that the environment's influence typically can neither be predicted offline, due to the many different objects that surround us, nor online as the density of radio links in conventional LPS is too small. Therefore, if there exist a feasible way to "sample" the space around an obstacle with sufficient frequency, meaning to establish multiple, partly overlapping radio links, and to be able to detect influenced links, it seems possible to narrow down the geographic location of the object by determining the overlapping area of some neighborhood of the affected links (see figure 4.1). As introduced in the introduction[1], this approach to localization is referred to as *Device-Free Localization (DFL)*. Summarizing, in order to enable DFL, a technology needs to be found which communicates over radio, is able to measure RSS of radio links and with which a multitude of physically adjacent radio links can be established without requiring too much effort regarding cost,

[1] see Sec. 1 on p. 10

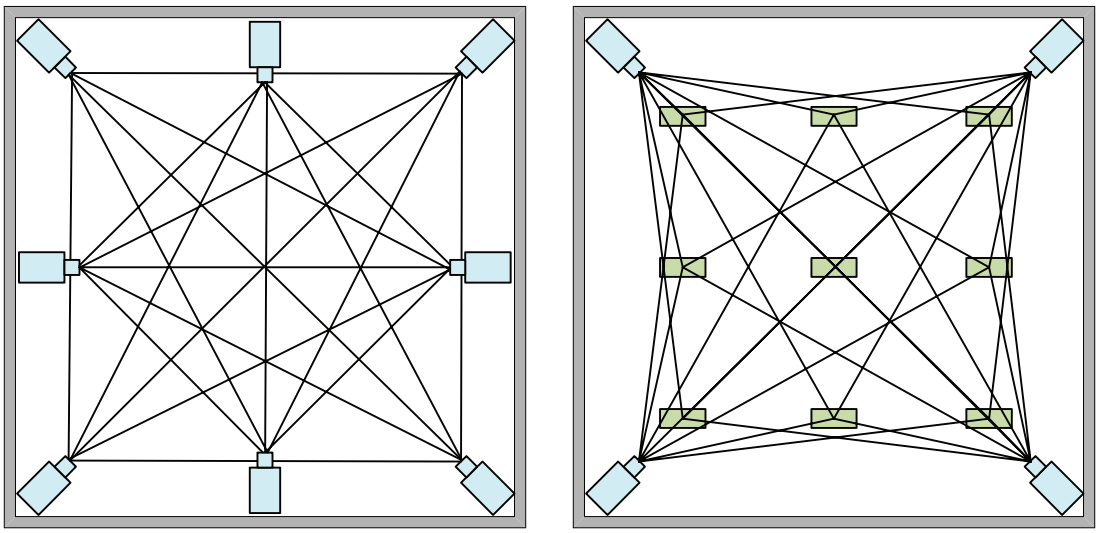

(a) Conventional LPS. **(b)** Passive RFID.

Figure 4.2: Passive RFID enables inexpensive deployment of a dense field of radio links. (denotes passive RFID tag, denotes a sensor).

installation and maintenance. In addition, as one of the important often cited properties of intelligent environments is that they "weave themselves into the fabric of everyday life", its parts should be physically, referring to its size, and visually not too attention-attracting[2].

The proliferation of *Automated IDentification technology (AutoID)* in the past centuries has resulted in the RFID technology. As illustrated in Sec. 1.2, this technology has several of the aforementioned properties. First, these systems communicate wireless and RSSI is often made available through the software API of the reader. Secondly, since the small and inexpensive passive tags are powered remotely by the reader, their size is very small and they can be attached to many objects and surfaces. Typically, UHF tags are about $10\,\text{cm} \times 1.5\,\text{cm}$ and thin as paper. Consequently, realization of a large number of radio links using passive RFID is facilitated while deployment of passive tags incurs only small cost (see figure 4.2b).

In the light of these considerations, this chapter investigates a localization method for coarsely populated environments which utilizes the change of RSS in a passive RFID

[2]Comment of Marc Weiser [3].

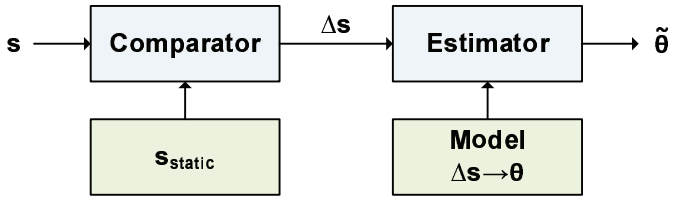

Figure 4.3: Overview on DFL which uses measurements of RSS to obtain an estimate $\tilde{\boldsymbol{\theta}}$ of the user location without requiring the user to carry localization devices. The approach is based on a model relating user location and change of RSS $\Delta\mathbf{s}$.

system to track the changes back to their origin which is regarded as the sought location. Figure 4.3 provides an overview on the approach. Online measurements of RSS are compared with static measurements that were conducted without user presence. The difference signal Δs is input to an estimator of location that utilizes a specific model of the relation between user location θ and Δs. It is noted that once the RFID system is installed, training measurements are carried out in a fully automated manner which does not require human interaction as is the case with conventional radio-map based localization algorithms [49]. Other key advantages are that 1) the accuracy of location estimates scales with the number of inexpensive passive tags, 2) the system does not require the user to be equipped with sensors and 3) provided the RFID-reader has fixed power supplies, the system has very small maintenance cost since, compared to conventional localization systems, tags are passive and do not need to be resupplied with batteries. Furthermore, the developed localization techniques yield sufficient accuracy to support many applications within intelligent environments.

The chapter is structured as follows. Sec. 4.1 focuses on recent applications of RFID systems and investigates the state-of-the-art regarding localization with passive RFID. Sections 4.2 and 4.3 investigate measurements conducted in a simplified scenario, develop the analytical observation model and derive localization techniques. Sec. 4.4 considers a larger deployment and focuses on statistical analysis of measurements and estimating the location of a stationary user. Before Sec. 4.6 summarizes the chapter, Sec. 4.5 investigates using computer simulations the applicability of RBEs to tracking the location of a mobile user.

4.1 Survey of Applications of RFID to Smart Environments

Due to its interesting properties, RFID has been used in many research projects considering pervasive and ubiquitous computing. This section presents the state-of-the-art of localization using RFID. The objective is to provide a solid basis to compare and evaluate the new approach.

The wide range of possible applications of RFID spans from logistics, asset and supply chain management over distributed information, guidance and navigation systems to health care applications and assisted living. Applications typically benefit from the small size, the inexpensiveness and low maintenance cost associated with RFID. Although this section aims at providing an overview, the scope of the survey is limited to applications related to ubiquitous environments and pervasive computing as to focus on the topics which are most related to the topic of this thesis. Therefore, determining and tracking of location of persons is the main focus. A recent survey on indoor localization can be found in [8, 49].

Liu, Corner and Shenoy investigated a prototype called *Ferret* which utilizes passive RFID-tags [85]. Ferret considers localization of nomadic objects and utilizes the directionality of RFID-readers. The idea is to exploit different poses of the reader to narrow the object location down. Ferret also utilizes a bistatic passive RFID-system similar to the one considered in the thesis. The Smart Watch prototype developed by Borriello et al. is a system that generates reminders for lost objects that have been tagged with passive RFID tags [15]. It utilizes stationary RFID readers that scan their environment and report the tagged objects using short-range broadcasts. These reports are input to the user's personal server which determines whether a reminder should be send.

While reminding users of important objects already provides some kind of ambient assistance, the research field of *assisted living* takes another step and considers supporting people in need of assistance in their everyday life. In particular, several approaches aim at supporting people with visual impairment and help them to navigate in unknown environments. For example, Kulyukin et al. investigate a robot-assisted guidance system. The robot is equipped with an RFID reader and the environment is augmented

with passive RFID tags [43]. Tag readings are used to create a virtual potential field which virtually repulses the robot away from tagged obstacles and attracts it towards the target location.

Willis and Helal consider a self-describing, localized information system which consists of a grid of passive RFID tags [83]. Tags are programmed upon installation with their geographical coordinates and a description of their surrounding. The authors adopt the *Smart Floor* [59] for establishing the RFID infrastructure and integrated RFID readers in the user's shoes which are connected to a PDA via Bluetooth. On the PDA runs a software which interprets the data from the RFID reader and issues voice outputs to inform the user about its location. When pointing with one shoe in a specific direction the system is also able to provide directional information.

In [7], Amemiya et al. present a prototype implementation of a navigation system for deaf-blind people. The approach comprises a localization system consisting of active RFID tags integrated in the floor, a tactile feedback system and a user worn bag pack containing a computer and RFID reader devices. The basic idea is that the user location at time t can be calculated as the centroid of RFID tags currently in range of the reader.

Besides applications that explicitly focus on supporting the user in an intelligent environment, other approaches simply focus on determining the location of users in indoor environments. One biometric approach is proposed by Orr et al. [59]. Within the Smart Floor Project, they consider using a grid of pressure sensors embedded in the floor to track and identify users. One distinguishing feature of the approach is that, similar to the approach presented in this chapter, the user does not need to carry devices dedicated to localization. Users are identified by matching the measured pressure profile to training data. This way a success rate of 93% is achieved regarding user identification. One drawback is that in order to enable the full detection accuracy, users need to step exactly on the presure sensors which is unrealistic in practice. Furthermore, since localization is based on proximity, the spacing between pressure sensors is critical to the location accuracy. In order to improve the resolution more sensors can be employed, however, with substantial additional cost since sensors are active, need to be connected with wires and are expensive compared with passive RFID tags.

Vorst et al. investigate in [80] localization of mobile devices like robots and

also persons in indoor environments. They consider three different radio technologies namely passive RFID, BlueTooth and WLAN. Each technology provides distinct measurements with different characteristics. The objective is to characterize the performance of the three technologies by tracking the position of a mobile robot. The authors show that in an experimental setting consisting of a mobile robot equipped with BlueTooth, RFID reader antennas and WLAN card can be localized accurately using RFID and BlueTooth while WLAN provides relatively coarse location information, however, with extended coverage. The approach's drawback is that the models for RFID need to be trained and have to be obtained a-priori. Furthermore, the robot itself carries the relatively large RFID antennas putting a high physical burden on the mobile object whereby it is not expected that these antennas will become significantly smaller in the future without decreasing their range.

Infineon financed the development of a localization prototype for tracking objects in an industrial waver production facility. Within this project, Thiesse et al. developed a localization system that utilizes active RFID and ultrasonic emitters to track and identify waver boxes [78]. The aim was to make the whole production cycle more transparent and provide a basis for optimizing lead times etc. The approach exploits the special topology of the production facility which consists mainly of long, narrow corridors. Specifically, a simplified lateration procedure was proposed that described the location as corridor X and a distance to one of the corridor ends rather than using metric coordinates. An accuracy of location estimates of 30 cm is reported.

Ni et al. propose *Landmarc*, a localization system that is based on stationary RFID readers and uses active tags. The purpose of active tags is twofold. First, several tags are attached to reference locations and their RSSI profile serves the readers as "landmarcs". The object to be tracked is also equipped with an active tag. The RSSI profile of the object tag is compared with that of the reference tags. The estimated location of the object is calculated as the centroid of the reference tags whose RSSI profile are most similar to the measurement. Basically, the use of reference tags aims at mitigating the impact of anisotropic radio propagation which is caused by obstacles, non-ideal antenna patterns etc. However, since the tags are active the approach is limited in the sense that maintenance cost limits the maximum number of references.

The previously reviewed approaches, except [59], have in common that the user

needs to be equipped with a communication device in order to enable localization. However, the proliferation of small and cost-effective miniaturized transmitter have fostered the idea to utilize the impact of the human body on radio communications for localization. Specifically, the commonly understood adverse effect of human presence to occlude the LOS of radio links and impact severely link quality, can be used to backtrack the information about which link is affected to localize the user. In the following, the state-of-the-art regarding the application of DFL is reviewed.

All previous works on exploiting the human impact on radio links for localization, i.e. radio tomographic imaging, considered wireless sensor motes [36, 40, 41, 61, 87–89]. Wireless sensor motes were the first technology to enable cost-effective and flexible establishment of radio links in numbers large enough to achieve feasible accuracy of DFL. Zhang et al. deployed a grid of ceiling mounted sensor motes and proposed to use the absolute change of RSSI to detect the passing of a human [89]. The authors report on the performance of their method in a $12\,\mathrm{m} \times 9\,\mathrm{m}$ deployment of 16 ceiling mounted sensors. Their method achieved 3 m localization error in 95% of test positions. In a later work, the authors improved localization accuracy to 2 m and reported on the ability to distinguish between multiple targets, however, without quantitive performance analysis.

Youssef et al. investigated the detection of changes and tracking of persons using the associated change of RSSI [87]. Regarding detection, they propose to use the moving average of RSSI or its variance whereby the use of variance yields increased success rate. Furthermore, they investigate tracking of a single person using an offline measured passive radio map. Basically, this map associates a change of RSSI with a specific location of the person.

Patwari and Agrawal coined the term radio tomographic imaging and reported on the similarity between tomographic imaging in medicine and other sciences and the impact of obstacles on radio links. In analogy to tomographic reconstruction, they consider the space between transmitter and receiver as a loss-field. In light of these considerations, they regard the attenuation of a radio link between any two points as given by a simple line integral over the loss field. Figure 4.4 illustrates the situation for one transmitter and two receivers. In this case, the presence of an obstacle for radio communications is represented by high values of the loss field at the corresponding

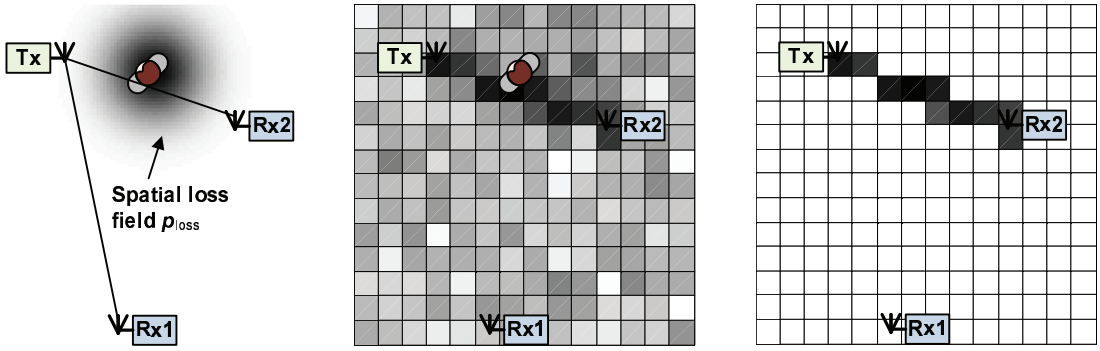

(a) Sample scenario. **(b)** Estimated loss field. **(c)** Estimated user location.

Figure 4.4: Referring to radio tomographic imaging, the attenuation on radio links can be modeled as line integrals over a spatial loss field. This model can be used to estimate the user location by detecting occluded radio links.

geographic locations. The attenuation a on the two links from Tx to either Rx1 or Rx2 is given by line integrals of the form $a \propto \int_{\mathbf{z}_{tx1}}^{\mathbf{z}_{rx}} \mathbf{p}_{loss}(\mathbf{y})\, dy$ whereby $\mathbf{z}_{rx}$ represents either the location of Rx1 or Rx2. Consequently, their approach is to estimate the loss field from measurements of RSSI and consider peaks of the loss field as target locations. The strength of their approach lies in the opportunity to apply existing techniques from the mature field of tomographic imaging to the new application domain.

As a first approach they showed in [61] that DFL is possible using a weighted linear least squares estimator. Furthermore, they published a video demonstrating the capability of their approach to track a person in a narrow area [62]. The coverage of the proposed method is, however, limited by the wireless range of the sensor motes whereas the accuracy scales according to the number of sensors. Since Patwari et al. utilize a linear estimator for non-linear[3] measurements, their approach is suboptimal. Furthermore, the application of their method is constrained by the physical size of the sensors. In order to achieve localization accuracy of less than one meter, one had to use a large number of sensors. Attaching sensors in such quantities in intelligent environments may distract the user visually or is merely not cost-efficient enough due to maintenance of the battery-powered sensors. Possible applications are to determine the location of sniper or hostages by police men. Also the technique can be used by first

[3] See Sec. 4.2 for detailed explanation.

responders looking for signs of life in buildings which are too dangerous to enter since the method's ad-hoc nature makes it especially applicable in these scenarios.

The method of Patwari et al. is further refined by Kanso and Rabbat [36]. They recognize that the measurements are sparse in situations where only few targets move in the deployment area which is the case during night times. They propose to use a variation of the weighted least squares estimator of [61] which they refer to as compressed RF tomography. Compressed RF tomography accounts for the sparsity of the measured RSSI signals and the authors propose centralized and decentralized versions of their algorithm.

Another approach which does not rely on user carried devices is to use the *Infrared Radiation (IR)* emanated by warm objects and also mammals and humans. Kemper and Linde investigate in [40, 41] the challenges and performance of this approach for localization. They installed three infrared sensor in the corners of a $5\,\mathrm{m} \times 4.7\,\mathrm{m}$ room and report a maximum localization accuracy of 80 cm. A drawback of the approach, as pointed out by the authors, is that the accuracy of IR localization is subject to several error sources. Some of the error sources are similar to the phenomena rendering indoor radio localization challenging. For example, IR can be reflected by metallic surfaces and is also subject to occlusion and background noise. However, the major drawback is that the IR signals are of rather limited usefulness for communications, two different technologies have to be implemented on the measurement device to enable sensing and communication. This makes application of the approach in WSN and smart environments difficult due to cost of installation and since the sensors constitutes specialized hardware and no *Commercial Off-The-Shelf (COTS)* products. A related approach is considered by Zhang et al. in [90].

Currently, the field of radio tomographic imaging, device- or transceiver-free localization, which refer to the exploitation of the same phenomenon to localize users, has attracted soaring research interest. Many of the presented works were published in 2008 / 2009.

The new approach presented in this chapter distinguishes itself from previous ones as it uses passive RFID to establish the large number of radio links in a cost-efficient and unobtrusive way. Furthermore, two novel estimators for the target location are proposed which are based on the newly developed analytical model of the impact of

the target's location on RSSI. In particular, the high accuracy of the model is the basis for the high accuracy of estimated locations and also enables tracking techniques like the EKF and PF. In the following, the works reviewed so far are compared regarding the following properties: tag and measurement type, whether they belong to DFL, lifetime, unobtrusiveness and whether they build on an accurate model of measurements. The figure of merits are explained in the following.

Type of measurements Does the approach utilize delay, phase and/or the strength decay of radio signals? Typically, radio localization exploits that characteristics of radio waves change while waves propagate through space. Furthermore, since radio waves propagate with a finite velocity, the delay between emitting and receiving radio waves can be used as an indicator of the distance between emitter and receiver.

Device-Free Localization Is it necessary to equip the target with devices to enable localization? While facilitating measurements, carrying radio tags imposes a further requirement the target has to adhere to. Therefore, approaches which do not require the target to carry such tags, so called device-free approaches, are attractive. It is noted that DFL does not rely on user carried tags but instead, the tags might rather be deployed in the environment.

Type of tags Are passive or active tags used? While active radio tags are equipped with batteries, passive tags solely use impinging radio energy for operation. Although active tags are more robust and long-range communication, passive tags have advantages in applications emphasizing low maintenance cost and long-term, unattended operations.

Lifetime The devices assumed by the algorithms are either battery-powered and have limited lifetime whereas those using fixed power supply have unlimited lifetime. Passive RFID-systems constitute a hybrid approach as the majority of sensors in these systems are passive and only the reader device needs fixed power supplies.

Unobtrusiveness The scale of the sensors that need to be deployed in the environment determines how aware the users will be of the system and its components. Although wireless sensors like the Mica2 mote have benefited from the ongoing miniaturization of MEMS, they appear large when compared with passive RFID tags that often are only $10\,\text{cm} \times 1\,\text{cm}$ large and thin as paper. The few RFID antennas can be easily incorporated in the environment, e.g. in the ceiling. In contrast incorporating a large number of COTS wireless sensor motes in the environment is considerably more difficult today in terms of maintenance, power supply etc.

Model-driven Model-driven approaches assume analytical relations between measurements and locations of objects and users to be localized which can be used to *predict* measurements. The strength of these algorithms is that they potentially yield highly accurate location estimates in case the model describes measurements correctly.

Table 4.1: Overview of related work.

	Tag Type	Measurement	DFL	Lifetime	Unobtrusive	Model-driven
Object Finding/Reminder						
Borriello et al. [15]	Passive	Connectivity	No	Unlimited	Yes	N / A
Ferret [85]	Passive	Connectivity	No	Unlimited	Yes	Yes
Assisted Living						
Willis et al. [83]	Passive	Connectivity	No	Limited	Yes	No
Amemiya et al. [7]	Passive	Connectivity	No	Limited	Yes	No
Kulyukin et al. [43]	Passive	Connectivity	No	Limited	n/a	Yes
Indoor User/Object Localization						
Orr et al. [59]	Active	Proximity	Yes	Limited	Yes	Yes
Landmarc [57]	Active	RSS	No	Limited	Yes	No
Thiesse et al. [78]	Passive	RSS/Sound	No	Limited	Yes	No
Vorst et al. [80]	Both	RSS/Conn./ToA	No	Limited	Partly	Yes
Device-Free Localization						
Zhang et al. [88, 89]	Active	RSS	Yes	Limited	No	Yes
Patwari et al. [61]	Active	RSS	Yes	Limited	No	Yes
Kemper et al. [40]	Active	IR	Yes	Limited	No	Yes
New approach	Passive	RSS	Yes	Unlimited	Yes	Yes

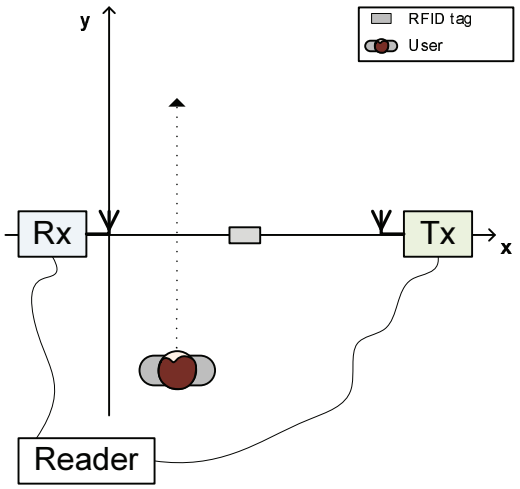

Figure 4.5: Set-up of measurements. The test person moves stepwise in the indicated direction while the RFID reader measures the RSSI of the radio link to the passive tag.

4.2 Initial Observations Using a Passive RFID-System

Having surveyed the state-of-the-art, this section focuses on the main idea of the novel localization approach. First, the results of an experiment conducted with a passive RFID system are analyzed and used as empirical evidence for the feasibility of the approach. Secondly, an analytical model of the empirical findings is derived which will be the basis for the subsequent sections. Finally, the parameters of the model are discussed.

4.2.1 Set-up and Procedure of Measurements

The main objective of the experiment is to provide evidence for the impact of a human on radio links of a bistatic, passive RFID system. For this purpose, a simple scenario was investigated which consisted of an RFID reader with one pair of transmitting and receiving antennas and one passive RFID tag. The measurements were conducted in a 8.15 m $\times$ 6 m rectangular room[4]. The circular polarized antennas are situated at coordinates (0,0) and (3.5,0) at a height of 1.8 m. One RFID-tag is attached to the carpet at coordinates (1.75,0) and its long axis parallel to the line connecting

[4]The room is located in the Institute of Applied Microelectronics and Computer Engineering in Rostock-Warnemünde and numbered 1227 in house 1.

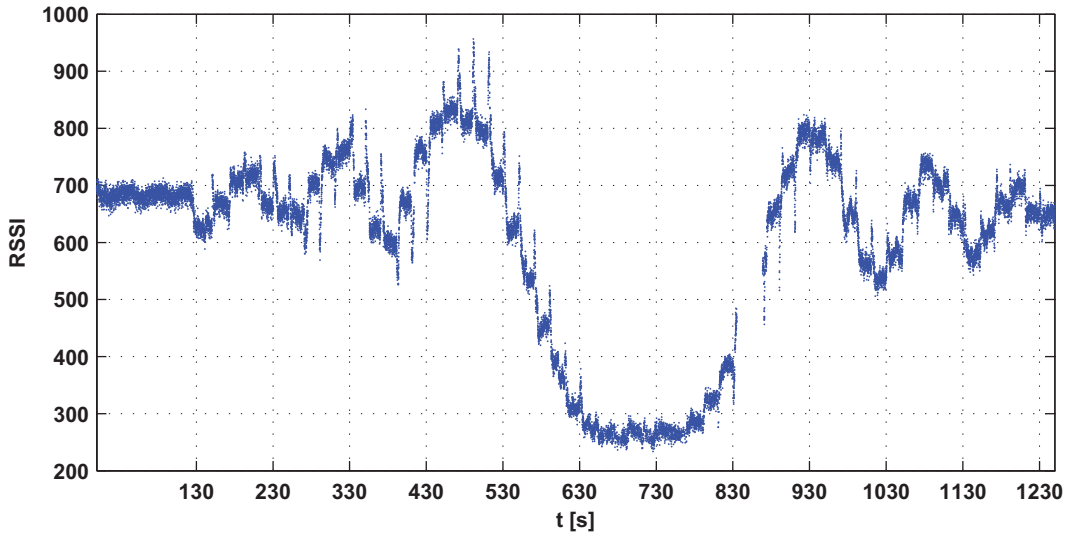

Figure 4.6: RSSI over time as measured by the deployment of Fig. 4.5. The spikes indicate the times when the test person moved forward.

the antennas (Fig. 4.5). There are $N_a = 1$ antenna pairs, $N_t = 1$ tags and, consequently, $N_{meas} = N_a N_t = 1$ radio links.

At the beginning of measurements, the test person was situated at $(0.865, -1.45)$. The measurement procedure was divided into time slots of 20 seconds. At the beginning of each time slot, the test person moved 0.05 meter in the positive y-direction which took no more than 5 seconds. After having moved, the test person remained stationary until the end of the time slot and continued moving in the next time slot. The RSSI is continuously measured by the RFID-reader which includes both stationary and movement phases. During the measurements, it was ensured that any objects other than the test person in the vicinity of communication links were stationary.

Analysis of Measurements

The stationary and movement phases of the test person are clearly indicated by spikes in the RSSI vs. t plot (Fig. 4.6). However, the average of RSSI measured in the stationary phase show are strongly affected if the test person is close to the LOS of the radio link, e.g. $y \approx 0\,\text{m}$, (Fig. 4.7). Outside this zone, however, the plot shows an oscillating behavior as RSSI is attenuated and amplified in turns. The results show that the

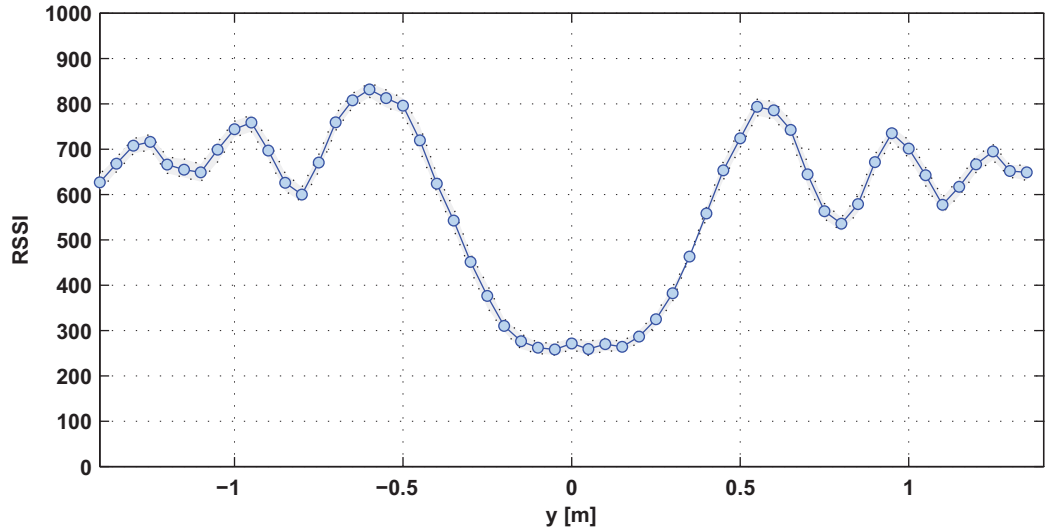

Figure 4.7: RSSI versus user location. The shaded area depicts the inner 90% quartile of measurements indicating their spread. (Initial measurements $t < 130\,\mathrm{s}$ and measurements during movements are omitted).

RSSI depends on the test person's location and is a combination of deterministic effects and random errors. Judging from the shape of the curve, the RSSI is a non-linear, non-injective function f of the user location. Due to the non-injectiveness, the mapping of RSSI to location is ambiguous as one RSSI value can be measured at multiple locations. Due to this property, it is not possible to unambiguously determine the person's location given an RSSI measurement on a single radio link. In particular, there are many locations that could potentially cause such a measurement.

To enable localization based on the above findings further investigations are needed. As a first step, Sec. 4.2.2 characterizes the functional dependence of RSSI on the target location in more detail.

4.2.2 Derivation of Observation Model

In this section, the measurements of Sec. 4.2.1 are regarded as the result of the superposition of radio waves. First, a model of the radio signals in the considered RFID-system is introduced. Then, the model is used to calculate the theoretical change of received signal strength at the receiver given the location of a person causing radio scatter.

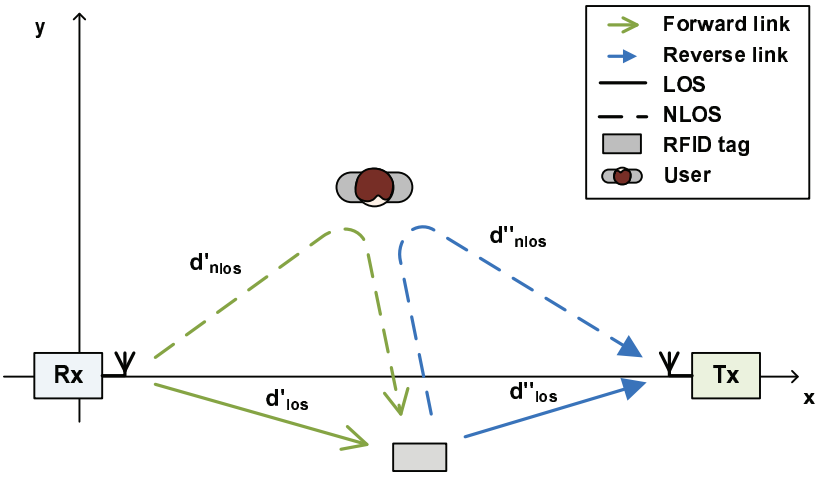

Figure 4.8: Humans contribute to the fluctuations on the RFID-link and lead to attenuation and amplification according to the phase difference of direct and reflected radio waves at the receiving antenna.

The RFID system operates in the 868 MHz *Industrial, Scientific, and Medical frequency band (ISM)* and transmissions allocate a bandwidth of 200 kHz. In such systems, the bandwidth is small compared with the carrier frequency. Since the current investigations focus on RSS, it is reasonable to approximate such radio signals as pure tones. On this basis, a typical radio signal can be described by its carrier (4.1).

$$\underline{A} = A\, e^{j\omega(t-d/c)} \tag{4.1}$$

Whereby c is the propagation speed of the signal, d the distance covered by the signal, $\omega = 2\pi c/\lambda$ and λ is the wave length. Without loss of generality, it is assumed that the initial phase of the signal equals zero.

In the following, the terms transmitter and receiver refer to the corresponding devices of the forward and reverse link of a bistatic RFID system as illustrated in Fig. 4.8. Transmitter denotes either transmitting antenna or tag depending on whether forward or reverse link is considered. Similarly, receiver either refers to the tag on the forward or to the receiving antenna on the reverse link. Furthermore, the path length of indirect and direct radio signals are indicated by subfixes $(\cdot)_{\mathrm{nlos}}$ and $(\cdot)_{\mathrm{los}}$.

The reference signal $\underline{A}_{\mathrm{los}}$ reaches the receiver on the direct path, hence, the re-

ceiver observes $\underline{A}_{\text{los}} = A_{\text{los}} e^{j\omega(t-d_{\text{los}}/c)}$. It is further assumed that a person is present in the vicinity of the line segment between transmitting and receiving antenna and reflects significant part of the radio energy. Therefore, a second signal $\underline{A}_{\text{nlos}}$ with same frequency but different energy $|\underline{A}_{\text{nlos}}|^2$ and phase interferes at the receiver $\underline{A}_{\text{nlos}} = A_{\text{nlos}} e^{j(\omega(t-d_{\text{nlos}}/c)+\phi_{\text{refl}})}$.

The signal energy, i.e. RSS $s = |\underline{A}|^2 = \underline{A}\underline{A}^*$, at the receiver can be formulated as the sum of the radio waves from the scattering object and from the transmitter:

$$\underline{A} = \underline{A}_{\text{los}} + \underline{A}_{\text{nlos}} \tag{4.2a}$$

$$= A_{\text{los}} e^{j(\omega(t+d_{\text{los}}/c))} + A_{\text{nlos}} e^{j(\omega(t+d_{\text{nlos}}/c))} e^{j\phi_{\text{refl}}} \tag{4.2b}$$

$$\begin{aligned} s = &\left(A_{\text{los}} e^{j(\omega(t+d_{\text{los}}/c))} + A_{\text{nlos}} e^{j(\omega(t+d_{\text{nlos}}/c)+\phi_{\text{refl}})}\right) \\ &\cdot \left(A_{\text{los}} e^{-j(\omega(t+d_{\text{los}}/c))} + A_{\text{nlos}} e^{-j(\omega(t+d_{\text{nlos}}/c)+\phi_{\text{refl}})}\right) \end{aligned} \tag{4.2c}$$

$$= A_{\text{los}}^2 + A_{\text{nlos}}^2 + 2A_{\text{los}}A_{\text{nlos}} \left[e^{-j\left(\omega\frac{d_{\text{nlos}}-d_{\text{los}}}{c}+\phi_{\text{refl}}\right)} + e^{j\left(\omega\frac{d_{\text{nlos}}-d_{\text{los}}}{c}+\phi_{\text{refl}}\right)}\right] \tag{4.2d}$$

$$= A_{\text{los}}^2 + A_{\text{nlos}}^2 + 4A_{\text{los}}A_{\text{nlos}} \cos\left(\frac{2\pi}{\lambda} d_{\text{exc}} + \phi_{\text{refl}}\right) \tag{4.2e}$$

Here, $(\cdot)^*$ denotes complex conjugation, ϕ_{refl} the phase shift due to reflection, $\underline{(\cdot)}$ a complex variable. The parameter d_{exc},, called *Excess Path Length (EPL)*, has been introduced which is important as it determines whether signals add constructively or destructively.

$$d_{\text{exc}} = d_{\text{nlos}} - d_{\text{los}} \tag{4.3}$$

To characterize the change of signal energy Δs, (4.2) is reformulated by subtracting the LOS signal energy:

$$\begin{aligned} \Delta s &= s - |\underline{A}_{\text{los}}|^2 \\ &\approx 4A_{\text{los}}A_{\text{nlos}} \cos\left(\frac{2\pi}{\lambda} d_{\text{exc}} + \phi_{\text{refl}}\right) \qquad A_{\text{los}} \gg A_{\text{nlos}} \end{aligned} \tag{4.4}$$

Equation (4.4) can be used to predict the change of RSS given the amplitudes of LOS

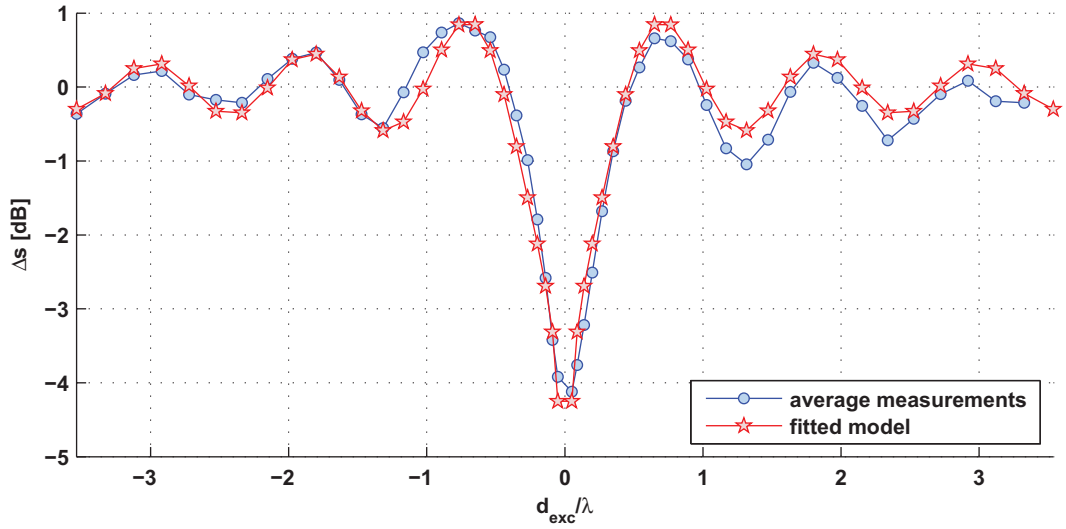

Figure 4.9: RSSI in dB vs. EPL d_{exc}. The blue line denotes the average of measurements and the red line the results provided by fitting the model (4.5). The parameters of the fit are $A = 0.34$, $B = -0.68$, $\lambda = 0.39\,\text{m}$ and $\phi_{\text{refl}} = 2.18$.

and *Non-Line-of-Sight (NLOS)* signals, the wave length λ, EPL d_{exc} and phase offset due to scattering ϕ_{refl} on forward and reverse links. It is noted that the amplitude of radio waves dissipates with distance and, therefore, the signal energy at the receiver does not only depend on the EPL but also on the absolute distances between the antennas and the obstacle. The amplitude $4A_{\text{los}}A_{\text{nlos}}$ of the superimposed radio wave is dominating by its smallest factor which is the amplitude of the indirect path A_{nlos}. Therefore, it is assumed that the amplitude of the superimposed radio signal for a given radio link obeys the power-law concerning the EPL which yields using (4.4) and parameters A, B, λ and ϕ_{refl}.

$$\Delta s \approx A d_{\text{exc}}^{B} \cos\left(\frac{2\pi}{\lambda} d_{\text{exc}} + \phi_{\text{refl}}\right) \tag{4.5}$$

Fitting the model (4.5) to the measurements presented in Sec. 4.2.1 in the least-squares error sense yields very good approximation (Fig. 4.9). It is noted that only the reverse link was considered for the fitting since the test person's influence on the forward link was assumed to be insignificant due to the large distance (Fig. 4.5).

It is noted that in general there will be more than one excess path. In this case, (4.4)

can be reformulated to accommodate for the interference between each pair of impinging signals.

$$\Delta s \approx \sum_{i=1}^{M} \sum_{j>i}^{M} 4A_i A_j \cos\left(\frac{2\pi}{\lambda} d_{\text{exc,i,j}} + \phi_{\text{refl,i,j}}\right) \tag{4.6}$$

Where A_1 denotes the LOS component, M denotes the total number of significant propagation paths and $A_1 \gg A_i \quad (i > 1)$. However, signals which undergo multiple reflections are most often too weak to be significant. Consequently, the simplified model of (4.5) is assumed and used in the remainder of the thesis.

4.3 Localization Techniques

In the following, two different approaches are followed to apply the findings of Sec. 4.2.2 to DFL. The first approach builds on the non-linear observation model which relates the user location to an predicted change of RSSI. A grid-based approach is utilized since the characteristics of the observation model (4.5) prevent an analytical calculation of the user location. The measurements are compared with the predictions calculated by the observation model assuming the user resides at a specific grid-point. The estimated location is regarded as the grid-point whose prediction best matches the measurements in the MLE sense.

The second approach is motivated by the observation that the largest change of RSS occurs whenever the user is very close to the LOS of a radio link. Therefore, points where strongly affected links intersect concentrate in the vicinity of the user. Based on these considerations, an estimator is developed which calculates the estimated user location as the centroid of the intersections of strongly affected links.

To facilitate the following investigations, several notations are introduced. N_t and N_a denote the total number of RFID tags and the number of antennas used for the experiments, respectively. The elements of the vector $\Delta\tilde{\mathbf{s}} = [\Delta\tilde{s}_{1,1}, \ldots, \Delta\tilde{s}_{1,N_\text{t}}, \Delta\tilde{s}_{2,N_\text{t}}, \ldots, \Delta\tilde{s}_{i,j}, \ldots, \Delta\tilde{s}_{N_\text{a},N_\text{t}}]^\text{T}$ denote the stacked measurements on the radio link corresponding to i-th antenna pair and j-th tag. The vector $\Delta\mathbf{s}$ has identical structure but its elements are given by the predicted change of RSSI

$\Delta s_{i,j}$ on a link. Each link corresponding to an element of $\Delta\tilde{\mathbf{s}}$ is identified by an index $l = 1,\ldots,N_{\text{meas}}$. In total there are $N_{\text{meas}} = N_{\text{a}}N_{\text{t}}$ measurements. The set of all links is denoted by $\mathcal{L} = \{l : l = 1,\ldots,N_{\text{meas}}\}$. Consequently, the measurements which satisfy a specific condition, e.g. $\Delta\tilde{s} > X$, can be referred to as the set $\{\Delta\tilde{s}_l : \Delta\tilde{s}_l > X, l \in \mathcal{L}\}$.

4.3.1 Maximum Likelihood Estimation

The Maximum Likelihood Estimator has been applied to problems in a large range of sciences. The method draws its popularity from the fact that it often allows to implement practical estimators in even complicated problems where the minimum variance estimator can not be found [39]. The method is based on the PDF p of a sequence of measurements and utilizes the dependence of p on the sought parameter. In the considered case, p is the PDF of measurement $\Delta\tilde{s}$ on a specific radio link and the user location $\boldsymbol{\theta}$ is its parameter. To characterize p further, an additive, white Gaussian error model of measurements is proposed and validated in Sec. 4.4.3. Stacking the N_{meas} measurements on all radio links yields the error model in vector form (4.7).

$$\Delta\tilde{\mathbf{s}} = \Delta\mathbf{s}(\boldsymbol{\theta}) + \mathbf{n} \tag{4.7}$$

$$n_i \propto N(0,\sigma_{\Delta s}^2) \qquad i = 1,\ldots,N_{\text{meas}} \tag{4.8}$$

Basically, the model suggests that measurements satisfy a Gaussian distribution with mean given by the theoretical change of RSS $\Delta\mathbf{s}$ and variance $\sigma_{\Delta s}^2$. To facilitate the following presentations, the dependence of the elements of $\Delta\mathbf{s}$ on θ are omitted wherever the context allows for it.

Concerning the current localization problem, the location $\tilde{\boldsymbol{\theta}}$ of the user is sought which best fits the measurements $\Delta\tilde{\mathbf{s}}$. In other words, the PDF $p(\Delta\tilde{\mathbf{s}};\boldsymbol{\theta})$ of measurements is regarded as a function of the true user location $\boldsymbol{\theta}$ as indicated by (4.7).

$$p(\Delta\tilde{\mathbf{s}};\boldsymbol{\theta}) = \frac{1}{(\sqrt{2\pi}\sigma_{\Delta s})^{N_{\text{meas}}}} \prod_{i=1}^{N_{\text{meas}}} \exp\left(-\frac{(\Delta\tilde{\mathbf{s}}_i - \Delta\mathbf{s}_i)^2}{2\sigma_{\Delta s}^2}\right) \tag{4.9}$$

Then the steps to determine the MLE are: 1) Calculate the negative log-likelihood

function

$$l(\Delta\tilde{\mathbf{s}};\boldsymbol{\theta}) = -\log(p(\Delta\tilde{\mathbf{s}};\boldsymbol{\theta})) \tag{4.10a}$$

$$= N_{\text{meas}} \log\left(\sqrt{2\pi}\sigma_{\Delta s}\right) + \sum_{i=1}^{N_{\text{meas}}} \frac{(\Delta\tilde{s}_i - \Delta s_i)^2}{2\sigma_{\Delta s}^2} \tag{4.10b}$$

2) Determine $\tilde{\boldsymbol{\theta}}$ as the point for which $l(\Delta\tilde{\mathbf{s}};\boldsymbol{\theta} = \tilde{\boldsymbol{\theta}})$ has a global minimum using a suitable optimization algorithm (in the work, gradient decent was used).

$$\tilde{\boldsymbol{\theta}}_{\text{mle}} = \arg\min_{\boldsymbol{\theta}\in\mathbb{R}^2} l(\Delta\tilde{\mathbf{s}};\boldsymbol{\theta}) \tag{4.11}$$

The location $\tilde{\boldsymbol{\theta}}$ is regarded as the most likely user location since the predictions $\Delta\mathbf{s}_i$ have smallest deviation from measurements. It is noted that the current approach assumes that elements of $\Delta\mathbf{s}$ and noise are uncorrelated. Since some radio links are geographically close to each other, correlation is, however, likely. Therefore, incorporation of correlation properties might improve estimation.

Furthermore, measurements analyzed in Sec. 4.4 show that the variance in (4.7) depend on EPL. Consequently, incorporating this dependence in the estimator improves the performance as is shown in the same section along with the model of $\sigma_{\Delta s}^2$.

4.3.2 Centroid of Intersection Points (CIP)

Since the MLE of Sec. 4.3.1 is computationally complex, this section investigates an estimator which trades accuracy for less complex calculations of estimates. The idea is to consider the *Intersection Points (IPs)* of links as potential locations of the user and find their weighted centroid. In short, the estimator discards insignificant links by applying a threshold, calculates the IPs of specific pairs of forward and reverse links and calculates the user location as the weighted centroid of IPs.

Before going into the details, the formulation of radio links as line equations is considered. The LOS of radio links can be formulated as line equations of the form $\mathbf{A}\boldsymbol{\theta} = \mathbf{b}$. The dimensionality of the problem is reduced to 2D because height information is not necessary, however, can be obtained by the approach. To increase the reliability of the

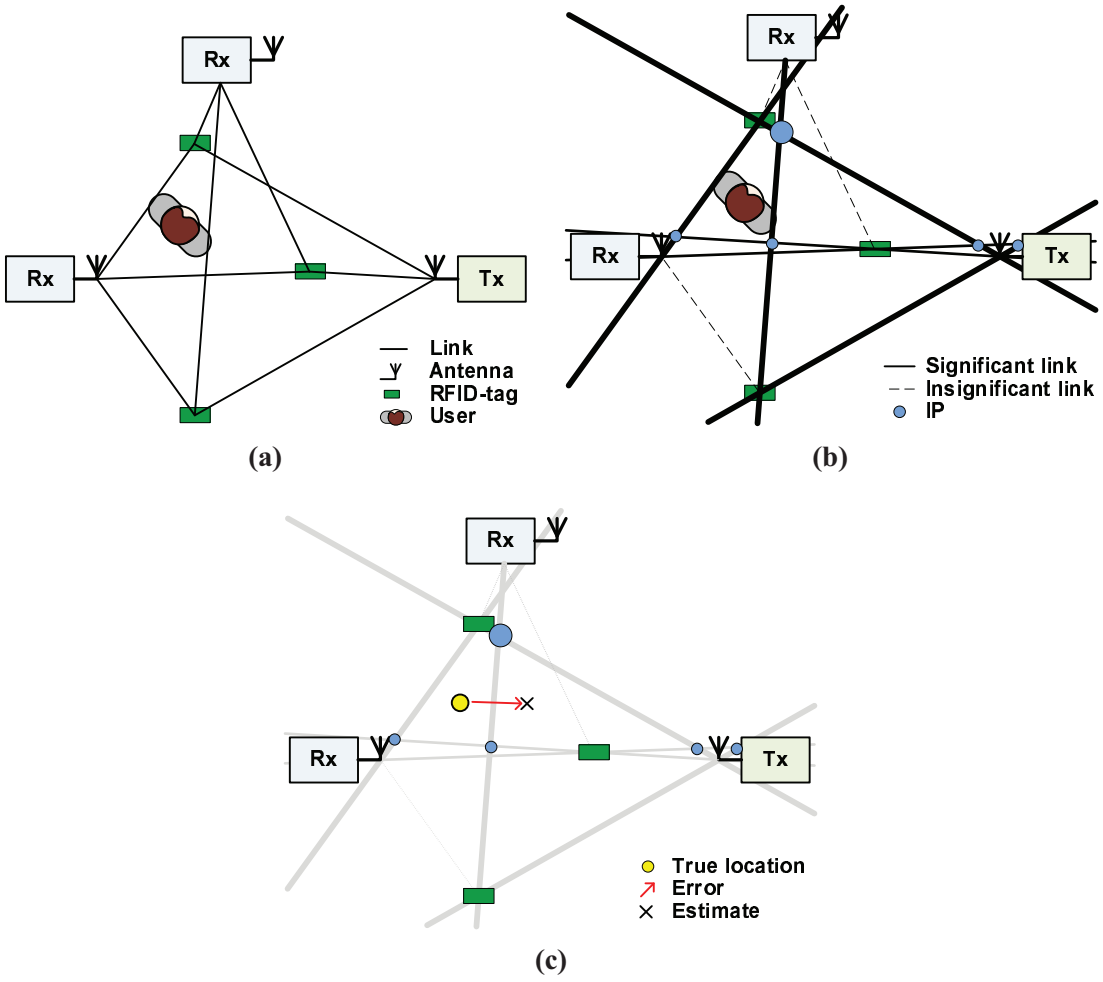

Figure 4.10: Principle of CIP localization. First, insignificant links, i.e. links unaffected by user, are discarded. Second, pairs of forward and reverse links are considered to calculate their IP. Only pairs of links are considered that do not belong to the same combination of transmitting and receiving antenna and RFID-tag. IPs are weighted using the minimum change of RSSI measured on the corresponding radio links. The estimated user location is the centroid of the weighted IPs.

Table 4.2: Calculation of IPs and corresponding weights.

```
1  procedure [θ_ip, w] CalculateIPs
2    k ← 1
3    for i = 1 to |S_f|
4      for j = 1 to |S_r|
5        if u_i = v_i
6          continue
7        end
8        A ← [ α_{u_i}  β_{u_i} ; α_{v_j}  β_{v_j} ]
9        b ← [γ_{u_i}, γ_{v_j}]^T
10       {θ_ip}_k ← (A^T A)^{-1} A^T b
11       {w_ip}_k ← min(|Δs̃_{u_i}|, |Δs̃_{v_j}|)
12       k ← k + 1
13     end
14   end
15 end procedure
```

estimator, only strongly affected links are considered which are denoted *significant* in the following. To be regarded as a significant link, the absolute change of RSSI needs to exceed thresholds T_f and T_r on forward and reverse links, respectively. The thresholds are derived in Sec. 4.4.2.

On this basis, the set of significant forward and reverse links are $\mathcal{S}_\mathrm{f} = \{l : l \in \mathcal{L}, |\Delta\tilde{s}_l| > T_\mathrm{f}\}$ and $\mathcal{S}_\mathrm{r} = \{l : l \in \mathcal{L}, |\Delta\tilde{s}_l| > T_\mathrm{r}\}$. To identify the index of significant links, the following vectors are introduced: The vectors $\mathbf{u} = [u_1, \ldots, u_{|\mathcal{S}_\mathrm{f}|}]^\mathrm{T}$ ($u_i \in \mathcal{S}_\mathrm{f}$) and $\mathbf{v} = [v_1, \ldots, v_{|\mathcal{S}_\mathrm{r}|}]^\mathrm{T}$ ($v_i \in \mathcal{S}_\mathrm{r}$) denote the indexes of forward and reverse links, respectively. Consequently, $\Delta\tilde{s}_{u_i}$ denotes the change of RSS on the i-th significant forward link. The IPs are the intersection points of forward and reverse links. Since the IPs of forward and reverse link of the same combination of antenna pair and tag is always located at the tag, these combinations are discarded when calculating IPs. The IPs can be calculated by LLS as illustrated in pseudocode in Table 4.2.

Finally, the estimated location of the user $\tilde{\boldsymbol{\theta}}_\mathrm{cip}$ is calculated as weighted centroid of IPs with weighting $\mathbf{w}_\mathrm{ip}$ corresponding to vector of the largest absolute value of $\Delta\tilde{s}$ on the considered pairs of links.

$$\tilde{\boldsymbol{\theta}}_\mathrm{cip} = \frac{1}{\sum_i \{\mathbf{w}_\mathrm{ip}\}_i} \sum_i \{\mathbf{w}_\mathrm{ip}\}_i \{\boldsymbol{\theta}_\mathrm{ip}\}_i \tag{4.12}$$

4.4 Estimating the Location of Stationary Users

In this section, a deployment of multiple passive RFID tags is considered. Keeping in mind the preliminary findings of Sec. 4.2, measurements of RSS are analyzed and investigated to determine the user location using the localization techniques developed in Sec. 4.3. Sec. 4.4.1 describes the measurement set-up and procedure. Before results of localization are presented in Sec. 4.4.3, a detailed analysis of measurements is given in Sec. 4.4.2.

4.4.1 Set-up and Procedure of Measurements

The measurement system consists of an RFID-reader operating on ISM 868 MHz frequency band and four antennas. Two circular polarized ($G = 5.5$ dB) and two linearly polarized ($G = 6$ dB) antennas are connected to the reader. All locations are relative to a coordinate system with origin as depicted in Fig. 4.11.

To facilitate the following investigations, several key parameters of the deployment are introduced: The experiment was conducted in an indoor room. $N_\mathrm{t} = 69$ passive RFID tags were deployed on the ground in a regular grid of side length 3.6 m. The $N_\mathrm{a} = 4$ antennas were situated near the edges of the deployment area at a height of 1.8 m whereby antennas of the same type were at opposite edges. The set-up was situated in the middle of a 8.15 m $\times$ 6 m room. To reduce the impact of reflection from adjacent walls, the antennas' main beam direction was aimed in an angle that all wall reflections needed to bounce on at least two walls before entering the deployment area.

The host computer was situated approximately 5 meters from the center of the deployment area. On the host computer ran a custom Java program to configure the RFID system and to fetch and store the measurement data utilizing the provided API.

For the measurements, only $N_\mathrm{ap} = 6$ of the 16 possible antenna pairs are considered to limit execution time of experiments (see table 4.3). During measurements, the RFID-system interrogates tags using a single antenna pair at a time and continuously cycles through all pairs. The parameters of the measurement series were the location and orientation of a test person (Fig. 4.12). Each measurement comprises three phases:

- 1. Phase: Static measurement of RSS

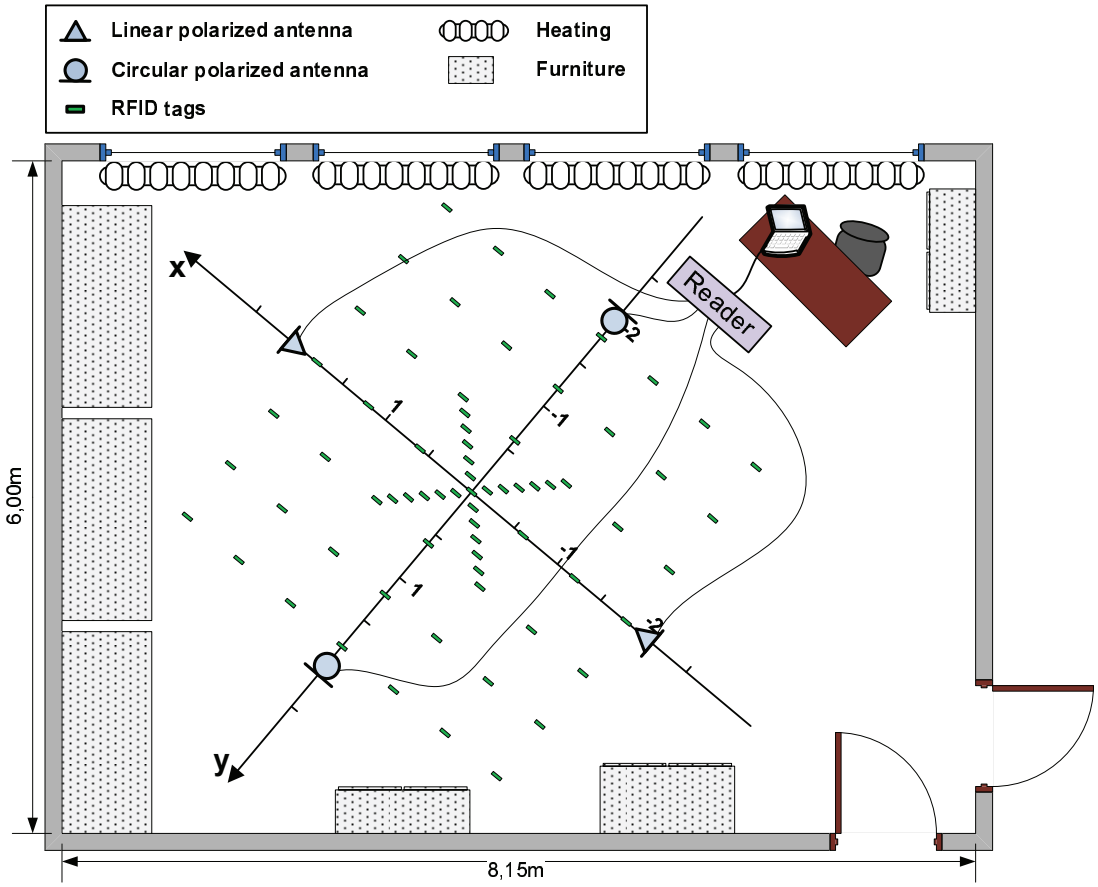

Figure 4.11: Measurement set-up of multiple-tag scenario.

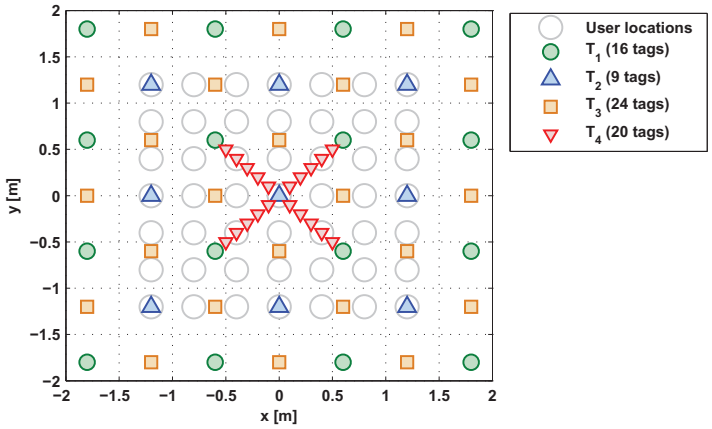

Figure 4.12: Location of tags and test person. Combinations of different subsets $T_i \quad i = 1, \ldots, 4$ of tags are used in the evaluation.

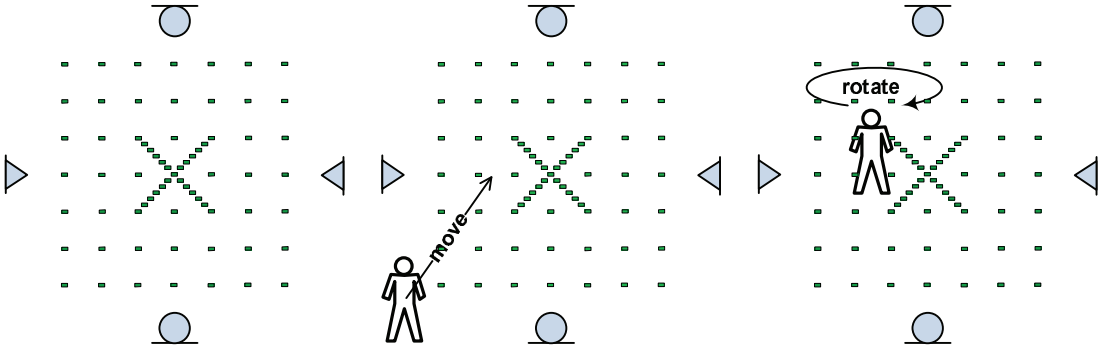

(a) Phase 1. **(b)** Phase 2. **(c)** Phase 3.

Figure 4.13: Procedure of measurements. Blue triangles and circles denote linear and circular polarized antennas, green rectangles denote passive RFID tags.

Table 4.3: 2D-locations (x,y) of antennas used as sender-receiver pairs.

	ID antenna pair					
	0	1	2	3	4	5
Tx location [m]	$(2,0)$	$(2,0)$	$(2,0)$	$(0,-2)$	$(0,-2)$	$(-2,0)$
Rx location [m]	$(0,-2)$	$(-2,0)$	$(0,2)$	$(-2,0)$	$(0,2)$	$(0,2)$

- 2. Phase: Test person moves to location
- 3. Phase: Alternating static measurements of RSS and rotation of test person.

The measurements of phases 1, denoted s_{static}, and 3, denoted s_{dynamic}, are used to calculate the measured change of RSS in [dB] using (4.13).

$$\Delta\tilde{s} = 10\log_{10}\frac{s_{\text{dynamic}}}{s_{\text{static}}} \tag{4.13}$$

49 different locations (x,y) of the test person were measured whereby at each location 8 different orientations α were tested. The range of parameters was $x,y \in \{-1.2,-0.8,-0.4\ldots,1.2\}$ meters and $\alpha \in \{0°,45°,90°,\ldots,315°\}$ respectively. The orientation α denotes the clockwise angle between the direction of view of the test person and the x-axis. The timing and anti-collision parameters of the RFID-system were chosen such that on average 10 RSSI values for each parameter set (location and

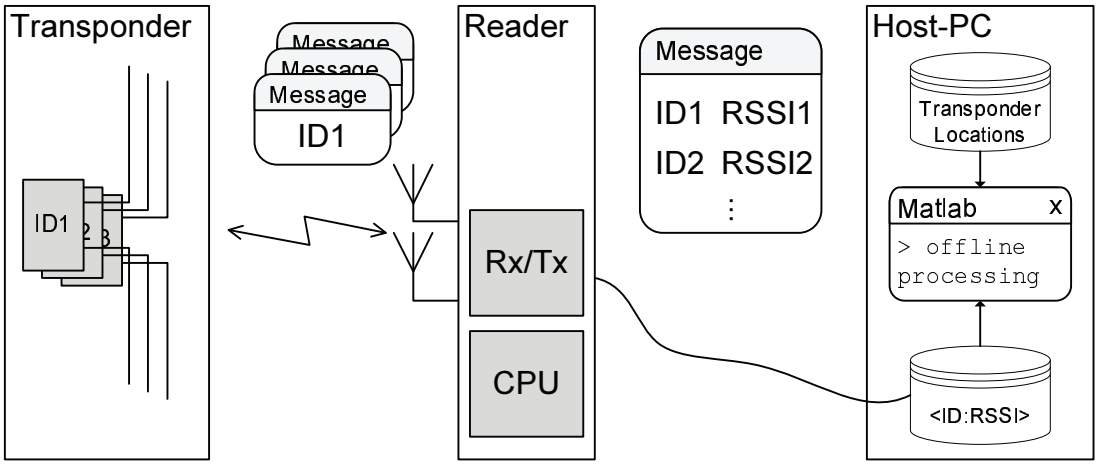

Figure 4.14: Message flow of multi-tag scenario.

orientation) could be acquired. The measurement data was stored on the host computer and analyzed afterwards. This shows that the communication protocol, standardized in ISO 18000-6[5], of the RFID system imposes an increasingly large delay when the number of tags to be interrogated is increased. This issue presents a lower bound on the measurement delay which impacts the performance of tracking techniques as will be elaborated on in Sec. 4.6 on page 121.

It is noted that, finally, the 2D location of the user are estimated since the z-coordinate, i.e. the height, is of minor importance. This stems from the fact that the source of the scatter can be at any height of the user. Consequently, the algorithms work on 2D coordinates if not stated otherwise.

4.4.2 Characterizing the Impact of Humans on RSS

Due to the ambiguity of single link measurements considered in Sec. 4.2, DFL can only be conducted with reasonable accuracy using multiple radio links. Due to the large number of radio links in the current set-up, the statistical properties of measurements are investigated using the concept of histograms. Specifically, the relation between user

[5]The freely available EPC Gen2 standard was adopted with minor modifications as ISO 18000-6C [4]

location and measurements is analyzed to investigate the validity of the observation model (4.5) in deployments with large numbers of RFID-tags.

Analysis of Joint Histogram

In this section, the joint histogram $P(\Delta\tilde{s}; d_{\text{exc}})$ of EPL d_{exc} and the variation of received signal strength $\Delta\tilde{s}$ is considered which is a two-dimensional bar plot showing the relative number of simultaneous occurrences of combinations of the two parameters.

Several quantities[6] are needed to calculate EPL d_{exc}. However, since the complexity of human body prohibits an analytical calculation, a simplified model is applied which regards the body as a cylinder of radius 0.15 m and height 1.9 m. This way, the path length of each NLOS path can be determined using simple ray tracing.

It is noted that the variation of RSSI can not be attributed specifically to either forward or reverse link since the system does only support RSSI between transmitting and receiving antennas. However, an obstacle can theoretically impact either forward or reverse link. Consequently, the following investigations will distinguish between forward and reverse links by assuming that changes of RSSI were caused by the influence of the test person on either forward or reverse link which is expressed mathematically by different values of d_{exc}. The goal of the following analysis is to determine whether the reverse *or* the forward link EPL explain the RSS variations best and how the perturbations of measurements can be reduced.

Figure 4.15 (a) and (b) depict $P(\Delta\tilde{s}; d_{\text{exc}})$ for forward and reverse links, respectively. The difference of the two histograms becomes more visible when considering the shaded plot in the bottom of the two figures. In general, the histogram values concentrate in the region $\{d_{\text{exc}}/\lambda \in (0, 0.25); \Delta\tilde{s} \in (-3.4, 1)\}$. It is shown that the forward link shows a wider spread of attenuations than the reverse link especially in the region $0.25 \leq d_{\text{exc}}/\lambda \leq 3$. In contrast, the histogram of the reverse link shows a more distinct relation between the two parameters. Furthermore, the histogram of the reverse link indicates more frequent and stronger attenuations (black area) than the forward link.

Figure 4.16 shows the two dimensional marginal histogram of $\Delta\tilde{s}$. It is shown that human presence causes more attenuation than amplifications since the CDF shows a

[6] see eq. (4.3) and Fig. 4.8 on p. 95

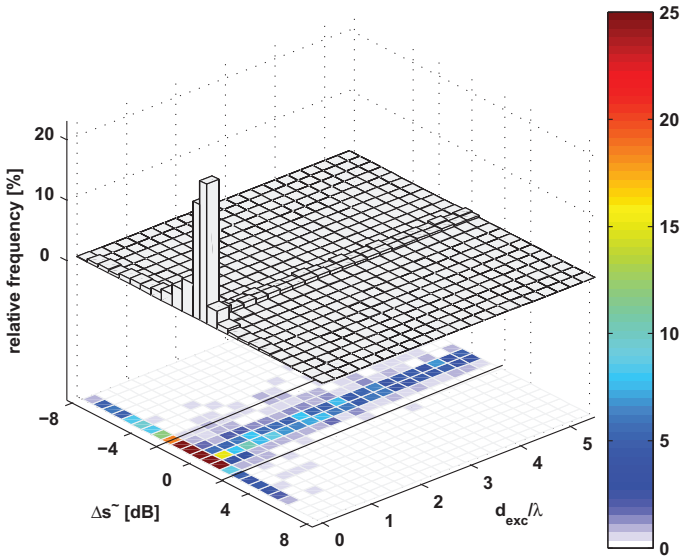

(a) Foward link.

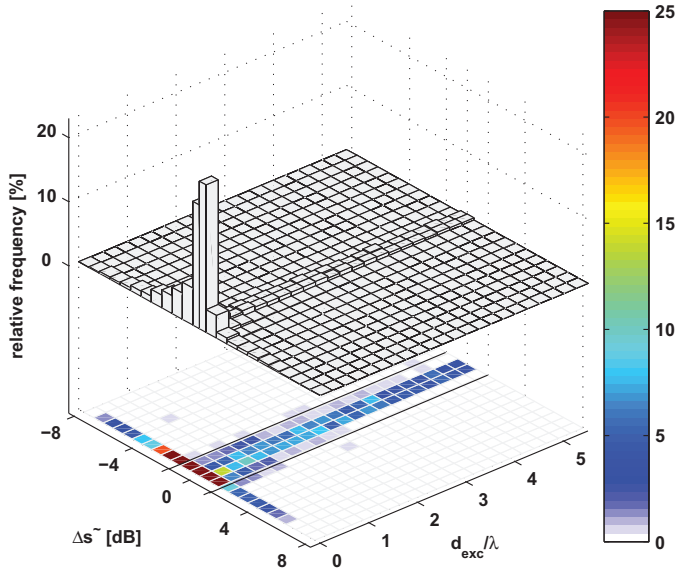

(b) Reverse link.

Figure 4.15: Histogram of measured RSS variations on radio links in a bistatic passive RFID system caused by human presence. The EPL d_{exc} is a measure of the distance between test person's location and radio links.

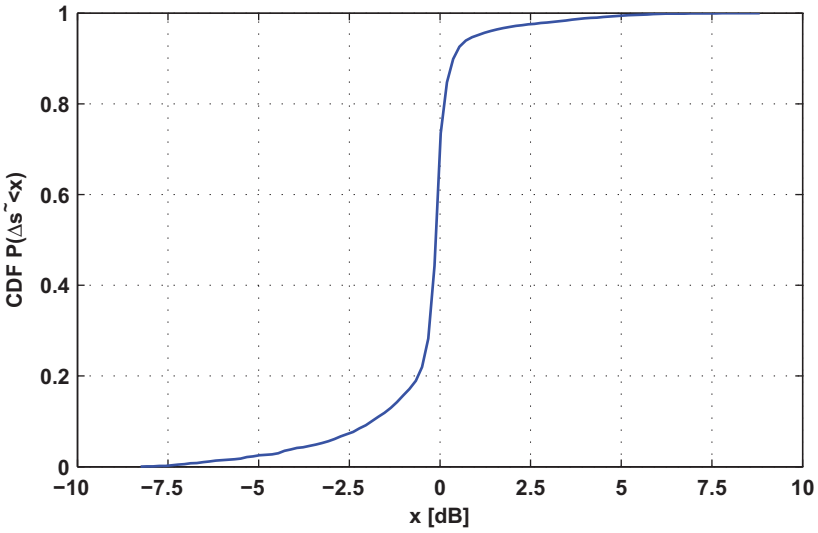

Figure 4.16: CDF of measured change of RSS.

steeper increase for $\Delta\tilde{s} \leq -1$ dB than for $\Delta\tilde{s} \geq 1$ dB. Furthermore, 80 % of RSSIs are in the range -1 dB $< \Delta\tilde{s} < 1$ dB. Considering figures 4.15a and 4.15b, it is observed that this region has non-zero relative frequencies also for large d_{exc} which makes infering d_{exc} from $\Delta\tilde{s}$ difficult.

Infering Excess Path Length from RSSI

Next, the success rate of mapping RSSI variations to an EPL is considered. One way of doing this, is to use the mutual information $I(\Delta\tilde{s}; d_{\text{exc}})$ (4.14) of the joint histogram. The mutual information tells us how much knowing one random variable, i.e. $\Delta\tilde{s}$, reduces the uncertainty about a second random variable, i.e. d_{exc}. The higher the mutual information the more information is contained in a value of RSSI about the EPL and, therefore, about the location.

$$I(\Delta\tilde{s}; d_{\text{exc}}) = \sum_{x \in \Delta\tilde{s}} \sum_{y \in d_{\text{exc}}} P(x,y) \log \frac{P(x,y)}{p(x)p(y)} \tag{4.14}$$

Where $p(\cdot)$ denotes marginal probability. Since measurements are defective, a method developed by Moddemeijer is used to estimate the mutual information [55]. Since the

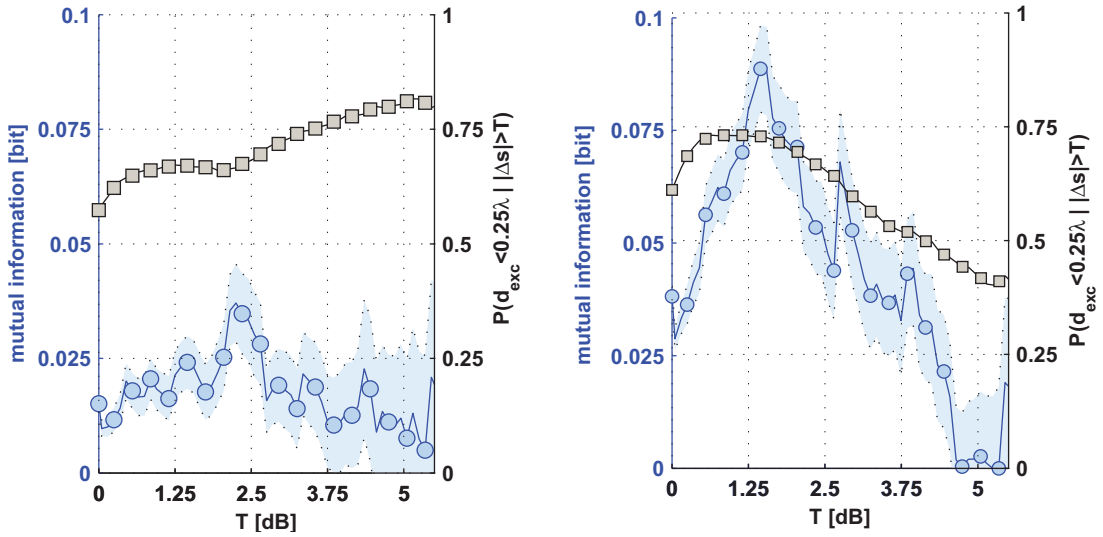

(a) Forward link. **(b)** Reverse link.

Figure 4.17: The figures depict the probability that a significant change of RSS was caused by a user close to the LOS of the affected radio link against the threshold (black curves and right vertical axis). Blue curves corresponding to the left vertical axis depict the mutual information between measurements and EPL.

joint histogram is strongly concentrated, the investigations focus on $d_{\text{exc}} < 0.25\lambda$ since the joint histogram is concentrates in this region.

Considering the joint histogram, it is observed that small variation of RSSI, e.g. $|\Delta\tilde{s}| < T$, occur for a wide range of EPL which makes inferring d_{exc} from $\Delta\tilde{s}$ difficult. Therefore, a threshold T is applied which effectively discards measurements with $|\Delta\tilde{s}| < T$. The question is: What is the optimal value of T to infer reliably d_{exc} from $\Delta\tilde{s}$?

Two metrics are considered in the following to answer this question. First, the probability that the user is within the region $d_{\text{exc}} < 0.25\lambda$ given a measurement $|\Delta\tilde{s}| > T$. The histograms indicate that this probability can be maximized by choosing the thresholds increasingly high. However, the higher the threshold the less measurements remain for analysis. Therefore, the second metric considered is the mutual information $I(\Delta\tilde{s}; d_{\text{exc}})$ which, if maximized, gives the threshold that maximizes the information about d_{exc} contained in measurements. These two quantities are depicted in Fig. 4.17

versus thresholds T for forward and reverse links, respectively. The shaded area around the mutual information depicts its standard deviation.

It is shown that the probability of correctly mapping $\Delta\tilde{s}$ to an EPL of $d_{\text{exc}}/\lambda < 0.25$ proceeds differently for forward and reverse links. Concerning forward links, it almost constantly grows, whereas it shows a maximum for reverse links. Consequently, choosing T is subject to a tradeoff: On the one hand, it must be assured that enough measurements are available to provide a statistically feasible basis which prefers smaller T. On the other hand, inferring d_{exc} from $\Delta\tilde{s}$ is more reliable the larger T is which is tantamount to maximizing $P(d_{\text{exc}} < 0.25\lambda \,|\, |\Delta\tilde{s}| > T)$. The mutual information $I(\Delta\tilde{s}; d_{\text{exc}})$ is considered to find a good tradeoff between the two extrema.

Comparison of $I(\Delta\tilde{s}; d_{\text{exc}})$ for forward and reverse links reveals that the mutual information shows a more distinct behavior for reverse links. The mutual information is maximized using thresholds $T_{\text{forw}} = 2.25$ dB and $T_{\text{rev}} = 1.45$ dB for forward and reverse links, respectively. Applying these thresholds reveals that the reverse link contains more than twice the information about d_{exc} compared with the forward link and is, therefore, slightly more important for localization. Also the probability of correct mapping is 0.73 for the reverse link versus 0.67 for the forward link in this case. This indicates that given a specific $\Delta\tilde{s}$, the EPL can more reliably be determined regarding the reverse link compared with the forward link.

The reason for these findings is that obstructions and interference on the forward link are more likely to cause RSSI to fall below the sensitivity of the tag and, thereby, causing a total loss of connection. As a consequence, the dynamic range of $\Delta\tilde{s}$ is cut below a certain level for forward links which can be regarded as quantization reducing the information contained in the corresponding measurements.

Fitting Measurements to Observation Model

Figure 4.18 depicts the measured RSSI $\Delta\tilde{s}$ against the EPL d_{exc} of forward and reverse link, respectively, for the linearly polarized antennas. The shaded area denotes the *Interquartile Range (IQR)* which includes the middle 50% of the sorted data and indicates the spread of measurements. Only the linearly polarized antennas are considered since the circular polarization seems to smooth the effect that the investigation focuses on.

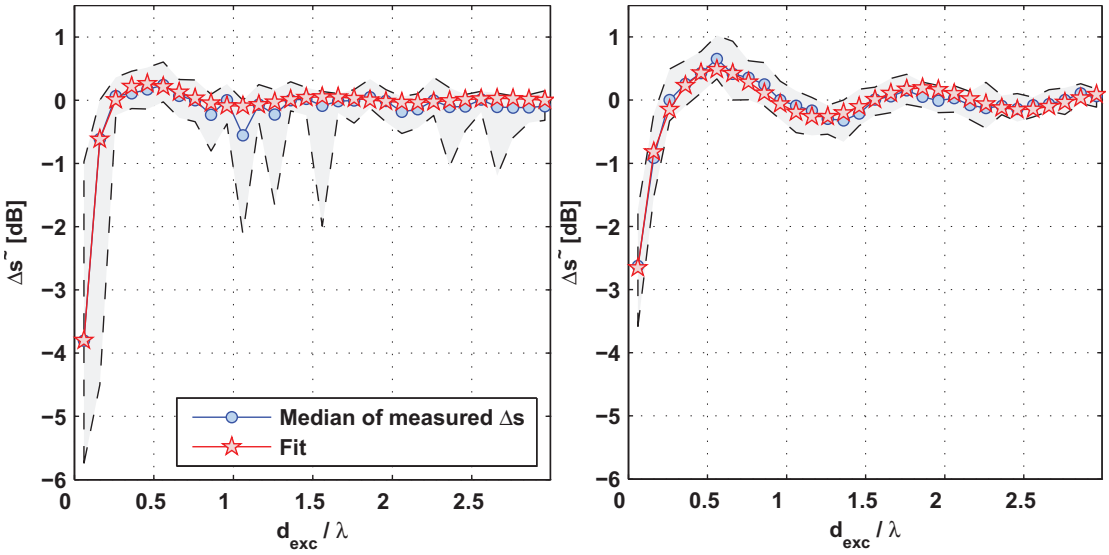

(a) Forward link.

(b) Reverse link.

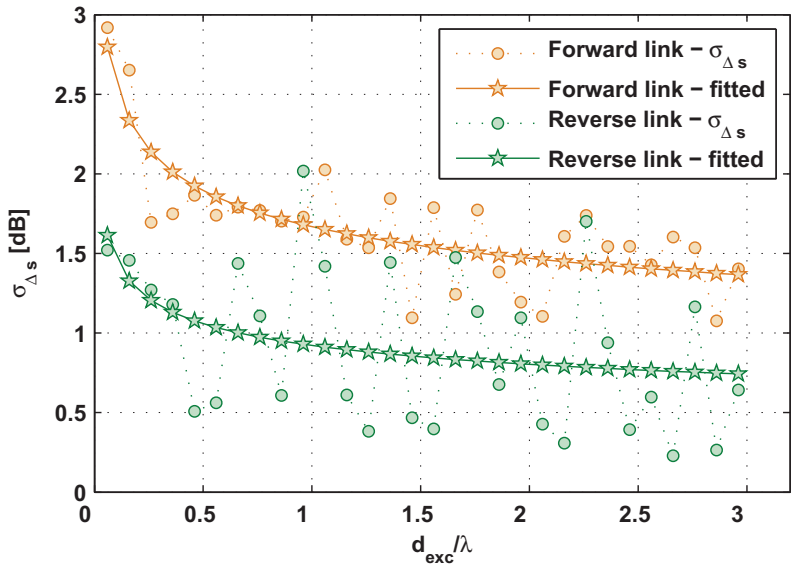

(c) Standard deviation.

Figure 4.18: The figures show the relation and the approximation using (4.15) and (4.16) between EPL d_{exc}, median measurements $\Delta\tilde{s}$ and $\sigma_{\Delta s}$. The results apply for linear polarized antennas and are averaged over all orientations of the user.

Table 4.4: Parameters of fitting the measurements.

Parameter	Forward link	Reverse link
A	0.025	0.14
B	−1.32	−0.79
$\tilde{\lambda}$	0.37	0.43
ϕ_{refl}	3.20	3.25
C	1.29	0.74
D	−0.19	−0.20
E	0.00	0.00

It is shown that comparatively large attenuations and large IQR can be associated with small d_{exc} on the forward link. However, $\Delta\tilde{s}$ is relatively constant for growing EPLs indicating that small variations of received power at the tag hardly influence RSSI.

In contrast, the reverse link shows a more characteristic relationship between $\Delta\tilde{s}$ and d_{exc}. Here, the curve shows a damped oscillation which indicates that reflections from farther test persons contribute significantly to the interference. This supports the findings presented in Sec. 4.4.2 that the reverse link contains more information about the location.

Next, the measurements are fitted to the observation model (4.5) with parameters $A, B, \tilde{\lambda}$ and ϕ_{refl}:

$$\Delta s(d_{\text{exc}}) = A d_{\text{exc}}^{B} \cos\left(2\pi \frac{d_{\text{exc}}}{\tilde{\lambda}} + \phi_{\text{refl}}\right) \tag{4.15}$$

The fitting can be regarded as a minimization of the squared error between $\Delta s(d_{\text{exc}})$ and measurements $\Delta\tilde{s}$. Input to the fitting are the parameters $A, B, \tilde{\lambda}, \phi_{\text{refl}}$ and the true location of the user which is used to calculated d_{exc}. Starting with an initial set of parameter values, the values are gradually refined using a gradient descent approach. Table 4.4 list the final parameters of the two fits. As shown in figure 4.18, the fitted curves represent a reasonable approximation to the measurements. As illustrated in table 4.4, the values of $\tilde{\lambda}$ agree well with the true wave length $\lambda = 0.344\,\text{m}$. It is noted that the determination of the model parameters requires knowledge of the true user location.

The IQR in Fig. 4.18 is also dependent on d_{exc}. Especially the forward link shows a comparably large spread of measurements for small EPL $d_{\text{exc}} < 0.25\lambda$ whereas on the reverse link IQR is only slightly increased compared to larger EPLs. Consequently, variance of measurements contain information about the user location and should be included in the model. A simple function which is monotonically decreasing on the range of d_{exc} is used for this purpose (4.16).

$$\sigma_{\Delta s}(d_{\text{exc}}) = C d_{\text{exc}}^{D} + E \tag{4.16}$$

4.4.3 Results and Conclusions

This section evaluates the new approach to indoor localization regarding its accuracy, scalability, and complexity. It was mentioned in the beginning of this chapter that passive RFID is well suited to the approach as many radio links can be established easily and cost-effectively using passive RFID tags. Consequently, the first part of the following analysis focuses on the accuracy of estimators, which were developed in Sec. 4.3, and how their performance and complexity scales with the number of tags. Finally, the assumption of Gaussian noise made in Sec. 4.3.1 is elaborated on.

Accuracy of Estimators

In the following, the accuracy of estimators developed in Sec. 4.3 is investigated on the basis of measurements analyzed in Sec. 4.4.2. The MSE is considered as figure of merit in terms of accuracy. It is calculated over the different orientations of the user (4.17)

$$\delta(\boldsymbol{\theta}) = \frac{1}{N_\alpha} \sum_{i=1}^{N_\alpha} \left\| \boldsymbol{\theta} - \tilde{\boldsymbol{\theta}}_{\alpha,i} \right\|^2 \tag{4.17}$$

where $\tilde{\boldsymbol{\theta}}_{\alpha,i}$ denotes the estimated location of either MLE or CIP, as indicated in the following, for any of the $N_\alpha = 8$ user orientations $\alpha \in \{0°, 45°, 90°, \ldots, 315°\}$. It is noted that this definition of MSE deviates from (2.11). However, (4.17) is better suited to evaluate the performance of algorithms as different orientations of the user have bigger impact on $\Delta\tilde{s}$ than measurement noise because of the shape of human body.

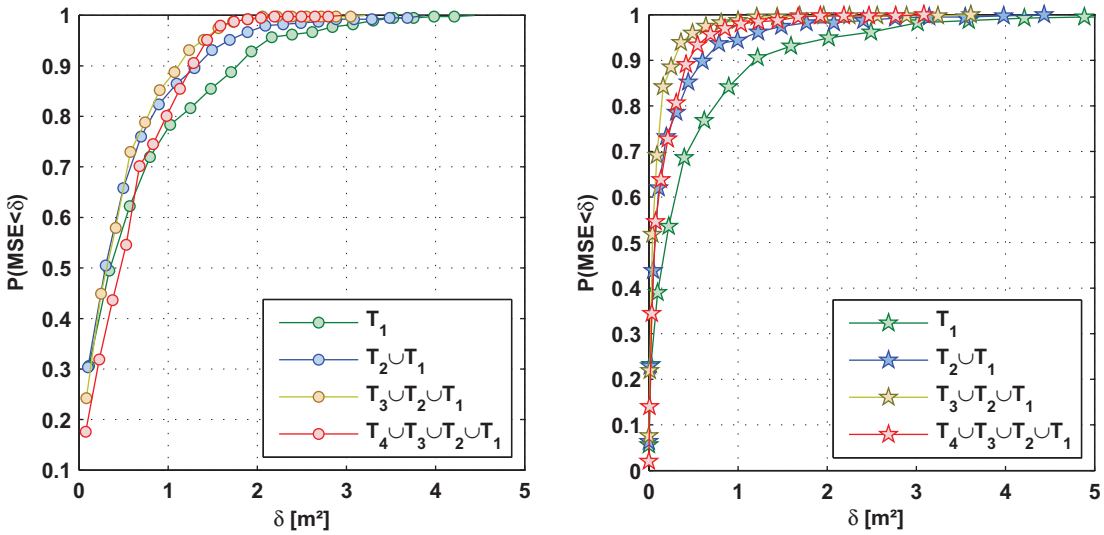

(a) CIP Localization. **(b)** MLE.

Figure 4.19: Performance of algorithms when using different subsets of tags $(T_1, \ldots, T_4)$ with $|T_1| = 16$, $|T_2 \cup T_1| = 25$, $|T_3 \cup T_2 \cup T_1| = 49$ and $|T_4 \cup T_3 \cup T_2 \cup T_1| = 69$ tags as depicted in Fig. 4.12. MLE yields most accurate location estimates for all sets of tags.

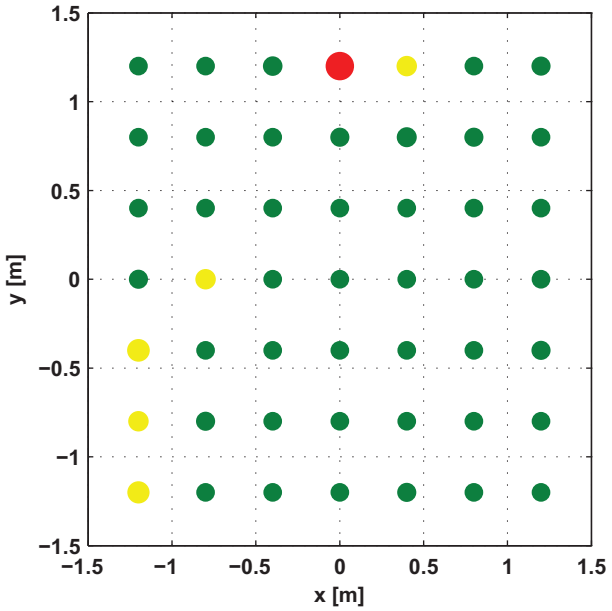

Figure 4.20: Spatial distribution of MSE for MLE averaged over all orientations (tags in $T_3 \cup T_2 \cup T_1$ used). Each dot represents the true location of the test person. The color of the dots indicate the MSE δ [m^2]: ● ($\delta \leq 0.33$), ● ($0.33 < \delta \leq 0.66$) and ● ($0.66 < \delta \leq 0.96$) .

MLE In the best configuration $(T_3 \cup T_2 \cup T_1)$, MLE achieves in 94% of tested locations an MSE of $\delta \leq 0.36\,\mathrm{m}^2$ (Fig. 4.19b). The estimator benefits strongly from increasing the number of tags. In particular, location error of MLE improves by approximately 88% when increasing the number of tags from 16 (T_1) to 49 $(T_3 \cup T_2 \cup T_1)$. However, the MSE does not monotonically decrease with the number of tags. Contrariwise, the location error slightly increases when increasing the number of tags from 49 to 69 $(T_4 \cup T_3 \cup T_2 \cup T_1)$.

Considering the spatial distribution of MSE, it is observed that $\delta \leq 0.33\,\mathrm{m}^2$ holds in large parts of the deployment (Fig. 4.20). However, the estimates of test location (0,1.2) m are considered an outlier since the adjacent test locations have been estimated with high accuracy. In contrast thereof, four adjacent test location at (-1.2,-1.2) m, (-1.2,-0.8) m, (-1.2,-0.4) m and (-0.8,0) m show comparatively large MSE. Generally, the MSE tends to be larger near the border of the deployment and the observed issue is most likely the result of a combination of unfavorable effects, i.e. interference of signals emanated from antenna cables or form the reader device.

It is noted that the algorithm uses 3D coordinates for the calculation of (4.10a) and integrates over the $z-$coordinate before searching the minimum of (4.11). This is necessary since the assumed model is susceptible to even small changes of distances and, therefore, discarding height information during calculation of EPL would increase localization error. Furthermore, the computational burden is reduced by computing (4.10a) on a grid of size $20 \times 20 \times 17$ in the deployment area.

Considering (4.10a), it is observed that the algorithm's applicability is subject to the accuracy of the model and the validity of the Gaussian noise assumption (4.7). Previous investigations have shown that the model agrees well with measurements 4.18. Therefore, the Gaussian noise assumption is elaborated on in the following. Figure 4.21 shows the histogram of the error between predictions and measurements $\Delta\tilde{s} - \Delta s$. It is shown that the Gaussian distribution can not explain all data values. However, the strong central tendency of measurements render the Gaussian distribution a feasible assumption.

CIP The CIP algorithm is used with the thresholds derived in Sec. 4.4.2 which are $T_\mathrm{f} = 2.25\,\mathrm{dB}$ on forward links and $T_\mathrm{r} = 1.45\,\mathrm{dB}$ on reverse links. Consequently, only

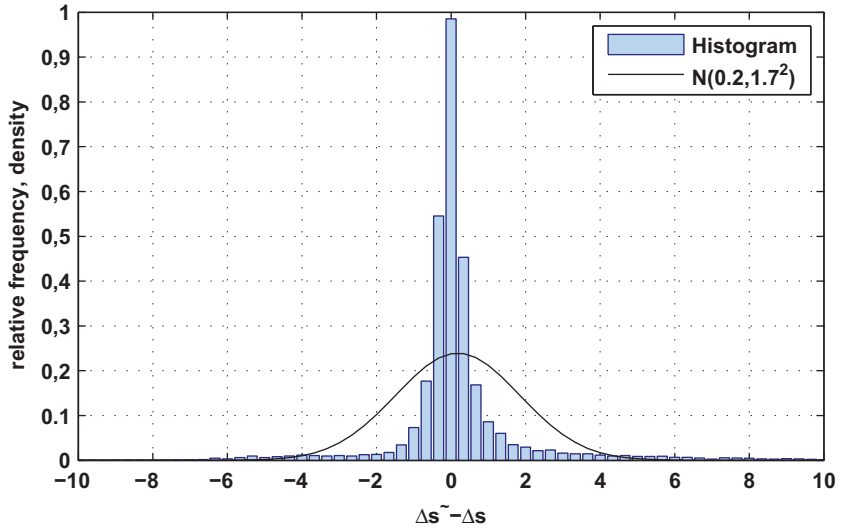

Figure 4.21: Histogram of errors between measurements and prediction vs. theoretical Gaussian distribution.

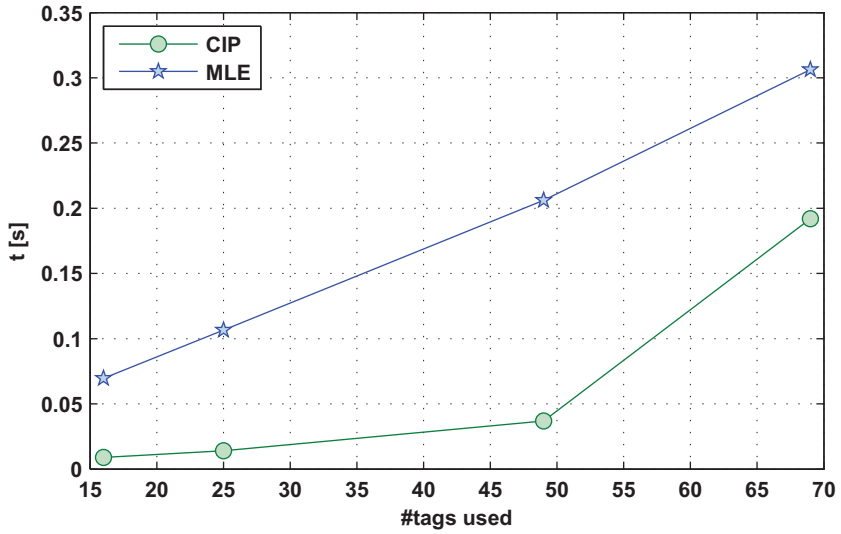

Figure 4.22: Complexity of algorithms in terms of execution time on a Pentium Core 2 Duo CPU@3.3 GHz.

measurements $|\Delta\tilde{s}| < T_\mathrm{f}$ and $|\Delta\tilde{s}| < T_\mathrm{r}$ are considered for forward and reverse links, respectively. CIP constantly yields a higher MSE compared with MLE and achieves in the best configuration an MSE of $\delta \leq 1.4\,\mathrm{m}$ in 95 %. CIP is able to decrease location error by 33 % when using tags $T_3 \cup T_2 \cup T_1$ instead of T_1.

Computational Complexity of Estimators

The two algorithms have different computational complexity. The extensive calculation of likelihood with the MLE leads to long execution times on the used computers compared with CIP (Fig. 4.22). In contrast, CIP is less complex and requires 90 % to 62 % less execution time. It is noted that MLE's complexity is linear in the number of tags used whereas that of CIP is superlinear.

4.5 Tracking the Location of Mobile User

In this section, two RBEs which were reviewed in Sec. 2.3.5 are used to continuously track the location of a mobile user using the DFL approach developed in Sec. 4.4. The main focus of this section is to investigate the performance of EKF and PF with target tracking in terms of MSE. In particular, the original Kalman Filter, which is an optimal estimator for Gaussian noise and linear models, can not be applied since the observation model is non-linear. Therefore, a major aspect to be investigated in the following is how the estimators deal with the non-linearity.

4.5.1 Set-up of Computer Simulations

The general simulation set-up consists of four antennas connected to a bistatic RFID reader, a varying number of passive RFID-tags and a user who moves through the deployment area on a predefined trajectory. The four antennas are situated at a height of 1.8 m in the corners of the deployment which is a $10\,\mathrm{m} \times 10\,\mathrm{m}$ square area. The tags are deployed in a regular grid whereby their number is a parameter of the simulations. The following assumptions are made:

- Tags and antennas have omnidirectional radiation pattern and all tags can be interrogated by any pair of antennas. For simplicity, only two of the 16 possible pairs of antennas are considered for measurements. The pairs consist of the antennas at opposite corners.
- Measurements of RSS are subject to additive zero-mean, white Gaussian noise with constant standard deviation $\sigma = 1\,\mathrm{dB}$. Perturbations are assumed to be independent in time and space dimensions but identically distributed.
- The static RSS is known a-priori, e.g. by means of a short automated measurement without user presence.
- The user moves on an S-shaped trajectory with constant velocity.
- The body of the user is approximated by a cylinder with 0.1 m radius and 1.9 m height for the calculation of EPL.

The computer simulations base on the *Recursive Bayesian Estimation Library (ReBEL)*[7]. ReBEL is a toolkit written for the software MatLab [2]. It facilitates state estimation using various recursive filters by defining generic data structures and interfaces to estimator routines. However, functions for observation and process models as well as movement patterns have to be contributed by the designer. Consequently, the toolkit has been extended for the current simulations by implementing the observation model (4.15) and the following models.

$$\boldsymbol{\theta} = [x, y, v_\mathrm{x}, v_\mathrm{y}]^\mathrm{T} \qquad \text{state} \tag{4.18a}$$

$$\boldsymbol{\theta}^{(t)} = \begin{bmatrix} 1 & 0 & T & 0 \\ 0 & 1 & 0 & T \\ 0 & 0 & 1 & 0 \\ 0 & 0 & 0 & 1 \end{bmatrix} \boldsymbol{\theta}^{(t-1)} + \mathbf{v}^{(t-1)} \qquad \text{process model} \tag{4.18b}$$

$$\Delta\tilde{\mathbf{s}}^{(t)} = \Delta\tilde{\mathbf{s}}^{(t)}_\mathrm{forw} + \Delta\tilde{\mathbf{s}}^{(t)}_\mathrm{rev} + \mathbf{n}^{(t)} \qquad \text{observation model} \tag{4.18c}$$

[7] A MatLab toolkit developed by Rudolph van der Merwe and Eric A. Wan and owned by the School of Science & Engineering, Oregon Health and Science University.

Table 4.5: Parameters for computer simulations of target tracking.

Parameter	Value
Velocity $\left\|\left[v_{\mathrm{x}}, v_{\mathrm{y}}\right]^{\mathrm{T}}\right\|$	$1.5\,\mathrm{m/s}$
Process noise	$\{\mathbf{v}\}_i \sim N(0, 0.01^2)$
Observation noise	$n_i \sim N(0,1)$
Sampling period	$T = 0.05\,\mathrm{s}$
# particles	$n_{\mathrm{p}} = 300$

Where time-discrete filtering is assumed with sampling period $T = 0.05\,\mathrm{s}$, t denotes a specific discrete time step ($t \in \mathbb{N}$) and $\Delta\tilde{\mathbf{s}}^{(t)}_{\mathrm{forw}}$, $\Delta\tilde{\mathbf{s}}^{(t)}_{\mathrm{rev}}$ denote the change of RSS on forward and reverse links, respectively. The parameters of simulations are summarized in table 4.5.

4.5.2 Results and Conclusions

The MSE is used to analyze tracking performance of each estimated locations $(\tilde{x}, \tilde{y})$ for each point of the simulated trajectory. The accuracy of tracking algorithms strongly depends on the number of tags (Figs. 4.23). Especially, the difference between EKF and PF become evident when algorithms use only 16 tags. Here, EKF looses track frequently whereas PF is able to follow the simulated trajectory. Both algorithms benefit from deploying more tags. However, EKF achieves similar performance for 36 tags compared with PF using only 16 tags. The reason for this is that PF is better suited to the non-linear observation model than EKF.

The Particle Filter shows superior tracking performance for all tag numbers. This is also supported by the cumulative histograms of RMSE in Fig. 4.24. It is shown that the tracking error of EKF slowly approaches that of PF. In particular, the EKF achieves only for 36 tags feasible position estimates while the accuracy of the PF only marginally improves with the number of tags.

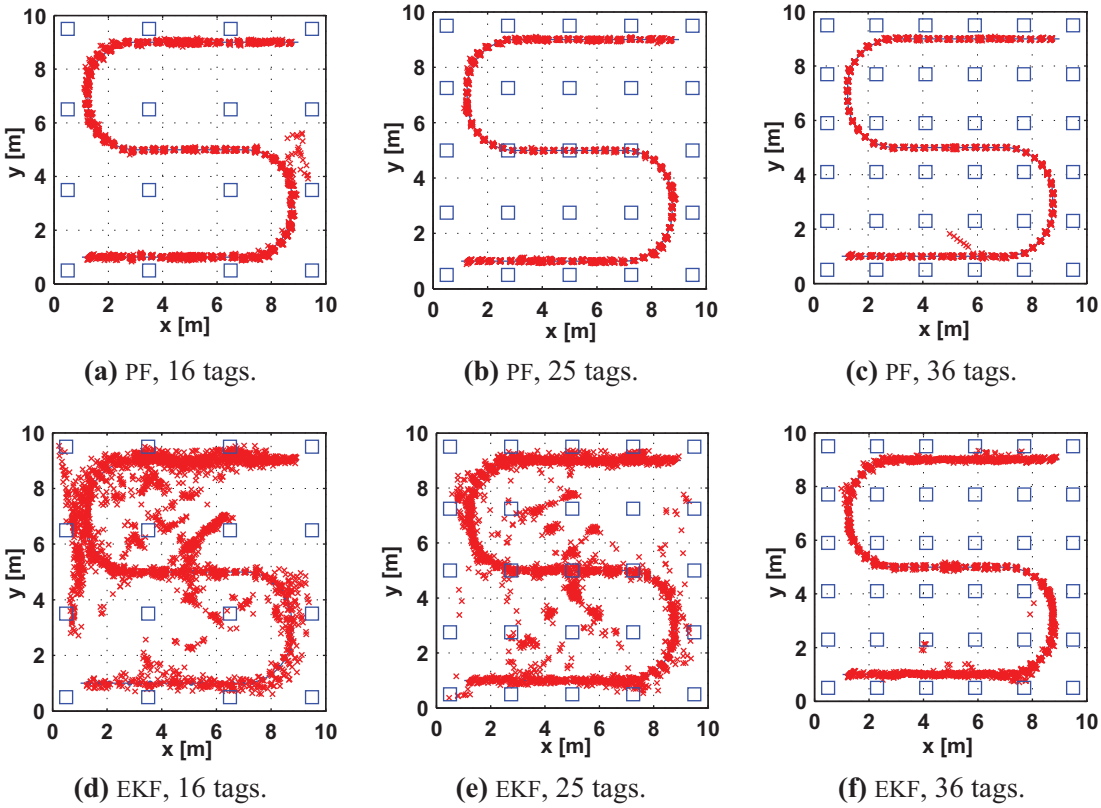

(a) PF, 16 tags. **(b)** PF, 25 tags. **(c)** PF, 36 tags.

(d) EKF, 16 tags. **(e)** EKF, 25 tags. **(f)** EKF, 36 tags.

Figure 4.23: MSE tracking error of a)-c) PF and d)-f) EKF. The four antennas are situated at the corners at (0,0), (0,10), (10,10) and (10,0). Estimated locations are depicted by red crosses, true locations by solid blue dots.

4.6 Summary

The investigations in this chapter considered DFL using a passive bistatic RFID system. Motivated by the suitability of passive RFID to DFL, a detailed observation model was developed which relates the user location to RSSI as measured by the RFID system. The validity and high accuracy of the model were analyzed using real world measurements (Sec. 4.2.2).

On this basis, two new estimators of user location were developed which differ in both accuracy of location estimates and complexity. The MLE shows superior accuracy while requiring comparatively complex calculations. The technique yielded MSE $\leq$

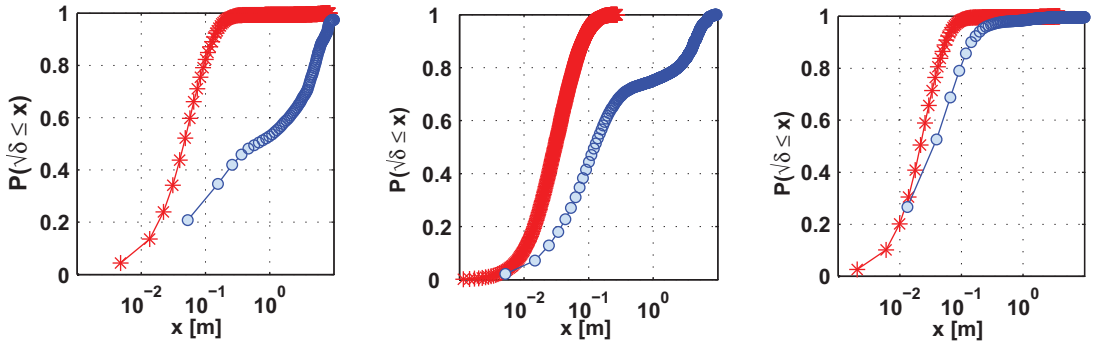

(a) 16 tags. **(b)** 25 tags. **(c)** 36 tags.

Figure 4.24: Cumulative histogram of tracking error RMSE $\sqrt{\delta}$ vs. number of tags. Red line with stars denotes PF and blue lines with circles denote EKF.

0.36 m^2 in 94% of measurements while requiring 0.20 s to calculate an estimate in a sample 3.6 m $\times$ 3.6 m deployment. The CIP algorithm achieved MSE $\leq$ 1.40 m^2 at 95% in the same scenario. However, calculating an estimate requires only 0.04 s with CIP, i.e. 80% less time (Sec. 4.4.3).

Furthermore, computer simulations were conducted to investigate the suitability of two often used tracking techniques, i.e. EKF and PF, to track the location of a mobile user with the DFL approach. Simulations showed that PF is better suited to the non-linear observation model than EKF which frequently lost track of the user. Both tracking techniques benefited from increasing the number of passive tags although the improvement was smaller with PF because of its already highly accurate estimates. In summary, this chapter has shown that passive RFID is well suited to DFL since it facilitates establishment of large numbers of radio links and, therefore, enables highly accurate localization.

Chapter 5

Conclusion and Future Research Directions

The thesis considered the localization of users and sensors in smart environments by processing measurements of RSS. The thesis approached the topic from two different point of views.

First, in chapter 3, networks of wireless sensors were considered which require relative locations of sensors for their operation. The thesis contributed to the state-of-the-art a new measure to characterize the energy efficiency of localization called LogarEEL. LogarEEL relates the normalized cost of localizing a sensor to its utility to the network as given by the normalized gain. The measure has the desirable property of being upper bounded which facilitates comparison of various algorithms for wireless localization. The second part of the same chapter was dedicated to the Sensor Selection Problem which considers selection of the most favorable location-aware sensors as anchors for the localization process to minimize location error and resource consumption. In this regard, a new distributed algorithm for the SSP, called local-crb, was developed and analyzed which achieved superior performance in computer simulations while limiting communication overhead to a minimum. Furthermore, algorithm local-dist, which is an extension of the existing distance-based sensor selection, was investigated successfully to further decrease the energy consumption of the selection process. Future work, can comprise the application of the findings within real-world testbeds. Furthermore, the

integration of the selection algorithms in existing localization algorithms promises to be a procreative research topic.

Chapter 4 considered Device-Free Localization which represents an approach to localize a user or moving object by backtracking their impact on the RSS of radio links. After extensively discussing the state-of-the-art, new models and methods for DFL using a passive, bistatic RFID system are developed and investigated in a real world testbed. In particular, the state-of-the-art was extended by a simple yet accurate model which relates the user location to changes of RSSI measured on a radio link and by two techniques to estimate the user location. The investigations showed that passive RFID is especially suited to DFL since large numbers of radio links can easily be established with the technology which enables highly accurate location estimates.

The downside of the approach is that the passive tags need to be deployed at known locations which contributes to the installation effort. However, this disadvantage will likely be relaxed in the near future since the inexpensive passive tags can easily be integrated in the environment, e.g. in carpets[1]. Furthermore, the applicability of the approach to real-time tracking of mobile users is currently limited by the delay of the RFID communication protocol. Further research is needed to investigate the different sources of latency during localization with the RFID system and develop a software module which finally enables tracking in real-time. In addition, the differentiation between different users in the coverage area is an open research question. In particular, from the current point of view, it seems possible to apply interference cancellation techniques that aim at isolating the contribution of a specific user, for example, by simply subtracting its influence as given by the observation model or by processing the baseband signals in the RFID reader. The applicability of such techniques and their performance, in terms of differentiating close by users, can be the task of future research.

[1]The company Vorwerk presented the first carpet with integrated RFID tags in 2004 (`http://www.vorwerk-carpet.com`)

Appendix A

Lists

Table A.1: Algorithms of class local-knowledge in pseudo-code. Code is executed at location-aware sensor s_i.

Local-crb

```
16  procedure ProcessLocalizationRequest(d̃_i, {d̃_{i,j} : s_j ∈ H}, t)
17      % calculate wait time
18      T_wait,i ← t + K · (d̃_{1,i} / r_tx)^α
19    H_i ← ∅
20    while true
21      flag ← 0
22      % update set of responders
23      if {Overheard response}
24        H_i ← H_i ∪ {current responder s_j}
25      end
26      if |H_i| = 1 then
27        if ∛(σ²_min(H_i ∪ s_i)) > r_tx
28          % quit current iteration without responding and try again next loop
29          continue
30        end if
31      elseif |H_i| = 2 then
32        % update wait time
33        T_wait,i ← t + K̃ · Δσ^α_min
34      end if
35      if t ≥ T_wait,i then
36        % broadcast response
37        respond(ownAddress, d̃_i, θ_i)
38        % exit procedure
39        return
40      end if
41    end while
42  end procedure
```

Local-dist

```
43  procedure ProcessLocalizationRequest(d̃_i, t)
44    % calculate wait time
45    T_wait,i ← t + K · (d̃_i / r_tx)^α
46    while true
47      if t ≥ T_wait,i then
48        % broadcast response
49        respond(ownAddress, θ_i)
50        % exit procedure
51        return
52      end if
53    end while
54  end procedure
```

Appendix B

Proofs

Definition B.1. *The Mean-Square Error (MSE) δ of an estimator $\tilde{\boldsymbol{\theta}}$ of a 2-dimensional location $\boldsymbol{\theta} = [x,y]^{\mathrm{T}}$ is $\delta = E\left((x-\tilde{x})^2 + (y-\tilde{y})^2\right)$.*

Definition B.2. *The bias bias $\left(\tilde{\boldsymbol{\theta}}\right)$ of an estimator $\tilde{\boldsymbol{\theta}}$ of a 2-dimensional location is the Euclidean distance of its expected value and $\boldsymbol{\theta}$, e.g.*

$$bias\left(\tilde{\boldsymbol{\theta}}\right) = \left\| E\left(\tilde{\boldsymbol{\theta}}\right) - \boldsymbol{\theta} \right\|. \tag{B.1}$$

Definition B.3. *The variance var $\left(\tilde{\boldsymbol{\theta}}\right)$ of an estimator $\tilde{\boldsymbol{\theta}}$ of a 2-dimensional location is the sum of variance of its elements, e.g.*

$$\begin{aligned} var\left(\tilde{\boldsymbol{\theta}}\right) &= var\left(\tilde{x}\right) + var\left(\tilde{y}\right) && \text{(B.2a)} \\ &= E\left(\left(x - E\left(x\right)\right)^2\right) + E\left(\left(y - E\left(y\right)\right)^2\right) && \text{(B.2b)} \end{aligned}$$

Theorem B.1. *The MSE of a vector estimator $\tilde{\boldsymbol{\theta}}$ equals var $\left(\tilde{\boldsymbol{\theta}}\right) + bias^2\left(\tilde{\boldsymbol{\theta}}\right)$.*

Proof.

$$
\begin{aligned}
E\left((x-\tilde{x})^2+(y-\tilde{y})^2\right) &= E\left(([\tilde{x}-E(\tilde{x})]+[E(\tilde{x})-x])^2\right) \\
&\quad + E\left(([\tilde{y}-E(\tilde{y})]+[E(\tilde{y})-y])^2\right) \\
&= E\left([\tilde{x}-E(\tilde{x})]^2+[E(\tilde{x})-x]^2+[\tilde{x}-E(\tilde{x})][E(\tilde{x})-x]\right) \\
&\quad + E\left([\tilde{y}-E(\tilde{y})]^2+[E(\tilde{y})-y]^2+[\tilde{y}-E(\tilde{y})][E(\tilde{y})-y]\right) \\
&= var(\tilde{x})+bias^2(\tilde{x})+E([\tilde{x}-E(\tilde{x})][E(\tilde{x})-x]) \\
&\quad + var(\tilde{y})+bias^2(\tilde{y})+E([\tilde{y}-E(\tilde{y})][E(\tilde{y})-y]) \\
&= var(\tilde{x})+bias^2(\tilde{x})+E\left(\tilde{x}E(\tilde{x})-\tilde{x}x-E(\tilde{x})^2+xE(\tilde{x})\right) \\
&\quad + var(\tilde{y})+bias^2(\tilde{y})+E\left(\tilde{y}E(\tilde{y})-\tilde{y}y-E(\tilde{y})^2+yE(\tilde{y})\right) \\
&= var(\tilde{x})+bias^2(\tilde{x})+E\left(E(\tilde{x})^2-E(\tilde{x})-E(\tilde{x})^2+E(\tilde{x})\right) \\
&\quad + var(\tilde{y})+bias^2(\tilde{y})+E\left(E(\tilde{y})^2-E(\tilde{y})-E(\tilde{y})^2+E(\tilde{y})\right) \\
&= var\left(\tilde{\boldsymbol{\theta}}\right)+bias^2\left(\tilde{\boldsymbol{\theta}}\right) \qquad \square
\end{aligned}
$$

Theorem B.2. *The error of estimated distances using lognormal distributed measurements of RSS is also lognormal distributed.*

Proof. The logarithm $\log_{10}(\tilde{d}) = \log_{10}(d_0) + \frac{P_0-P_i}{K}$ of estimated distances is Gaussian distributed because P_i is Gaussian distributed (2.6a),(2.9). The probability density of the a new random variable $X = \log_{10}(\tilde{d})$ is considered in B.3.

$$
f_X(\tilde{d}) = \frac{K}{\sqrt{2\pi}\sigma_{\mathrm{db}}} \exp\left\{ -K^2 \frac{\left(\log_{10}(\tilde{d}) - \log_{10}(d)\right)^2}{2\sigma_{\mathrm{db}}^2} \right\} \tag{B.3}
$$

Since $\tilde{d} = 10^X$, the following transformation of $f_X(\tilde{d})$ can be conducted to yield $f_{\tilde{d}}(\tilde{d})$.

$$y = 10^X \tag{B.4}$$

$$\frac{dy}{dX} = 10^X \log(10) \tag{B.5}$$

$$f_{\tilde{d}}(\tilde{d}) = \frac{f_X(\tilde{d})}{\left|\frac{dy}{dX}\right|} \tag{B.6}$$

Substitute X, change the base of the logarithm to 10 and substitute $K = 10\varepsilon$ yields (B.7) which presents a lognormal distribution.

$$f_{\tilde{d}}(\tilde{d}) = \frac{K \log_{10}(e)}{\sqrt{2\pi}\sigma_{\mathrm{db}}\tilde{d}} \exp\left\{ -K^2 \frac{\left(\log_{10}(\tilde{d}) - \log_{10}(d)\right)^2}{2\sigma_{\mathrm{db}}^2} \right\} \tag{B.7}$$

□

Eidesstattliche Erklärung

Ich erkläre an Eides statt, dass ich die vorliegende Arbeit selbstständig und nur unter Verwendung der angegebenen Quellen und Hilfsmittel angefertigt habe. Die Arbeit wurde bisher in gleicher oder ähnlicher Form weder veröffentlicht noch einer anderen Prüfungsbehörde vorgelegt.

Rostock, 17. September 2010 Dominik Lieckfeldt

Thesen

1. Wireless networks of battery-powered sensing devices that are capable of measuring parameters of their environment, so called *Wireless Sensor Network (WSN)*, constitute a major source of context-information in smart environments.
2. For information processing and to enable local decision making in various operation areas (message routing, measurement aggregation, etc.), relative locations of sensors need to be known. However, these can often not be provided prior to deployment due to prohibitively large configuration effort in large networks or because sensors are mobile.
3. Energy-efficient operations, given by the ratio of utility and cost, is a major design goal of WSNs since the lifetime of these networks is limited by the finite capacity of sensors' batteries.
4. The novel measure *Logarithmic Energy Efficiency of Localization (LogarEEL)* facilitates comparison of different localization algorithms in terms of energy efficiency as it considers the bounds on utility and cost of a localization process.
5. Location-unaware sensors can calculate estimates of their location using relative distances to location-aware sensors which can be obtained by measuring the *Received Signal Strength (RSS)* of wireless communication. These estimates deviate from the true location due to the impact of measurement errors. The corresponding location errors are typically characterized using the *Mean-Square Error (MSE)*.
6. The degree with which measurement errors propagate to location errors depends on the geographical configuration of location-aware and location-unaware sensors.
7. Selecting subsets of c out of N_A location-aware sensors to be used to localize a location-unaware sensor can yield different MSE of estimated location.
8. The energy consumption attributable to localization can be reduced by using only those subsets of location-aware sensors that yield favorable geographical configurations.

9. The fully distributed algorithm local-crb selects small subsets of location-aware sensors that lead to comparatively small MSE without introducing additional communication overhead.
10. The extension of distance-based selection of location-aware sensors, called algorithm local-dist, enables optimization of the energy efficiency of the localization process.
11. *Device-Free Localization (DFL)* of users in smart environments has, compared with conventional approaches, the advantages to not require the user to carry communication devices. Therefore, DFL can enable new application in the smart environment domain.
12. The accuracy of DFL depends strongly on the number of radio links in a specific region.
13. Passive *Radio Frequency Identification (RFID)* is especially suited to DFL as its small, inexpensive, passive tags facilitate deployment of large numbers of radio links which are mandatory to ensure highly accurate location estimates.
14. Using measurements of RSS, the location of a user can be determined by backtracking its impact on close by radio links with the considered passive RFID system.
15. The model developed in the thesis relates the interference between *Line-of-Sight (LOS)* radio signals and reflections caused by the user and can accurately describe the impact of humans on RSS which forms the basis for localization of the user.
16. The localization algorithm which bases on the maximum likelihood principle achieves highly accurate estimated locations with MSE $\leq 0.36\,\mathrm{m}^2$ in 95% of investigated user locations in a testbed implementation of DFL.
17. The *Particle Filter (PF)* is better suited to tracking the location of mobile users compared with *Extended Kalman Filter (EKF)*.

Kurzreferat

Die Dissertation behandelt die Lokalisierung, das heißt die Bestimmung der Position von Sensoren und Nutzern in intelligenten Umgebungen. Zu diesem Zweck können bestimmte Eigenschaften von Funkwellen gemessen und ausgewertet werden. Unter den möglichen Messgrößen konzentriert sich die vorliegende Arbeit auf die Messung der Empfangssignalstärke, da diese von den meisten Funkempfängern ausgewertet werden kann.

Die vorliegende Arbeit nähert sich dem Thema aus zwei unterschiedlichen Richtungen. Zunächst werden Netzwerke von drahtlos kommunizierenden Sensoren betrachtet, deren relative Positionen für die Konfiguration und Erhaltung des Netzes benötigt werden. Die Dissertation leistet einen Beitrag zum Stand der Forschung, indem ein neues Maß zur zahlenmäßigen Bewertung der Energieeffizienz von Algorithmen zur Positionsbestimmung entwickelt und auf einige häufig eingesetzte Verfahren angewendet wird. Des Weiteren wird das Sensorauswahlproblem betrachtet, dessen Ziel es ist, diejenigen Sensoren mit bekannten Positionen als Referenzpunkte für die Lokalisierung anderer Sensoren zu wählen, die zur Positionsschätzung mit kleinstem Fehler und geringstem Energieverbrauch führen. Hierzu wird ein neuer, verteilt arbeitender Algorithmus mit Namen local-crb entwickelt und untersucht. Dieser Algorithmus erreicht in den Computer-Simulationen Positionsschätzwerte mit geringstem Fehler im Vergleich mit anderen Verfahren und minimiert gleichzeitig den Kommunikationsaufwand. Darüber hinaus wird die existierende distanzbasierte Sensorauswahl in einer Art und Weise erweitert, die es erlaubt, diesen Ansatz hinsichtlich des Energieverbrauchs zu optimieren.

Der zweite Teil der Arbeit behandelt die gerätefreie Lokalisierung von Nutzern, die Nutzer oder auch mobile Objekte anhand ihres Einflusses auf die Empfangssignalstärke von Funkverbindungen lokalisiert. Neue Modelle und Methoden für die gerätefreie Lokalisierung werden entwickelt und angewendet. Insbesondere wird der Stand der Forschung durch ein einfaches, jedoch

exaktes Model erweitert, das einen analytischen Zusammenhang zwischen Nutzerposition und Veränderungen in der Empfangssignalstärke beschreibt und somit die Grundlage für die Lokalisierung bildet. Schließlich werden Algorithmen zur Lokalisierung eines Nutzers auf Messwerte angewendet, wobei ein mittlerer quadratischer Fehler von $\leq 0{,}36\,\mathrm{m}^2$ erreicht wird.

Abstract

The thesis considers determination of location of sensors and users in smart environments. For this purpose, measurements of propagation properties of radio waves between two sensors are used. The thesis focuses on the Received Signal Strength of radio communications among the various types of measurements since it is available on most wireless communication devices.

The thesis approaches the topic from two different point of views. First, Wireless Sensor Network are considered which require relative locations of sensors for their operation. The thesis contributes to the state-of-the-art a new measure to characterize the energy efficiency of localization called LogarEEL. Furthermore, the Sensor Selection Problem is examined which considers selection of the most favorable location-aware sensors as anchors for the localization process to minimize location error and resource consumption. In this regard, a new distributed algorithm, called local-crb, is developed and analyzed. The novel algorithm achieves superior location accuracy in computer simulations while limiting communication overhead to a minimum. Furthermore, algorithm local-dist, which is an extension of the existing distance-based sensor selection, is examined successfully to further decrease the energy consumption of the selection process.

Furthermore, Device-Free Localization is considered which represents an approach to localize a user or moving object by backtracking their influence on the RSS of radio links. Novel models and methods for DFL using a passive, bistatic RFID system are developed and investigated in a real world testbed. In particular, the state-of-the-art is extended by a simple yet accurate model which relates the user location to changes of RSS measured on a radio link and by two localization techniques. Evaluation using the real-world measurements demonstrate mean square location error $\leq 0.36\,\mathrm{m}^2$.

Bibliography

[1] *Precision Agriculture*. Springer. ISSN: 1573-1618, http://www.springerlink.com/content/103317/. 4

[2] http://www.mathworks.com/products/matlab/. 119

[3] http://www.ubiq.com/hypertext/weiser/SciAmDraft3.html. 81

[4] *EPC Gen2 standard*, 2005. http://www.epcglobalinc.org/standards/uhfc1g2. 106

[5] I. Akyildiz, W. Su, Y. Sankarasubramaniam, and E. Cayirci. A survey on sensor networks. *Communications Magazine, IEEE*, 40(8):102–114, Aug 2002. ISSN 0163-6804. doi: 10.1109/MCOM.2002.1024422. 4, 50

[6] J. Albowicz, A. Chen, and L. Zhang. Recursive position estimation in sensor networks. In *Proceedings IEEE ICNP*, pages 35–41, Los Alamitos, CA, USA, 2001. IEEE Computer Society. ISBN 0-7695-1429-4. doi: http://doi.ieeecomputersociety.org/10.1109/ICNP.2001.992758. 59

[7] T. Amemiya, J. Yamashita, K. Hirota, and M. Hirose. Virtual leading blocks for the deaf-blind:a real-time way-finder by verbal-nonverbal hybrid interface and high-density rfid tag space. In *Virtual Reality Conference, IEEE*, volume 0, page 165, Los Alamitos, CA, USA, 2004. IEEE Computer Society. doi: http://doi.ieeecomputersociety.org/10.1109/VR.2004.1310070. 84, 91

[8] I. Amundson and X. Koutsoukos. A survey on localization for mobile wireless sensor networks. In *Mobile Entity Localization and Tracking in GPS-less Environments*, volume 5801, pages 235–254, September 2009. ISBN 978-3-642-04378-9. doi: 10.1007/978-3-642-04385-7_16. 83

[9] T. Arampatzis, J. Lygeros, and S. Manesis. A survey of applications of wireless sensors and wireless sensor networks. In *Intelligent Control, 2005. Proceedings of the 2005 IEEE International Symposium on, Mediterrean Conference on Control and Automation*, pages 719–724, June 2005. doi: 10.1109/.2005.1467103. ISBN: 0-7803-8936-0. 4

[10] J. Ash and L. Potter. Sensor network localization via received signal strength measurements with directional antennas. *Proceedings of the Forty-Second Annual Allerton Conference on Communication, Control, and Computing*, pages 1861–1870, September 2004. 20

[11] G. Barrenetxea, F. Ingelrest, G. Schaefer, and M. Vetterli. The hitchhiker's guide to successful wireless sensor network deployments. In *SenSys '08: Proceedings of the 6th ACM conference on Embedded network sensor systems*, pages 43–56, New York, NY, USA, 2008. ACM. doi: http://doi.acm.org/10.1145/1460412.1460418. ISBN: 978-1-59593-990-6. 4

[12] R. Behnke and D. Timmermann. AWCL: Adaptive Weighted Centroid Localization as an efficient Improvement of Coarse Grained Localization. In *Positioning, Navigation and Communication, 2008. WPNC 2008. 5th Workshop on*, pages 243–250, Mar. 2008. doi: 10.1109/WPNC.2008.4510381. 27

[13] F. Bian, D. Kempe, and R. Govindan. Utility based sensor selection. In *IPSN '06: Proceedings of the fifth international conference on Information processing in sensor networks*, pages 11–18, New York, NY, USA, 2006. ACM. ISBN 1-59593-334-4. doi: http://doi.acm.org/10.1145/1127777.1127783. 60

[14] J. Blumenthal, F. Reichenbach, and D. Timmermann. Minimal transmission power vs. signal strength as distance estimation for localization in wireless sensor

networks. In *Sensor and Ad Hoc Communications and Networks, 2006. SECON '06. 2006 3rd Annual IEEE Communications Society on*, volume 3, pages 761–766, Sept. 2006. ISBN 1-4244-0626-9. doi: 10.1109/SAHCN.2006.288558. 59

[15] G. Borriello, W. Brunette, M. Hall, C. Hartung, and C. Tangney. Reminding about tagged objects using passive rfids. *UbiComp 2004: Ubiquitous Computing*, 3205:36–53, 2004. ISSN 0302-9743. `http://www.springerlink.com/content/b8y4p8tvbhp1gmhp`. 83, 91

[16] I. Bose and R. Pal. Auto-id: managing anything, anywhere, anytime in the supply chain. *Commun. ACM*, 48(8):100–106, 2005. ISSN 0001-0782. doi: http://doi.acm.org/10.1145/1076211.1076212. 7

[17] N. Bulusu, J. Heidemann, and D. Estrin. Gps-less low cost outdoor localization for very small devices. *IEEE Personal Communications Magazine*, 7(5):28–34, October 2000. ISSN 1070-9916. doi: 10.1109/98.878533. 26, 35

[18] N. Bulusu, D. Estrin, and J. Heidemann. Adaptive beacon placement. In *Proceedings of the 21st International Conference on Distributed Computing Systems*, volume 0, pages 489–498, Los Alamitos, CA, USA, 2001. IEEE Computer Society. ISBN 0-7695-1077-9. doi: http://doi.ieeecomputersociety.org/10.1109/ICDSC.2001.918979. 59

[19] K.-Y. Cheng, V. Tam, and K.-S. Lui. Improving aps with anchor selection in anisotropic sensor networks. In *Proceedings of ICAS/ICNS*, page 49, Los Alamitos, CA, USA, 2005. IEEE Computer Society. ISBN 0-7695-2450-8. doi: http://doi.ieeecomputersociety.org/10.1109/ICAS-ICNS.2005.55. 59

[20] M. Chu, H. Haussecker, and F. Zhao. Scalable Information-Driven Sensor Querying and Routing for Ad Hoc Heterogeneous Sensor Networks. *International Journal of High Performance Computing Applications*, 16(3):293–313, 2002. doi: 10.1177/109434200201600309O1. `http://hpc.sagepub.com/cgi/content/abstract/16/3/293`. 56, 60

[21] S. Coleri, S. Y. Cheung, and P. Varaiya. Sensor networks for monitoring traffic. In *42th Annual Allerton Conference on Commuinication, Control, and Computing*, 2004. 4

[22] D. J. Cook and S. K. Das. How smart are our environments? an updated look at the state of the art. *Pervasive and Mobile Computing*, 3(2):53 – 73, 2007. ISSN 1574-1192. doi: 10.1016/j.pmcj.2006.12.001. Design and Use of Smart Environments. 41

[23] J. A. Costa, N. Patwari, and I. Alfred O. Hero. Distributed weighted-multidimensional scaling for node localization in sensor networks. *ACM Transactions on Sensor Networks*, 2(1):39–64, February 2006. 59

[24] T. L. Dinh, W. Hu, P. Sikka, P. Corke, L. Overs, and S. Brosnan. Design and deployment of a remote robust sensor network: Experiences from an outdoor water quality monitoring network. In *Local Computer Networks, 2007. LCN 2007. 32nd IEEE Conference on*, pages 799–806, October 2007. doi: 10.1109/LCN.2007.39. ISSN: 0742-1303. 4

[25] E. Ertin, J. W. Fisher, and L. C. Potter. Maximum mutual information principle for dynamic sensor query problems. In *Information Processing in Sensor Networks*, volume 2634/2003, pages 405–416. Springer-Verlag, 2003. ISBN 978-3-540-02111-7. doi: 10.1007/3-540-36978-3_27. 57, 58

[26] H. Feng, R. Yuan, and C. Mu. An energy-efficient localization scheme with specified lower bound for wireless sensor networks. In *Proceedings of the Sixth IEEE CIT*, page 232, Washington, DC, USA, 2006. IEEE Computer Society. ISBN 0-7695-2687-X. doi: http://dx.doi.org/10.1109/CIT.2006.46. 44, 59

[27] K. Finkenzeller. *RFID-Handbuch, Grundlagen und praktische Anwendungen induktiver Funkanlagen, Transponder und kontaktloser Chipkarten*. Number 3-446-40398-1. Hanser, 4 edition, 2006. v, 7

[28] K. P. Fishkin, B. Jiang, M. Philipose, and S. Roy. I sense a disturbance in the

force: Unobstrusive detection of interactions with rfid-tagged objects. *Ubicomp*, pages 268–282, 2004. 20

[29] M. Gudmundson. Correlation model for shadow fading in mobile radio systems. *Electronics Letters*, 27(23):2145–2146, Nov. 1991. ISSN 0013-5194. doi: 10.1049/el:19911328. 21

[30] I. Guvenc, C.-C. Chong, and F. Watanabe. Analysis of a linear least-squares localization technique in los and nlos environments. *Vehicular Technology Conference, 2007. VTC2007-Spring. IEEE 65th*, pages 1886–1890, April 2007. ISSN 1550-2252. doi: 10.1109/VETECS.2007.391. 54

[31] H. Hashemi. The indoor radio propagation channel. *Proceedings of the IEEE*, 81 (7):943–968, Jul 1993. ISSN 0018-9219. doi: 10.1109/5.231342. 20, 21

[32] L. Holmquist, H. Gellersen, G. Kortuem, S. Antifakos, F. Michahelles, B. Schiele, M. Beigl, and R. Maze. Building intelligent environments with smart-its. *Computer Graphics and Applications, IEEE*, 24(1):56–64, Jan-Feb 2004. ISSN 0272-1716. doi: 10.1109/MCG.2004.1255810. 41

[33] A. Howard, M. J. Mataric, and G. S. Sukhatme. Mobile sensor network deployment using potential fields: A distributed, scalable solution to the area coverage problem. In *Proceedings of the 6th International Symposium on Distributed Autonomous Robotics Systems*, pages 299–308, 2002. `http://citeseerx.ist.psu.edu/viewdoc/summary?doi=10.1.1.12.8990`. 6

[34] L. Hu and D. Evans. Localization for mobile sensor networks. In *MobiCom '04: Proceedings of the 10th annual international conference on Mobile computing and networking*, pages 45–57, New York, NY, USA, 2004. ACM. ISBN 1-58113-868-7. doi: http://doi.acm.org/10.1145/1023720.1023726. 6

[35] P. Juang, H. Oki, Y. Wang, M. Martonosi, L. S. Peh, and D. Rubenstein. Energy-efficient computing for wildlife tracking: design tradeoffs and early experiences with zebranet. *SIGOPS Oper. Syst. Rev.*, 36(5):96–107, 2002. doi: http://doi.acm.org/10.1145/635508.605408. ISSN:0163-5980. 4

[36] M. A. Kanso and M. G. Rabbat. Compressed rf tomography for wireless sensor networks: Centralized and decentralized approaches. *Lecture Notes in Computer Science*, 5516:173–186, 2009. ISSN 0302-9743. doi: 10.1007/978-3-642-02085-8_13. 86, 88

[37] L. Kaplan. Global node selection for localization in a distributed sensor network. *Aerospace and Electronic Systems, IEEE Transactions on*, 42(1):113–135, Jan. 2006. ISSN 0018-9251. doi: 10.1109/TAES.2006.1603409. 58, 60

[38] L. Kaplan. Local node selection for localization in a distributed sensor network. *Aerospace and Electronic Systems, IEEE Transactions on*, 42(1):136–146, Jan. 2006. ISSN 0018-9251. doi: 10.1109/TAES.2006.1603410. 58, 60

[39] S. M. Kay. *Fundamentals of Statistical Signal Processing, Volume I: Estimation Theory*. Prentice Hall PTR, 1993. ISBN 0133457117. 28, 29, 54, 99

[40] J. Kemper and H. Linde. Challenges of passive infrared indoor localization. pages 63–70, March 2008. ISBN 978-1-4244-1798-8. doi: 10.1109/WPNC.2008.4510358. 86, 88, 91

[41] J. Kemper, M. Walter, and H. Linde. Human-assisted calibration of an angulation based indoor location system. In *Sensor Technologies and Applications, 2008. SENSORCOMM '08. Second International Conference on*, pages 196–201, Aug. 2008. ISBN 978-0-7695-3330-8. doi: 10.1109/SENSORCOMM.2008.17. 86, 88

[42] C. Knapp and G. Carter. The generalized correlation method for estimation of time delay. In *Acoustics, Speech and Signal Processing, IEEE Transactions on*, pages 320–327, 1976. 17

[43] V. Kulyukin, C. Gharpure, J. Nicholson, and S. Pavithran. Rfid in robot-assisted indoor navigation for the visually impaired. In *Intelligent Robots and Systems, 2004. (IROS 2004). Proceedings. 2004 IEEE/RSJ International Conference on*, volume 2, pages 1979–1984 vol.2, Sept.-2 Oct. 2004. ISBN 0-7803-8463-6. doi: 10.1109/IROS.2004.1389688. 84, 91

[44] K. Langendoen, A. Baggio, and O. Visser. Murphy loves potatoes: experiences from a pilot sensor network deployment in precision agriculture. In *Parallel and Distributed Processing Symposium, 2006. IPDPS 2006. 20th International*, April 2006. doi: 10.1109/IPDPS.2006.1639412. ISBN: 1-4244-0054-6. 4

[45] C. L. Lawson and R. J. Hanson. *Solving Least Squares Problems*. Society for Industrial Mathematics, 1995. ISBN: 0-89871-356-0. 32

[46] J. Lee, K. Cho, S. Lee, T. Kwon, and Y. Choi. Distributed and energy-efficient target localization and tracking in wireless sensor networks. *Computer Communications*, 29(13-14):2494–2505, 2006. 62

[47] D. Lieckfeldt, J. You, and D. Timmermann. An algorithm for distributed beacon selection. In *4th IEEE International Workshop PerSeNS*. PerCOM, March 2008. 60, 61, 72

[48] S. E. Lindley, R. Harper, and A. Sellen. Designing for elders: exploring the complexity of relationships in later life. In *BCS-HCI '08: Proceedings of the 22nd British HCI Group Annual Conference on HCI 2008*, pages 77–86, Swinton, UK, UK, 2008. British Computer Society. ISBN 978-1-906124-04-5. ISBN:978-1-906124-04-5. 8

[49] H. Liu, H. Darabi, P. Banerjee, and J. Liu. Survey of wireless indoor positioning techniques and systems. *Systems, Man, and Cybernetics, Part C: Applications and Reviews, IEEE Transactions on*, 37(6):1067–1080, Nov. 2007. ISSN 1094-6977. doi: 10.1109/TSMCC.2007.905750. 24, 82, 83

[50] J. Liu, J. Reich, and F. Zhao. Collaborative in-network processing for target tracking. *EURASIP JOURNAL ON APPLIED SIGNAL PROCESSING*, pages 378–391, 2003. 57, 58, 60, 73

[51] J. Liu, Y. Zhang, and F. Zhao. Robust distributed node localization with error management. In *Proc. ACM MobiHoc '06*, pages 250–261. ACM Press, 2006. ISBN 1-59593-368-9. doi: http://doi.acm.org/10.1145/1132905.1132933. 5, 59

[52] J. P. Lynch. An overview of wireless structural health monitoring for civil structures. *Philosophical Transactions of the Royal Society A: Mathematical, Physical and Engineering Sciences*, 365(1851):345–372, 2007. doi: 10.1098/rsta.2006.1932. `http://rsta.royalsocietypublishing.org/content/365/1851/345.abstract`. 4

[53] A. Mainwaring, D. Culler, J. Polastre, R. Szewczyk, and J. Anderson. Wireless sensor networks for habitat monitoring. In *Proceedings of the 1st ACM WSNA*, pages 88–97, New York, NY, USA, 2002. ACM. ISBN 1-58113-589-0. doi: http://doi.acm.org/10.1145/570738.570751. 4

[54] G. Mao, B. Fidan, and B. D. O. Anderson. Wireless sensor network localization techniques. *Comput. Netw.*, 51(10):2529–2553, 2007. ISSN 1389-1286. doi: http://dx.doi.org/10.1016/j.comnet.2006.11.018. 24

[55] R. Moddemeijer. On estimation of entropy and mutual information of continuous distributions. *Signal Processing*, 16(3):233–246, 1989. 109

[56] W. Navidi, W. S. Murphy, Jr., and W. Hereman. Statistical methods in surveying by trilateration. *Comput. Stat. Data Anal.*, 27(2):209–227, 1998. ISSN 0167-9473. doi: http://dx.doi.org/10.1016/S0167-9473(97)00053-4. 32

[57] L. M. Ni, Y. Liu, Y. C. Lau, and A. P. Patil. Landmarc: Indoor location sensing using active rfid. *Wireless Networks*, 10(6):701+, 2004. ISSN 1022-0038. doi: 10.1023/B:WINE.0000044029.06344.dd. `http://dx.doi.org/10.1023/B:WINE.0000044029.06344.dd`. 20, 91

[58] E. Olson, J. J. Leonard, and S. Teller. Robust range-only beacon localization. In *IEEE AUV*, 2004. 59

[59] R. J. Orr and G. D. Abowd. The smart floor: a mechanism for natural user identification and tracking. In *CHI '00: CHI '00 extended abstracts on Human factors in computing systems*, pages 275–276, New York, NY, USA, 2000. ACM. ISBN 1-58113-248-4. doi: http://doi.acm.org/10.1145/633292.633453. 84, 85, 91

[60] N. Patwari. *Location Estimation in Sensor Networks*. Dissertation, University of Michigan, 2005. `http://www.ece.utah.edu/~npatwari/`. 20

[61] N. Patwari and P. Agrawal. Effects of correlated shadowing: Connectivity, localization, and rf tomography. *Information Processing in Sensor Networks, 2008. IPSN '08. International Conference on*, pages 82–93, April 2008. doi: 10.1109/IPSN.2008.7. 21, 86, 87, 88, 91

[62] N. Patwari and J. Wilson. Radio tomographic imaging. YouTube, March 2009. `http://www.youtube.com/watch?v=fzAzbmgL-d0`. 87

[63] N. Patwari, A. O. Hero III, M. Perkins, N. Correal, and R. O'Dea. Relative location estimation in wireless sensor networks. In *IEEE TSP*, volume 51, pages 2137–2148, August 2003. 29, 33

[64] N. Patwari, J. Ash, S. Kyperountas, R. Moses, and N. Correal. Locating the nodes: Cooperative localization in wireless sensor networks. *IEEE Signal Processing Magazine*, 22:54–69, July 2005. `citeseer.ist.psu.edu/patwari05locating.html`. 20

[65] J. Polastre, J. Hill, and D. Culler. Versatile low power media access for wireless sensor networks. In *SenSys '04: Proceedings of the 2nd international conference on Embedded networked sensor systems*, pages 95–107, New York, NY, USA, 2004. ACM. ISBN 1-58113-879-2. doi: http://doi.acm.org/10.1145/1031495.1031508. xi, 70

[66] N. B. Priyantha, A. Chakraborty, and H. Balakrishnan. The cricket location-support system. In *ACM/IEEE MobiCom*, 2000. doi: http://doi.acm.org/10.1145/345910.345917. ISBN:1-58113-197-6. 18, 59

[67] T. S. Rappaport. *Wireless Communications: Principles and Practice*. Prentice Hall, 2001. ISBN 0130422320. 21

[68] F. Reichenbach and D. Timmermann. Comparing the efficiency of localization algorithms with the power-error-product (pep). In *Second IEEE International Workshop on Wireless Mesh and Ad Hoc Networks (WiMAN)*, June 2008. 44

[69] F. Reichenbach, A. Born, D. Timmermann, and R. Bill. A distributed linear least squares method for precise localization with low complexity in wireless sensor networks. In *DCOSS*, volume 4026 of *Lecture Notes in Computer Science*, pages 514–528. Springer, 2006. ISBN 3-540-35227-9. 33

[70] K. Romer and F. Mattern. The design space of wireless sensor networks. *Wireless Communications, IEEE*, 11(6):54–61, Dec. 2004. doi: 10.1109/MWC.2004.1368897. ISSN: 1536-1284. 4

[71] H. Rowaihy, S. Eswaran, M. Johnson, D. Verma, A. Bar-Noy, T. Brown, and T. L. Porta. A survey of sensor selection schemes in wireless sensor networks. In E. M. Carapezza, editor, *Unattended Ground, Sea, and Air Sensor Technologies and Applications IX*, number 1. SPIE, 2007. doi: 10.1117/12.723514. 51, 55

[72] S. Sarma, D. Brock, and D. Engels. Radio frequency identification and the electronic product code. *Micro, IEEE*, 21(6):50–54, Nov/Dec 2001. ISSN 0272-1732. doi: 10.1109/40.977758. 7

[73] A. Savvides, C.-C. Han, and M. B. Strivastava. Dynamic fine-grained localization in ad-hoc networks of sensors. In *MobiCom '01: Proceedings of the 7th annual international conference on Mobile computing and networking*, pages 166–179, New York, NY, USA, 2001. ACM. ISBN 1-58113-422-3. doi: http://doi.acm.org/10.1145/381677.381693. 20

[74] Y. Shang, W. Rumi, Y. Zhang, and M. Fromherz. Localization from connectivity in sensor networks. *Parallel and Distributed Systems, IEEE Transactions on*, 15 (11):961–974, Nov. 2004. ISSN 1045-9219. doi: 10.1109/TPDS.2004.67. 35

[75] V. Shnayder, M. Hempstead, B.-r. Chen, G. W. Allen, and M. Welsh. Simulating the power consumption of large-scale sensor network applications. In *SenSys '04: Proceedings of the 2nd international conference on Embedded networked sensor systems*, pages 188–200, New York, NY, USA, 2004. ACM. ISBN 1-58113-879-2. doi: http://doi.acm.org/10.1145/1031495.1031518. xi, 70

[76] K. Sinha and A. D. Chowdhury. A beacon selection algorithm for bounded error location estimation in ad hoc networks. In *IEEE ICCTA*, pages 87–93. IEEE Computer Society, 2007. ISBN 978-0-7695-2770-3. doi: http://doi.ieeecomputersociety.org/10.1109/ICCTA.2007.1. `http://dblp.uni-trier.de/db/conf/iccta/iccta2007.html`. 59

[77] W.-Z. Song, R. Huang, M. Xu, A. Ma, B. Shirazi, and R. LaHusen. Air-dropped sensor network for real-time high-fidelity volcano monitoring. In *MobiSys '09: Proceedings of the 7th international conference on Mobile systems, applications, and services*, pages 305–318, New York, NY, USA, 2009. ACM. ISBN 978-1-60558-566-6. doi: http://doi.acm.org/10.1145/1555816.1555847. 4

[78] F. Thiesse, E. Fleisch, and M. Dierkes. Lottrack: Rfid-based process control in the semiconductor industry. *Pervasive Computing, IEEE*, 5(1):47–53, Jan.-March 2006. ISSN 1536-1268. doi: 10.1109/MPRV.2006.9. 8, 85, 91

[79] M. Vieira, J. Coelho, C.N., J. da Silva, D.C., and J. da Mata. Survey on wireless sensor network devices. In *Emerging Technologies and Factory Automation, 2003. Proceedings. ETFA '03. IEEE Conference*, volume 1, pages 537–544 vol.1, Sept. 2003. doi: 10.1109/ETFA.2003.1247753. 42

[80] P. Vorst, J. Sommer, C. Hoene, P. Schneider, C. Weiss, T. Schairer, W. Rosenstiel, A. Zell, and G. Carle. Indoor positioning via three different rf technologies. In *4th European Workshop on RFID Systems and Technologies (RFID SysTech 2008)*, Freiburg, Germany, June 10-11 2008. ISBN 978-3-8007-3106-0. `http://www.ra.cs.uni-tuebingen.de/publikationen/2008/ambisense2008positioning-rfid-systech.pdf`. 84, 91

[81] H. Wang, K. Yao, G. Pottie, and D. Estrin. Entropy-based sensor selection heuristic for target localization. In *Proceedings of the third international symposium on Information processing in sensor networks (IPSN'04)*, pages 36–45. ACM Press, April 2004. `citeseer.ist.psu.edu/wang04entropybased.html`. 57, 58, 60, 74

[82] G. Welch and G. Bishop. An introduction to the kalman filter. Technical report, University of North Carolina, Chapel Hill, NC, USA, June 2006. http://citeseerx.ist.psu.edu/viewdoc/download?doi=10.1.1.79.6578&rep=rep1&type=pdf. 37

[83] S. Willis and S. Helal. A passive RFID information grid for location and proximity sensing for the blind user. Technical report, 2004. ftp://ftp.cise.ufl.edu/cise/ftp-pub/tech-reports/tr04/tr04-009.pdf. 84, 91

[84] J. Wilson and N. Patwari. Through-wall tracking using variance-based radio tomography networks. Arxiv.org, October 2009. http://arxiv.org/abs/0909.5417. 9

[85] P. S. Xiaotao Liu, Mark D. Corner. Ferret: Rfid localization for pervasive multimedia. *Ubicomp 2006*, 2006. 8, 83, 91

[86] W. Ye, J. Heidemann, and D. Estrin. Medium access control with coordinated adaptive sleeping for wireless sensor networks. *IEEE/ACM Trans. Netw.*, 12(3): 493–506, 2004. ISSN 1063-6692. doi: http://dx.doi.org/10.1109/TNET.2004.828953. 42

[87] M. Youssef, M. Mah, and A. Agrawala. Challenges: device-free passive localization for wireless environments. In *MobiCom '07: Proceedings of the 13th annual ACM international conference on Mobile computing and networking*, pages 222–229, New York, NY, USA, 2007. ACM. ISBN 978-1-59593-681-3. doi: http://doi.acm.org/10.1145/1287853.1287880. 86

[88] D. Zhang and L. M. Ni. Dynamic clustering for tracking multiple transceiver-free objects. *Pervasive Computing and Communications, IEEE International Conference on*, 0:1–8, 2009. doi: http://doi.ieeecomputersociety.org/10.1109/PERCOM.2009.4912777. 91

[89] D. Zhang, M. Jian, Q. Chen, and L. Ni. An rf-based system for tracking transceiver-free objects. In *5th Annual IEEE International Conference on Per-*

vasive Computing and Communications, PerCom 2007, pages 135–144, White Plains, NY, 2006. doi: http://dx.doi.org/10.1109/PERCOM.2007.8. 86, 91

[90] Z. Zhang, X. Gao, J. Biswas, and J. K. Wu. Moving targets detection and localization in passive infrared sensor networks. In *Information Fusion, 2007 10th International Conference on*, pages 1–6, July 2007. ISBN 978-0-662-45804-3. doi: 10.1109/ICIF.2007.4408178. 88

[91] F. Zhao, J. Shin, and J. Reich. Information-driven dynamic sensor collaboration. *Signal Processing Magazine, IEEE*, 19(2):61–72, Mar 2002. ISSN 1053-5888. doi: 10.1109/79.985685. 55, 58, 60, 74

[92] Y. Zou and K. Chakrabarty. Energy-aware target localization in wireless sensor networks. In *Pervasive Computing and Communications, 2003. (PerCom 2003). Proceedings of the First IEEE International Conference on*, pages 60–67, March 2003. ISBN 0-7695-1893-1. 58, 60